U.S. DEPARTMENT OF INTERIOR

U.S. GEOLOGICAL SURVEY

Petrology and mineralogy of alkaline rocks from the Elk massif, northeastern Poland

by

Theodore J. Armbrustmacher[1] and Peter J. Modreski[1]

Open-File Report 94-145

[1]Denver, Colorado

1994

CONTENTS

ILLUSTRATIONS

TABLES

ABSTRACT

The Elk alkaline massif is one of a group of intrusive centers within the crystalline basement of the Precambrian Baltic Shield in northeastern Poland. The Elk massif is composed mainly of syenite; it is about 400 km^2 in areal extent and is buried beneath 800-900 m of Mesozoic and Cenozoic sedimentary rocks. Nine drill holes have been bored into rocks of the massif since 1954. This report describes the results of a joint study of core samples from seven of these drill holes, including major- and minor-element analyses, petrographic and cathodoluminescence observations, and electron microprobe mineral analyses.

Thirty-one chemically analyzed core samples comprise five lithologic types: nepheline-sodalite-cancrinite-aegirine syenite (foid-bearing syenite), foid-less aegirine-augite syenite (foid-less syenite), aegirine-arfvedsonite syenite (amphibole syenite), quartz-bearing syenite (quartz syenite), and monzogabbro. Some of the rocks show evidence of incipient fenitization, which results in major modifications of their original alkali and silica contents.

Clinopyroxene in the rocks ranges from augite in monzogabbro, to aegirine-augite in the foid-less syenite, to highly sodic aegirine in the feldspathoidal syenite (X_{Ac} = 0.61-98) and arfvedsonite syenite. Clinopyroxenes in some of the syenite and feldspathoidal syenites are notably zoned, with aegirine-augite cores surrounded by more sodic rims. Biotite is partly altered to chlorite. Increasing Mn enrichment in biotite is observed in the more felsic and feldspathoid-rich rocks. One monzogabbro contains sparse orthopyroxene (En_{75}). Blue-green to yellow pleochroic amphiboles in the aegirine-arfvedsonite syenite are sodium- and fluorine-rich arfvedsonite. Monzogabbro contains greenish-brown, calcic hornblende.

In addition to nepheline, sodalite, and cancrinite, the feldspathoidal syenite contains analcime, natrolite, and perhaps thomsonite. Many of the syenitic rocks contain phenocrysts of microperthite composed of orthoclase and albite, plus late-appearing, interstitial albite. Orthoclase exhibits bright-red cathodoluminescence as does late albite in the arfvedsonite syenite; albite in other syenites luminesces pink to blue. Feldspars in quartz syenite and monzogabbro luminesce blue to bluish green. Monzogabbro contains zoned plagioclase phenocrysts, and sanidine, more sodic plagioclase, and quartz in some samples.

All rock types are sodic except quartz syenite, which is potassic, in terms of $CaO:Na_2O:K_2O$ ratios. Nepheline and arfvedsonite syenites are peralkaline; foid-less syenite is metaluminous to weakly peralkaline, and quartz syenite and monzogabbro are metaluminous. Agpaitic indexes (mol. $Na_2O + K_2O > Al_2O_3$) range from 1.01 to1.24 in nepheline syenite, 1.09 to 1.14 in arfvedsonite syenite, 0.94 to 1.02 in foid-less syenite, 0.82 to 0.97 in quartz syenite, and 0.43 to 0.51 in monzogabbro. However, mineralogical characteristics of these rocks are more similar to miaskitic syenites. Differentiation indexes range from 76.53 to 95.37 for syenites and from 44.22 to 47.32 for monzogabbro. All analyzed rocks show light rare-earth-element enrichment, but rare-earth-element fractionation trends are variable. Most rocks have negative Eu anomalies, although three samples have positive Eu anomalies, and monzogabbro and unaltered quartz syenite have no Eu anomalies.

The Elk rocks may represent more than one magmatic differentiation series, although this interpretation is complicated by late- to post-magmatic alteration involving introduction of albite, orthoclase, amphibole, sericite, chlorite, and carbonate; some syenites may be fenitized. Absence of a protolith for the fenitized rocks and contacts between various lithologies in the drill core complicate efforts of determining the origin of the Elk massif rocks.

INTRODUCTION

The information described here represents the results of a 3-year cooperative study conducted by the U.S. Geological Survey (USGS) and Panstwowy Instytut Geologiczny (PGI) of the geology and mineral resource potential of the Elk alkaline intrusive massif and other alkaline massifs, including the Tajno massif, in northeastern Poland. The cooperative study was sponsored by the Polish-U.S. Joint Commission, the Maria Sklodowska-Curie Joint Fund II.

In addition to the Elk massif, at least four other alkaline massifs intrude the crystalline basement of northeastern Poland. These massifs were originally discovered by PGI using gravity and magnetic geophysical techniques, and some of the resultant geophysical anomalies were investigated by core drilling. These alkaline massifs include intrusions at Elk, Pisz, Mlawa, Olsztynek, and Tajno (Fig. 1) (Karaczun and others, 1982). This report discusses the results of petrologic and mineralogic studies

conducted by the USGS on samples of core drilled by the PGI into the Elk massif.

Several earlier studies of the Elk massif were conducted chiefly by members of PGI. English-language reports include those by Dziedzic (1984), Dziedzic and Ryka (1983), and Bareja and Kubicki (1983). The structural setting of the Elk massif is discussed by Kubicki and Ryka (1982). The geology of the syenites at Elk are described (in Polish) by Juskowiak (1969).

ANALYTICAL METHODS

In April, 1989, 12 samples of drill core from the Elk massif were collected from the PGI core repository at Iwiczna, Poland; in July, 1991, 21 additional samples were collected from the Elk massif at Iwiczna and the core repository at Szurpily, Poland. These samples were analyzed in the laboratories of the USGS. Major-element abundances were determined by X–ray fluorescence spectrometry (Taggart and others, 1987); FeO, CO_2, and H_2O were determined by classic rock analysis techniques (Jackson and others, 1987); 44 minor- and trace-element abundances were determined by optical spectroscopy (Lichte, Golightly, and Lamothe, 1987); uranium and thorium were determined by delayed neutron counting (McKown and Millard, 1987); and rare-earth elements (REE) were determined by inductively coupled plasma-optical emission spectroscopy (Crock and Lichte, 1982; Lichte, Meier, and Crock, 1987). Minerals and rock textures were studied using standard petrographic techniques. Scanning electron microscopy (SEM) techniques were used for further identification of minerals and cathodoluminescence (CL) properties of minerals were examined using the luminoscope.

Chemical compositions of pyroxene, amphibole, biotite, alkali feldspar, and plagioclase in representative samples of the various rock types were determined using an electron microprobe. Compositions of selected rock-forming minerals in a variety of rock types were determined on the ARL-SEMQ electron microprobe at the USGS. Operating conditions for quantitative analysis were 15kV accelerating voltage and 15nA specimen current. Beam diameter was between 20 μm and about 1 μm depending on sample grain size and the need to minimize volatilization of hydrous or alkali-containing minerals. Counting times were generally 20 seconds on peak and on background positions. Data reduction was with the ZAF-type matrix correction program "MAGIC IV" (Colby, 1968).

Sodium, potassium, magnesium, calcium, manganese, iron, aluminum, silica and titanium contents were determined in all minerals studied; in selected samples, strontium, barium, chromium, fluorine, and chlorine were also determined. A variety of standards, including acmite (Na, Fe, Si), albite (Na, Al, Si), anorthite (Ca), augite (Ca, Al), BaF_2 (Ba), biotite (Cl), celsian (Ba), diopside (Ca, Mg), fayalite (Fe), fluorphlogopite (F, Mg, K, Al, F), halite (Cl), hematite (Fe), hornblende (Ti), magnesiochromite (Cr), olivine (Mg), orthoclase (K), rhodonite (Mn), rutile (Ti), scapolite (Cl), spessartine (Mn), and $SrTiO_3$ (Sr,Ti), were used to analyze the various minerals.

Table 2 is a summary of the minerals analyzed in 14 selected rock samples, representing the nepheline (nepheline-sodalite-cancrinite) syenite, amphibole-bearing syenite, foidless syenite, and monzogabbro from the Grajewo drill hole. Most quartz syenite and most of the primary mineral phases contained therein (drill holes K1, P1, and P2) are extensively altered; no minerals in these rocks have been analyzed. Compositional data on rock-forming minerals in the Elk rocks are given in table 3 (clinopyroxene), table 4 (biotite), table 5 (amphibole), and table 6 (feldspar). Figures 13-16 are plots of these mineral data.

GEOLOGICAL FRAMEWORK

The alkaline intrusive massif at Elk intrudes crystalline rocks of the East-European Precambrian Platform (fig. 1), which form the Baltic and the Ukrainian Shields in eastern Europe. At Elk, in northeastern Poland, the Platform is covered by 800-900 m of Mesozoic and Cenozoic sedimentary rocks. Consequently, rocks of the Elk massif are not exposed and are only accessible through drilling.

The Platform consists of several tectonic-lithologic units (Ryka, 1984a). The oldest rocks are pre-Karelian (Archean) granite gneiss massifs or domes, including the Mazowsze massif that host the alkaline massifs, and folded metamorphic rocks that have some characteristics of greenstone belts. The gneissic rocks consist chiefly of quartz, orthoclase, microcline, oligoclase, muscovite, biotite, and minor cordierite and they are spatially associated with granite and granodiorite plutons. Chemical compositions of the gneissic rocks indicate that they are homogeneous over large areas. Potassium-argon ages indicate a maximum age of 2,650 Ma, but some of the ages have apparently been reset by metasomatic

events that occurred during Gothian time, about 1644-1143 Ma (Kubicki and Ryka, 1982). The folded metamorphic rocks are characterized by steep isoclinal folds and local strong cataclasis. These rocks originated by metamorphism of thick volcanic tuff and lava flow sequences to two-pyroxene granulite, charnockite, and pyroxene gneiss, and by the metamorphism of arkosic sedimentary rocks to cordierite gneiss. These rocks were later intruded by tholeiitic mafic dikes. Granite gneiss massifs and folded metamorphic rocks are separated by mylonite zones as much as several hundred meters thick. A younger pre-Karelian metamorphic event accompanied diapiric intrusion of calc-alkalic magmas (Ryka, 1985).

Following the pre-Karelian episode, a different sequence of volcanic-sedimentary rocks was metamorphosed to amphibolite and hornblende gneiss in Karelian time (Proterozoic). These rocks were subsequently eroded from most areas of the pre-Karelian basement. The Karelian metamorphic event was accompanied by tectonism that caused detachment of these rocks from the pre-Karelian basement forming a set of disharmonious folds.

Rocks of the Platform were then subjected to an episode of intense alkali metasomatism (granitization) and migmatization during Gothian time (Ryka, 1984b). Granitization was intense at boundaries between the granite massifs and folded metamorphic rocks and along contacts between Karelian and pre-Karelian structures; contacts between Karelian and pre-Karelian structures were intruded by Gothian granite (Ryka, 1984b). East-west Karelian faults along the southern boundary of the Mazowsze massif were reactivated at this time and were the locus of rapakivi granite intrusion. Anorthosite massifs of the Platform were formed at essentially the same time. Potassium-argon dates indicate that the rapakivi granite formed 1,472 Ma; the Gothian granite in the Mazowsze massif formed 1,360 Ma. Synchronously, the Platform was faulted into rectangular segments resulting in the formation of elongate troughs and equidimensional depressions.

After Gothian time, a thin cover of clastic sediments was deposited in tectonic grabens and at other sites. This sedimentation was accompanied by an episode of volcanism. These sedimentary and volcanic rocks were subsequently metamorphosed to an assemblage of quartzite and related rocks known as the Biebrza massif (equivalent to Jothnian in other parts of the Platform), which are preserved in small areas mainly

associated with the rocks of the Mazowsze massif.

During Devonian-Carboniferous time, the East-European Platform crystalline rocks were intruded by a series of at least five alkaline massifs in northeastern Poland. These massifs contain rocks ranging in composition from mafic-ultramafic rocks to syenitic rocks; carbonatite was also intruded into alkaline rocks of at least one of the alkaline massifs. After another episode of uplift and erosion, several hundred meters of sedimentary rocks of Mesozoic and Cenozoic age were deposited on top of the rocks of the Platform.

ALKALINE INTRUSIVE MASSIFS

East-European Precambrian Platform rocks located in northeastern Poland were intruded by a series of intrusions consisting of alkaline rocks and carbonatite (fig. 1). Isotopic dating of carbonatite and silicate rocks from the Tajno massif (Bell and Ryka, in press) yielded ages of 330 Ma by several techniques. Blusztajn (in press) indicates that rocks of the Elk massif formed 355 ± 4 Ma. These ages are similar to those (380-360 Ma) for the Paleozoic Kola Alkaline Province of the Commonwealth of Independent States and Finland (Kramm and others, 1993). Isotopic ages are not available for the other Polish alkaline massifs.

The characteristics of the intrusions at Pisz and Mlawa are poorly known; each has been penetrated by a single drill hole. The intrusion at Olsztynek has not been drilled; the presence of alkaline rocks is implied by geophysical signatures similar to those of the other drilled alkaline massifs. The massif at Tajno contains a series of alkaline rocks ranging from melteigite to nepheline syenite and alkaline volcanic rocks cut by carbonatite dikes (Krystkiewicz and Krzeminski, 1992; Ryka, 1992; Ryka and others, 1992).

As of 1984, the Elk massif had been penetrated by nine holes drilled by PGI (fig. 2); the first hole was drilled in 1954 near the center of a strong negative gravity anomaly (Dziedzic, 1984). The massif occupies at least 400 km^2, as indicated by geophysical data, and is buried under 800-900 m of Mesozoic and Cenozoic sedimentary rocks. According to Dziedzic (1984), the drill core consists chiefly of a variety of agpaitic and miaskitic syenites and minor mafic rocks.

Several episodes of igneous activity have been delineated by geophysical and drill-hole data at Elk (Dziedzic, 1984). Rocks of the first

episode consist of ring-shaped intrusions composed of granite and diorite with several textural types; rocks of the second episode are dominated by ring-shaped intrusions of quartz syenite, locally hydrothermally altered. Intrusion of the quartz syenite was followed by collapse of the central part of the massif. Rocks of the third episode consist of microperthite syenite; rocks of the fourth episode include several varieties of agpaitic syenite and related rocks; a fifth episode predicted by Dziedzic (1984) to contain eudialyte syenite and carbonatite, was not yet discovered as of 1984. Dziedzic has pointed out the existence of "carbonatite" of metasomatic-hydrothermal origin in the Elk massif (Dziedzic and Ryka, 1983). Discussions of Zr-Nb-REE-U-Th mineralization in drill holes E3 and E4 were given by Dziedzic (1984) and by Bareja and Kubicki (1983).

Petrography of rocks of the Elk massif

Petrographic and chemical data were combined to establish rock nomenclature of five rock types identified in drill core of the Elk massif. Five different mineralogic types of intrusive rock were defined by petrographic examination of 31 core samples from 7 drill holes. The following chemical names, in parentheses, are derived from figure 3 (modified from De la Roche and others, 1980) and are prefixed by the mineralogic identifications obtained through petrographic observations: nepheline-sodalite-cancrinite aegirine-augite syenite (nepheline syenite) (drill holes E2 and E3); foid-less aegirine-augite syenite with nepheline in the norm (foid-less syenite) (drill hole E3); aegirine-augite, eckermannite-arvfedsonite syenite ± fluorite (amphibole syenite) (drill hole E4); quartz-bearing syenite (quartz syenite) (drill holes K1, P1, and P2); and quartz-bearing, plagioclase-potassic feldspar rock of more mafic composition (monzogabbro) (drill hole G1). Nepheline syenite pegmatite and metasomatized zones (in drill holes E3 and E4) described by Dziedzic (1984) and metasomatized carbonate rocks, considered carbonatite by Dziedzic (1984), were not identified in the samples collected for this study.

Nepheline syenite

The feldspathoid-bearing nepheline syenite samples are medium to coarse grained and equigranular to slightly porphyritic with phenocrysts

of equant perthitic alkali feldspar; a few samples have trachytoid textures with lath-shaped feldspars. The perthitic feldspar is a mixture of slightly altered untwinned potassic feldspar and unaltered albitic plagioclase phase. Fresh, late-appearing plagioclase is interstitial to the feldspars, especially along boundaries between adjacent perthitic alkali feldspars. Sodalite, cancrinite, and nepheline, mostly in close spatial association with each other, are interstitial to the feldspars and appear to have crystallized late in the paragenetic sequence. Sodalite is medium to coarse grained and contains abundant solid and fluid inclusions; inclusions are not apparent in the other feldspathoids. Subhedral to anhedral aegirine-augite is the main ferromagnesian mineral in the rocks. It is slightly zoned and usually spatially associated with opaque oxide minerals and biotite. Yellow-brown to brown pleochroic biotite forms discrete grains and alteration products of aegirine-augite. Opaque oxide minerals, partly oxidized to hematite, are fine to medium grained. Chlorite results from alteration of biotite. Sparse apatite occurs in a few samples.

In samples E2-1850 and E2-2001.4 (sample numbers consist of a notation of the drill hole number followed by the depth, in meters) the slightly altered potassic feldspar phase of the microperthite luminesces bright red; the fresher appearing plagioclase phase luminesces partly pink, partly light blue. Interstitial, late albitic plagioclase luminesces bright blue. Sodalite luminesces bright orange, cancrinite does not luminesce. Secondary carbonate is calcitic (it luminesces bright golden yellow), fluorite is bright bluish gray (silvery), and secondary zeolite (thomsonite?) luminesces medium blue. Mafic minerals and accessory minerals such as titanite do not luminesce.

Foid-less syenite

Several samples from drill hole E3 (fig. 2) have the chemistry of nepheline syenite (fig. 3) but do not contain identifiable modal feldspathoids; some of the samples have pyroxene composed of acmite rims surrounding aegirine-augite cores. Perthitic feldspars are selectively altered; potassic feldspars are slightly altered, clear, sodic plagioclase, which occurs in perthite and as interstitial, late grains, is unaltered. Ferromagnesian minerals in samples from near the top of the massif are partly to completely replaced by fine-grained aggregates of

sericitic mica, unidentified, fine-grained isotropic minerals, and poorly crystallized iron oxides. Titanite and fine-grained needles of apatite are accessory constituents. Carbonate, chiefly calcite, is a sparse secondary mineral.

Dziedzic (1984) stated that the interval between 1070 and 1385.5 m in drill hole E3 was an interval characterized by radioactive anomalies and mineralized rock associated with a zone of metasomatic-hydrothermal alteration. Several samples from that interval appear to be altered but not necessarily mineralized. In sample E3-1019, the potassic feldspar luminesces bright red, whereas relatively fresh-appearing plagioclase phase luminesces bright blue. In sample E3-1230, most of the feldspar luminesces blue. The CL features of other minerals are similar to those described for E2 samples, except feldspathoidal minerals are absent. Our samples from interval 1070-1385.5 show zones of metasomatized rock interspersed with less altered rock; anomalously radioactive and mineralized rock was not observed in our samples of drill core.

Amphibole syenite

Core from drill hole E4 contains a suite of minerals similar to that in drill hole E3 samples except for the presence of pleochroic bluish-gray eckermannite-arfvedsonite that is spatially associated with aegirine-augite in most places; this rock is classified as syenite. Fluorite, titanite, apatite, and opaque oxide minerals are accessory minerals. All feldspar, including both feldspars in microperthite and interstitial, late albitic plagioclase in samples E4-1129 and E4-1267.7 luminesces bright red. All other CL observations are similar to those for previously described samples.

Quartz syenite

Quartz syenite in drill holes K1, P1, and P2 consists chiefly of medium- to coarse-grained porphyritic rock with phenocrysts of equidimensional microperthite; lath-shaped feldspars occur in the medium-grained groundmass. These rocks, which contain interstitial quartz, biotite, chlorite replacing biotite, and accessory apatite and zircon, are altered; carbonate minerals partly replace some pre-existing minerals and

the feldspars are sericitized.

In samples from drill hole P2, the quartz faintly luminesces a dark bluish gray and the feldspars luminesce medium blue and shades of bluish green. Apatite luminesces bright yellow and secondary carbonate luminesces bright red.

Monzogabbro

The rocks intersected by drill hole G1 are unlike the rocks in the other drill cores. They consist chiefly of quartz, plagioclase, augite, biotite partly replacing augite, hornblendic amphibole, chlorite replacing biotite, minor sanidine, and sulfide and oxide opaque minerals. The chemistry of this rock would be classified as monzogabbro (De la Roche and others, 1980), but its petrography is closer to that of monzonite. Carbonate is a secondary constituent; apatite and olivine are accessory minerals in some of the samples. Myrmekitic intergrowths of quartz and sanidine are present. Feldspars in samples G1-1411.3 and G1-1952.7 display compositional zoning under the luminoscope; the cores of crystals are slightly darker blue than an intermediate zone, which in turn is rimmed by feldspar that luminesces pale reddish-blue. Apatite luminesces bright silvery and quartz luminesces dark bluish-purple.

Major-element geochemistry

Major-element analyses for 31 samples of drill core from the Elk massif are presented in table 1. A plot of normative nepheline or quartz as a function of silica content (fig. 4) shows that the nepheline syenite is the most undersaturated with respect to silica; the altered quartz syenite is the least undersaturated. Figure 4 also suggests that alteration of the quartz syenite occurred under conditions of constant SiO_2 but increasing normative quartz content; alteration of the monzogabbro occurred under conditions of increasing SiO_2 and increasing normative quartz. A plot of total alkalies versus silica (fig. 5) shows that all the rocks analyzed are alkaline. Most nepheline syenite samples plot in the foid-bearing, strongly alkaline field of Saggerson and Williams (1964), whereas the other rock types fall in the foid-less, mildly alkaline field. On figures 4 and 5, as well as other diagrams, the monzogabbro samples form a distinctive group and appear to be unrelated to the other rock types. The

CaO-Na2O-K2O diagram (fig. 6) illustrates the sodic nature of all the rock types except the quartz syenite which exhibits a potassic affinity. Harker diagrams (fig. 7) depict the distinctive nature of the unaltered monzogabbro; it contains lesser amounts of SiO2 and alkalies and greater amounts of MgO, CaO, total iron, P2O5, and TiO2 than the other rock types. The various mineralogic syenite types form fairly distinctive though overlapping groups. The Harker diagrams on figure 7 are of limited value for defining differentiation trends exhibited by chemical analyses of the Elk rocks because of the relatively narrow range of SiO2 content in those rocks. In addition, the Harker diagrams offer little, if any, evidence for derivation of Elk rocks from a common parental magma by fractionation of constituent minerals.

The analyses of samples of Elk syenite were also plotted against MgO (fig. 8), which is a better differentiation index for rocks with small SiO_2 variation (Dorais and Floss, 1992). Again, data show considerable scatter, but there appears to be a suggestion of a continuum progressing from nepheline syenite to foid-less syenites to quartz syenite as MgO increases. This suggests the possibility of derivation of the syenitic rocks from the same parental magma, but this possibility is rather remote.

Nepheline syenite from the Elk massif is peralkaline (mol. $Na_2O + K_2O > Al_2O_3$) as indicated by its normative acmite content and an agpaitic index between 1.01 to 1.10; the index of one sample (E3-2005.7) is unusually high (1.24). Foid-less syenite is metaluminous to barely peralkaline and the agpaitic index is 0.94-1.02. Amphibole syenite is peralkaline; the agpaitic index is 1.09-1.14. Quartz syenite is metaluminous; the agpaitic index is 0.82-0.97. Monzogabbro is metaluminous; unaltered samples have agpaitic indexes of 0.43-0.51; altered rocks have an index of 0.78. Although some of these rocks would be considered agpaitic because their index is ≥ 1, most of the mineralogical characteristics of the rocks (Sorensen, 1974) are similar to those of miaskitic syenite; however, compositions of amphiboles in these rocks suggest that they are agpaitic.

Differentiation indexes (DI = normative q + or + ab + ne + lc + kp) (Thornton and Tuttle, 1960) for all of the syenites range from 76.53 (E3-1286.5) to 95.37 (E3-1259); unaltered monzogabbro ranges from 44.22 to 47.32. Plots of DI versus major elements (fig. 9) also show some grouping of lithologic types but only a limited sense of differentiation because of

the narrow range in composition of the rocks.

Feldspathoid-bearing nepheline syenite contains the highest Al_2O_3, alkalies, and Na_2O and the lowest MgO and TiO_2 of the syenitic rocks (fig. 7). Syenite has the lowest Al_2O_3 content and, in terms of chemical composition, is the most homogeneous of the syenite types. All "nepheline" syenite samples have similar compositions, except E3-1286.5, which is somewhat more mafic than other syenite samples (DI = 76.53; average of all syenite samples = 91.81). Chemical compositions of quartz syenite samples from drill hole P2 are nearly identical; samples from K1 and P1 differ from the P2 samples because they are altered.

Minor-element geochemistry

Rocks from the Elk massif have a range of rare-earth element (REE) concentrations (table 1), although REE patterns (fig. 10) are generally similar. Total REE and La/Yb_{CN} (chondrite-normalized lanthanum/ytterbium) values for nepheline syenite range from 207 to 1588, and 7 to 38, respectively; foid-less "nepheline" syenite, which includes some of Dziedzic's (1984) "altered and mineralized rocks ," ranges from 446 to 1,213, and from 22 to 44, respectively; syenite ranges from 552 to 1,224, and from 34 to 52, respectively; quartz syenite ranges from 330 to 768, and from 25 to 35, respectively; and monzogabbro ranges from 270 to 374, and 21 to 29, respectively. All rocks show light REE enrichment. All syenitic rocks show fairly steep slopes from lanthanum (La) to europium (Eu); monzogabbro samples have relatively more gradual slopes (fig. 10). Two nepheline syenite samples, E3-2005.7 and E2-1844, show relatively elevated concentrations of heavy REE, resulting in a concave-shaped pattern. The fractionation of titanite and (or) apatite, (Brotzu, and others, 1989), or the fractionation of clinopyroxene and (or) amphibole (Hanson, 1978) may result in a concave-shaped pattern . The nepheline syenite samples show considerable range in total REE abundances compared with other Elk samples; all samples except E3-1810 have a negative Eu anomaly. "Nepheline" syenite samples have negative Eu anomalies, except E3-1230, which has a positive Eu anomaly; E3-1230 and E3-1019 also may exhibit positive cerium (Ce) anomalies. The amphibole syenite samples consistently have small negative Eu anomalies; samples E4-1074 and E4-1256 also may exhibit small Ce anomalies. The altered quartz syenite samples K1-965.3 and P1-974.2 have, respectively, a

positive and a negative Eu anomaly, whereas the relatively fresh quartz syenite samples have no Eu anomalies. Eu anomalies are usually formed by the addition or subtraction of feldspar to or from the parental magma. Monzogabbro samples, fresh and altered, do not have any Eu anomalies; samples G1-829.7 and G1-845.6 are altered and both have greater concentrations of light REE.

Abundances of several trace elements are plotted against DI (fig. 11). Data for the various syenite types tend to cluster on these plots, but there is no indication that the rocks of the Elk massif are related through fractionation processes. Sample E2-1844, a nepheline syenite, is somewhat enriched in Ce, La, and thorium (Th), and sample E3-2005.7, also a nepheline syenite, is enriched in niobium, zinc, and gallium, relative to the other rock samples. Samples from within Dziedzic's metasomatized and mineralized zone (E3-1072 to 1384.5 m) do not contain higher concentrations of REE, niobium, uranium, or thorium than other syenitic samples. The monzogabbro samples have low Ce, La, niobium, beryllium, uranium, and thorium, intermediate barium, lithium, zinc, gallium, and yttrium, and high strontium concentrations relative to those in the syenite samples.

Spider diagrams (fig. 12) for nepheline syenite, foid-less "nepheline" syenite, and amphibole syenite have large barium, strontium, phosphorous, and titanium troughs. Troughs for Sr, P, and Ti result from fractionation of plagioclase, apatite, and Fe-Ti oxides, respectively, during the evolution of the parental magma (Thompson and others, 1982; Cameron and others, 1986); barium troughs may reflect alkali feldspar fractionation (Cameron and others, 1986). Altered quartz syenite samples have increased concentrations of, niobium, strontium, and REE relative to the unaltered samples; although all the quartz syenite samples have strontium, phosphorous, and titanium troughs, the strontium troughs of the altered samples are deeper. The fresher quartz syenite samples have pronounced niobium troughs, whereas the altered samples do not. The differences in the background levels of the spider diagrams and the depths of the troughs for barium, strontium, phosphorous, and titanium may reflect varying degrees of fractionation in these syenitic rocks. Fresh monzogabbro samples have relatively shallow titanium troughs and an overall concave shape; altered monzogabbro samples have moderately deep strontium, phosphorous, and titanium troughs. The overall gross similarity of the spider diagrams of the syenite samples suggests that

they may be derived from a similar magmatic parent; monzogabbro appears to be derived from different magmas.

Mineral chemistry

Pyroxene

Clinopyroxene compositions range from diopsidic augite to acmite. Pyroxenes were analyzed in 11 of the rock samples studied, including 4 of the nepheline syenites, 3 foid-less "nepheline" syenites, 2 amphibole syenites, and 2 monzogabbros. Table 7 is a summary of the results with regard to acmite (soda) component of the pyroxenes, and table 3 gives the complete analytical results.

A variety of methods are available for computing formula proportions from pyroxene analyses and for inferring the Fe^{2+}/Fe^{3+} ratio, including normalizing proportions to 6 oxygen atoms and (or) to 4 total cations, from microprobe analyses. The most successful method for the analyses presented here appears to be to compute Fe_2O_3 assuming that the atomic proportion of Fe^{3+} and Na are equal, and to normalize the proportions to 6 total oxygens; this is followed in the analyses of table 3 (if Na>Fe, then all Fe = Fe^{3+}).

The pyroxene data are plotted on fig. 13, the pyroxene quadrilateral, and again on fig. 14 in terms of atomic proportions of Fe^{3+}, (Fe^{2+}+Mn^{2+}), and Mg. The latter diagram, representing respectively the acmite, hedenbergite-ferrosilite-johannsenite, and diopside-enstatite components, is used here because many of the analyzed pyroxenes contain a predominance of the acmite component and therefore are outside the pyroxene quadrilateral.

Clinopyroxene compositions vary from slightly sodic augite in the monzogabbro to nearly pure acmite in the nepheline and amphibole syenites. Pyroxenes in three of the nepheline syenites (E2-1850, E2-1856 and E3-1810) show pronounced zoning, with acmite-rich overgrowths surrounding aegirine-augite cores.

One monzogabbro sample (G1-2000.0) contains a few phenocrysts (xenocrysts?) of orthopyroxene (bronzite), with Mg/(Fe+Mg) = 0.75 (table 3).

Biotite

Biotite is present in most of the rocks, including the nepheline syenite, foid-less "nepheline" syenite, and monzogabbro; however, it is absent from the amphibole syenite. Microprobe analyses of biotite are given in table 4 and are plotted in terms of atomic Mg-Fe-Mn on figure 15. For lack of a reliable way to infer Fe^{3+} content from the microprobe analyses, the analyses are presented here with all iron expressed as FeO, recognizing that some proportion of the iron in these micas is ferric iron.

Compositions of biotite in the three analyzed monzogabbro samples are fairly uniform, centering near $Mg_{60}Fe_{40}$, with a very low Mn content (table 4, fig. 15). This mica would have the composition of phlogopite if one uses 1:1 Mg:Fe as the boundary between phlogopite and biotite, but it is still classified as biotite by the commonly adopted boundary of 2:1 Mg:Fe (Deer and others, 1966).

In the syenites, biotite compositions range from about Fe_{43} to Fe_{82}. In many of these rocks, biotite is significantly zoned; the most extreme example of zoning is in the nepheline syenite E2-1850, where biotite compositions range from Fe_{57} to Fe_{82}. Within each rock sample, biotite compositions define a linear trend of increasing Fe:Mg and relatively constant Mn content. Each rock can be characterized by the Mn content of its biotite: biotite in nepheline syenite and amphibole syenite (E3-1230, E3-1286.5, E3-1810, and E3-2013.5) is Mn_3-Mn_6, nepheline syenite E2-1850 is Mn_8-Mn_{10}, nepheline syenite E2-1856 is $Mn_{11\text{-}13}$, and biotite in nepheline syenite E2-1844 shows a very strong enrichment in manganese, with Mn_{16} (table 4; fig. 15). The trend of increasing Mn content in these rock samples parallels fractionation indicated by the acmite content of their clinopyroxenes (table 3; fig. 13). The very low Mn content of biotite in the monzogabbro, $Mn_{0.2}$-$Mn_{0.4}$, is quite distinct from that of the Mn-rich syenites.

Amphibole

Amphibole syenite from Elk drill hole E4 contains blue-green to yellow pleochroic sodic amphibole. Associated minerals in these rocks include aegirine, potassic feldspar, and albite. Microprobe analyses of the amphibole in three of these syenites are given in table 5. The amphiboles are high in sodium and low in aluminum and calcium; iron and magnesium

abundances (by atomic proportion) present are comparable. A significant amount of potassium and fluorine (about 3 weight percent), equivalent to about 1.4 F anions per $[Si_8O_{22}]$ formula unit, are also present. The high sodium (nearly 3 cations per formula unit) and low aluminum content place the amphibole in the arfvedsonite-magnesio-arfvedsonite series, ideally $Na_3(Fe^{2+},Mg)_4Fe^{3+}Si_8O_{22}(OH,F)_2$, as opposed to eckermannite, $Na_3(Mg,Fe^{2+})_4AlSi_8O_{22}(OH,F)_2$, or riebeckite, $Na_2(Fe^{2+},Mg)_3Fe^{3+}{}_2Si_8O_{22}(OH)_2$ (Leake and Winchell, 1978; Hawthorne, 1981). The bulk atomic proportions of iron and magnesium are nearly equal in the amphiboles (table 5); however assignment of a reasonable proportion of the iron as Fe^{3+} to satisfy the charge-balance requirement for one trivalent cation per formula unit in the octahedral sites leaves $Mg/(Mg+Fe^{2+})$ slightly >0.5 in the remaining sites, yielding an amphibole composition of arfvedsonite rather than magnesio-arfvedsonite. Different schemes for recalculating the formulas and partitioning ferrous and ferric iron in these amphiboles yield various inferred species names. Some of the alternate calculation procedures in the AMPHIBOL program of Richard and Clarke (1990) assign amphibole names ranging from arfvedsonite and magnesio-arfvedsonite to ferro-eckermannite for the same analyses.

A small amount of blue-green amphibole appears to be present in at least two nepheline syenite samples from drill hole E3, samples no. E3-2005.7 and E3-2013.5. The amphibole is late forming, and some grains poikilitically surround aegirine needles.

Amphiboles are also present in some of the plagioclase- and quartz-bearing monzogabbro. Microprobe analyses of this greenish-brown, moderately pleochroic amphibole (samples G1-1394.5 and G1-1408.0) indicate a calcic amphibole composition, similar to those in the range between magnesio-hornblende and actinolitic hornblende (Leake and Winchell, 1978); these amphiboles are notably less sodic than those in the amphibole syenites.

Feldspar

Analyses of alkali and plagioclase feldspars are given in table 6, and the feldspar compositions are plotted in a Na-K-Ca diagram in figure 17. Table 8 is a summary of the alkali and plagioclase feldspar compositions.

The syenitic rocks contain only alkali feldspar. Typical coarse-grained phenocrysts are sanidine microperthite. Analyzing these grains is

difficult because it is hard to avoid adjacent sodic and potassic exsolution lamellae. Experiments with different beam diameters were made in the course of the microprobe analysis, but it was not possible to determine whether intermediate compositions obtained during analysis represented an average composition of unmixed feldspar or whether random proportions of Na- and K-rich lamellae were analyzed. Potassium-rich orthoclase is present in some samples: amphibole syenite E4-950.2, Or_{98}; nepheline syenites E3-2005.7 (Or_{90-94}), E2-1850 (Or_{95}), E2-1856 (Or_{95}), and E3-1810 (Or_{95}); and foid-less syenite E3-1286.5 (Or_{96}). In contrast, non-end member potassic feldspar was found in nepheline syenite E2-1844 (Or_{15-83}), and in foid-less syenite E3-1230 (near Or_{37}); and both nearly pure orthoclase ($Or_{97.5}$) and apparent intermediate sanidine (Or_{76-91}) were found in amphibole syenite E4-1256. The structural states of these potassic feldspars were not determined.

Most of the rocks also contain albite, often as a late-stage, interstitial mineral which appears to be a result of metasomatic introduction of Na_2O or a product of unmixing. Albite is very near end-member composition in the amphibole syenites ($Ab_{99.5}$), near to slightly less pure in the nepheline syenites ($Ab_{97-99.5}$), and in the compositional range Ab_{94-98} in the other syenites.

Monzogabbro from the Grajewo drill hole G-1 is the only rock examined that contained plagioclase. Its composition ranges from sodic labradorite to oligoclase (table 6), and it is accompanied in one case (G1-1394.5) by sodic plagioclase near albite (Ab_{96}) in composition, and in another case (G1-1408.0) by potassium-rich feldspar (Or_{68-88}).

PETROGENESIS

The concealed nature of the Elk massif and lack of definitive cross-cutting relations between various types of syenites in the drill cores preclude establishing the relative ages of the various syenites. The absence of mafic alkaline rocks such as those in the Tajno massif in any of the drill cores observed by us and the lack of geophysical evidence of mafic rocks in the Elk massif make it difficult to define potential parental magmas for the syenitic rocks. Thus, direct evidence for the evolution of a primary magma or identification of more primitive or less evolved species is not viable.

Luminoscope examination of the Elk rocks indicates that samples of drill cores E2, E3, and E4 have been subjected to internal fenitization (Marshall, 1988). In this process, late-stage alkaline magmatic fluids become enriched in alkalis, and iron in the system becomes stablized in the ferric state as crystallization proceeds. Subsequently, late-stage fluids react with earlier formed primary rock-forming minerals. Primary feldspars are replaced by ferric iron-substituted feldspar; because ferric iron is an activator element, it luminesces bright red under electron bombardment and is readily distinguished from the blue-luminescing ferric iron-poor feldspar. This closed system alteration is similar to the process of deuteric alteration. Alternatively, the internal fenitization may be a primary igneous phenomenon and indicates conditions of strong oxidation or high alkalinity. Augite is replaced in part by aegirine-augite at grain boundaries. The formation of cancrinite at the expense of nepheline may also result from internal fenitization. The inferred metasomatic episode may also be responsible for the introduction of fluorite and calcite into these rocks. The presence of late-stage, interstitial albitic plagioclase that luminesces blue suggests that an even later process occurred. This process resulted not from fenitizing solutions but from sodium metasomatism in which the fluids enabled nucleation of albitic plagioclase lacking ferric iron impurities. Thus, it appears that the syenitic rocks have experienced an unusual late-magmatic to post-magmatic history, and the discovery of a unifying process for the origin of all the syenitic rocks will be difficult. Another possibility is that the syenites in drill holes E2, E3, and E4 represent rheomorphic fenites, that is, rocks of unknown original composition, perhaps granitic, that were remobilized and reintruded during intense fenitization. The composition of the parent magma and the resulting unaltered rock formed from it are also unknown. The quartz syenite samples are not deuterically altered as are the other syenites, but the close proximity between the P1 drill holes and the contact with the pre-Karelian granitic host rocks suggests that the quartz syenite may be the result of contamination of a parent magma by host granitic rocks. CL evidence for replacement of feldspars by ferric iron-rich fluids is lacking which suggests that the quartz syenites were not formed by fenitization of the host pre-Karelian rocks. Rubidium-strontium and samarium-neodymium isotopic systematics might help determine the relation between the various syenites.

Compositional variations among the Elk syenitic rocks are complicated by late- to post-magmatic events, and variation diagrams suggest that the rocks are not easily interpreted as being related through simple fractionation. The lack of systematic relations between various element pairs suggests that the rocks do not represent a single liquid line of descent. The scattering of data results from considering samples that represent random limited sampling of magmas at different stages of evolution from a suite of parental magmas with similar compositions. Variation diagrams suggest that the rocks in drill hole G1 may not be genetically related to the syenitic rocks. Drill hole G1 is located at the town of Grajewo, near the southeastern contact of the massif, and may have been drilled into pre-Karelian granitic rocks that host the massif.

REFERENCES CITED

Bareja, E., and Kubicki, S., 1983, Mineralization in zones of metasomatic hydrothermal alterations of Elk syenites, NE Poland: Kwartalnik Geologiczny, v. 27, p. 215-223.

Bell, Keith, and Ryka, Waclaw, in press, Isotopic systematics of the Tajno carbonatite complex, Poland and implications for fluorite mineralization: Canadian Mineralogist.

Blusztajn, J., in press, The Elk syenite intrusion: Rb-Sr and fission track dating, thermal history and tectonic implications: Prace Instytutu Geologicznego.

Brotzu, P., Beccaluva, L., Conte, A., and others, 1989, Petrological and geochemical studies of alkaline rocks from continental Brazil. 8. The syenitic intrusion of Morro Redondo, RJ: Geochimica Brasiliensis, v. 3, p. 63-80.

Cameron, Maryellen, Cameron K.L., and Carman, M.F., Jr. 1986, Alkaline rocks in the Terlingua-Big Bend area of Trans-Pecos Texas, in, Price, J.G., Henry, C.D., Parker, D.F., and Barker, D.S., eds., Igneous geology of Trans-Pecos Texas: Field trip guide and research articles, Bureau of Economic Geology, Texas Mining and Mineral Resources Research Institute, Guidebook 23, p. 123-142.

Colby, J.W., 1968, Quantitative microprobe analysis of thin insulating films: Advances in x-ray analysis, v. 11, p. 287-305.

Crock, J.G. and Lichte, F.E., 1982, Determination of rare earth elements in geological materials by inductively coupled argon plasma/atomic emission spectrometry: Analytical Chemistry, v. 54, p. 1329-1332.

De la Roche, H., Leterrier, J., Grandclaude, P., and Marchal, M., 1980, A classification of volcanic and plutonic rocks using R_1R_2-diagram and major-element analyses --Its relationships with current nomenclature: Chemical Geology, v. 29, p. 183-210.

Deer, W.A., Howie, R.A., and Zussman, J., 1966, An introduction to the rock-forming minerals: New York, John Wiley and Sons, 528 p.

Dorais, M.J. and Floss, C., 1992, An ion and electron microprobe study of the mineralogy of enclaves and host syenites of the Red Hill complex, New Hampshire, USA: Journal of Petrology, v. 33, p. 1193-1218.

Dziedzic, A., 1984, Elk syenite intrusion: Biuletyn Instytutu Geologicznego, v. 347, p. 39-47.

Dziedzic, A., and Ryka, W., 1983, Carbonatites in the Tajno intrusion (NE Poland): Archiwum Mineralogiczne, v. 38, p. 4-34.

Hanson, G.N., 1978, The application of trace elements to the petrogenesis of igneous rocks of granitic composition: Earth and Planetary Science Letters, v. 38, p. 26-43.

Hawthorne, F., 1981, Crystal chemistry of the amphiboles: Mineralogical Society of America Reviews in Mineralogy, v. 9A, p. 1-102.

Jackson, L.L., Brown, F.W. and Neil, S.T., 1987, Major and minor elements requiring individual determination, classical whole rock analysis, and rapid rock analysis, in, Baedecker, P.A., ed., Methods for geochemical analysis: U.S. Geological Survey Bulletin 1770, p. G1-

G23.

Juskowiak, O., 1969, Syenites from the Elk complex [in Polish]: Kwartalnik Geologiczny, v. 13, p. 691-692.

Karaczun, K., Kubicki, S. and Ryka, W., 1982, Lithological map of crystalline basement surface in Polish part of East-European Platform: Warszawa, Wydawnictwa Geologiczne, Table 2.

Kramm, U., Kogarko, L.N., Kononova, V.A ., and Vartiainen, H., 1993, The Kola Alkaline Province of the CIS and Finland: Precise Rb-Sr ages define 380-360 Ma age range for the magmatism: Lithos, v. 30, p. 33-44.

Krystkiewicz, E., and Krzeminski, L., 1992, Petrology of the alkaline ultrabasic Tajno complex: Prace Panstwowego Instytutu Geologicznego, v. 139, p. 19-35.

Kubicki, S. and Ryka, W., 1982, Geologic atlas of crystalline basement in Polish part of the East-European Platform: Warsaw, Wydawnictwa Geologiczne, 24 maps, 24 p.

Leake, B.E., and Winchell, H., 1978, Nomenclature of amphiboles: American Mineralogist, v. 63, p. 1023-1052.

Lichte, F.E., Golighty, D.W. and Lamothe, P.J., 1987, Inductively coupled plasma-atomic emission spectrometry, in, Baedecker, P.A., ed., Methods for geochemical analysis: U.S. Geological Survey Bulletin 1770, p. B1-B10.

Lichte, F.E., Meier, A.L., and Crock, J.G., 1987, Determination of the rare earth elements in geological materials by inductively coupled plasma mass spectrometry: Analytical Chemistry, April 15, 1987, p. 1150-1157.

Marshall, D.J., 1988, Cathodoluminescence of Geological Materials: Boston, Unwin Hyman, 146 p.

McKown, D.M. and Millard, H.T., Jr., 1987, Determination of uranium and thorium by delayed neutron counting, in, Baedecker, P.A., ed., Methods for geochemical analysis: U.S. Geological Survey Bulletin 1770, p. I1-I12.

Miyashiro, A., 1978, Nature of alkalic volcanic rock series: Contributions to Mineralogy and Petrology, v. 66, p. 91-104.

Morimoto, N., Fabries, J., Ferguson, A.K., Ginzburg, I.V., Ross, M., Seifert, F.A., Zussman, J., Aoki, K., and Gottardi, G., 1988, Nomenclature of pyroxenes: American Mineralogist, v. 73, p. 1123-1133.

Nakamura, N., 1974, Determination of REE, Ba, Fe, Mg, Na, and K in carbonaceous and ordinary chondrites: Geochimica et Cosmochimica Acta, v. 38, p. 757-775.

Richard, L.R., and Clarke, D.B., 1990, AMPHIBOL: a program for calculating structural formulae and for classifying and plotting chemical analyses of amphiboles: American Mineralogist, v. 75, p. 421-423.

Ryka, W., 1984a, Deep structure of the crystalline basement of the Precambrian Platform in Poland: Publication of the Institute of Geophysics of the Polish Academy of Science, v. A-13 (160), p. 47-61.

_____ 1984b, Precambrian evolution of the East-European Platform in Poland: Biuletyn Instytutu Geologicznego, v. 347, p. 17-28.

_____ 1985, The evolving of old Precambrian structures in the marginal zone of the East-European Platform: Publication of the Institute of Geophysics of the Polish Academy of Science, v. A-16 (175), p. 29-42.

_____ 1992, Geology of the Tajno massif carbonatites: Prace Panstwowego Instytutu Geologicznego, v. CXXXIX, p. 43-77.

Ryka, W., Armbrustmacher, T.J., and Modreski, P.J., 1992, Geochemistry and petrology of the alkaline rocks of the Tajno complex

(Preliminary report): Prace Panstwowego Instytutu Geologicznego, v. CXXXIX, p. 37-41.

Saggerson, E.P. and Williams, L.A.J., 1964, Ngurumanite from southern Kenya and its bearing on the origin of rocks in the northern Tanganyika alkaline district: Journal of Petrology, v. 5, p. 40-81.

Sorensen, H., 1974, Glossary of alkaline and related rocks, in, Sorensen, H., ed., The alkaline rocks: London, John Wiley and Sons, p. 558-577.

Taggart, J.E., Jr., Lindsay, J.R., Scott, B.A., Vivit, D. ., Bartel, A.J. and Stewart, K.C., 1987, Analysis of geologic materials by wavelength-dispersive X-ray fluorescence spectrometry, in, Baedecker, P.A., ed., Methods for geochemical analysis: U.S. Geological Survey Bulletin 1770, p. E1-E19.

Thompson, R.N., Dickin, A P., Gibson, I.L., and Morrison, M.A., 1982, Elemental fingerprints of isotopic contamination of Hebridean Paleocene mantle-derived magmas by Archaean Sial: Contributions to Mineralogy and Petrology, v. 79, p. 159-168.

Thornton, C. P. and Tuttle, O. F., 1960, Chemistry of igneous rocks. I. Differentiation index: American Journal of Science, v. 258, p. 664-684.

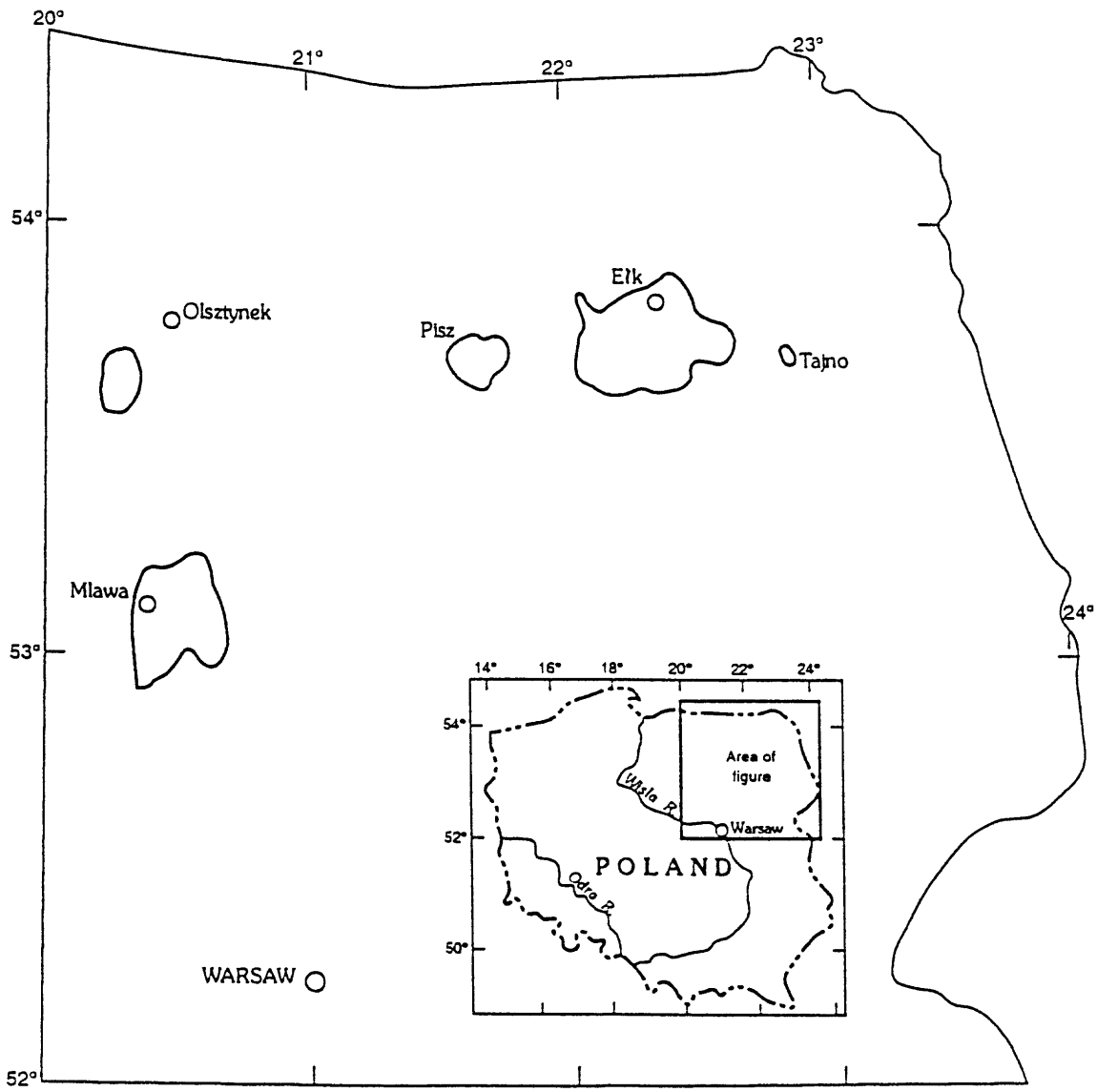

Figure 1. Map of northeastern Poland showing the location of the alkaline massifs. Modified from Table 2b of Kubicki and Ryka (1982).

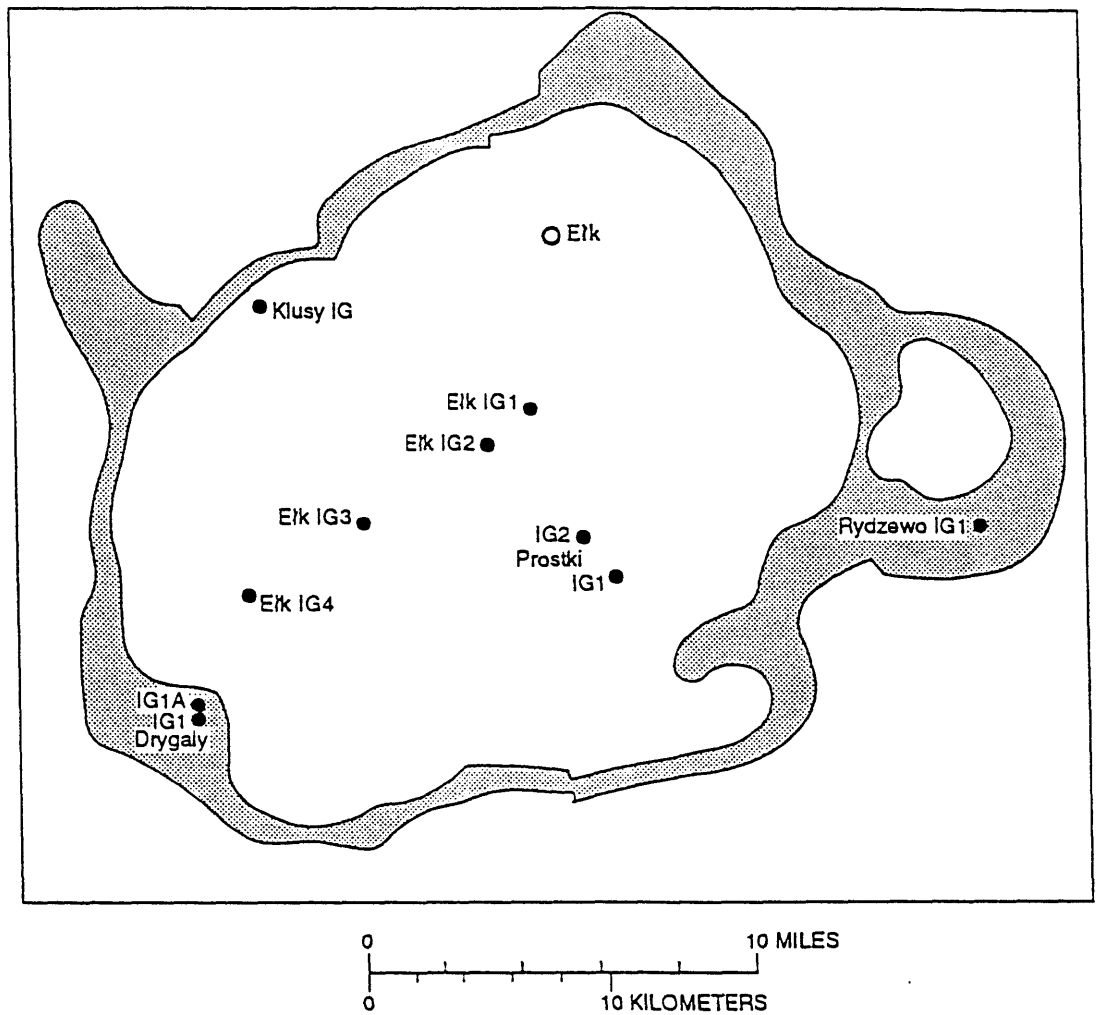

Figure 2. Map of the Elk massif showing the location of bore holes. The shaded area is shown by Kubicki and Ryka (1982) to be metasomatized granitoids at the contact with syenites of the massif. Modified from Table 5 of Kubicki and Ryka (1982).

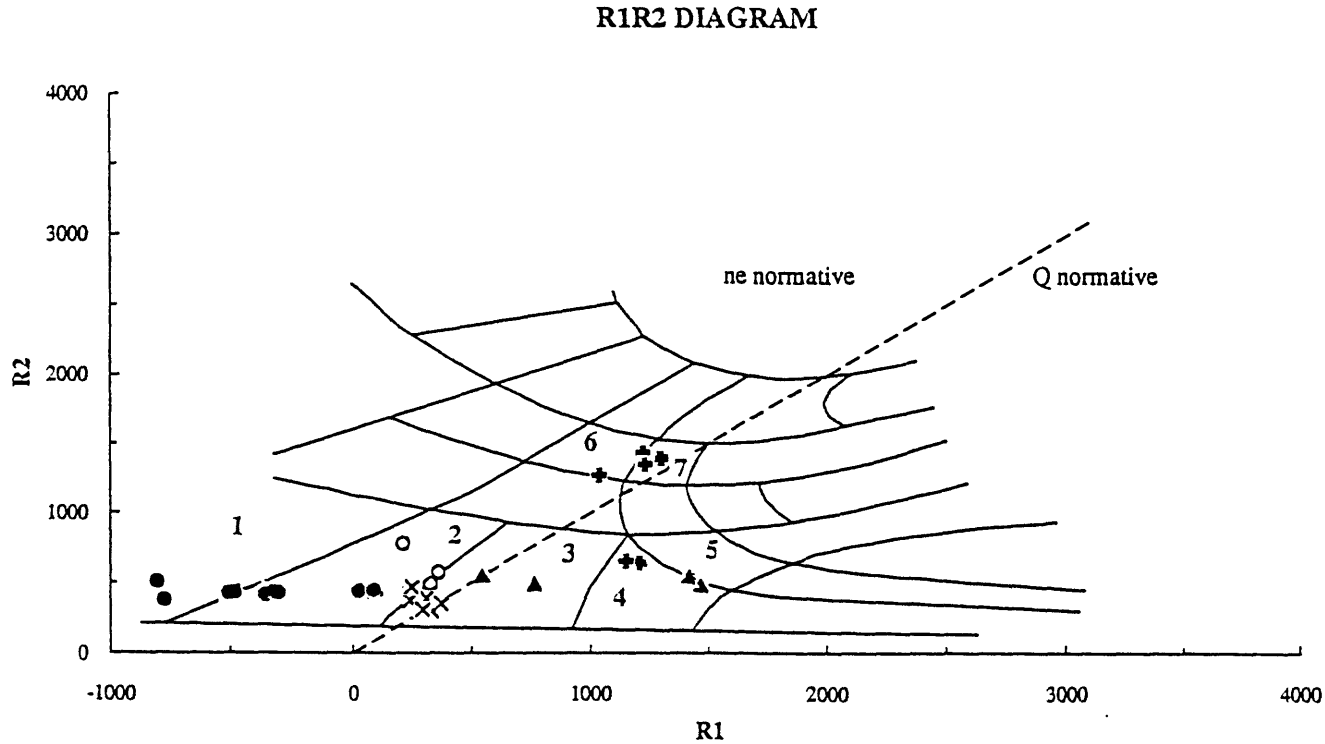

Figure 3. Plot of rock compositions using the illustration of De la Roche and others(1980). Solid circles are nepheline syenite, open circles are foid-less syenite, X's are amphibole syenite, filled triangles are quartz syenite, and crosses are monzogabbro. Field 1 is nepheline syenite, field 2 is also nepheline syenite, field 3 is syenite, field 4 is quartz syenite, field 5 is quartz monzonite, field 6 is syenogabbro and field 7 is monzogabbro.

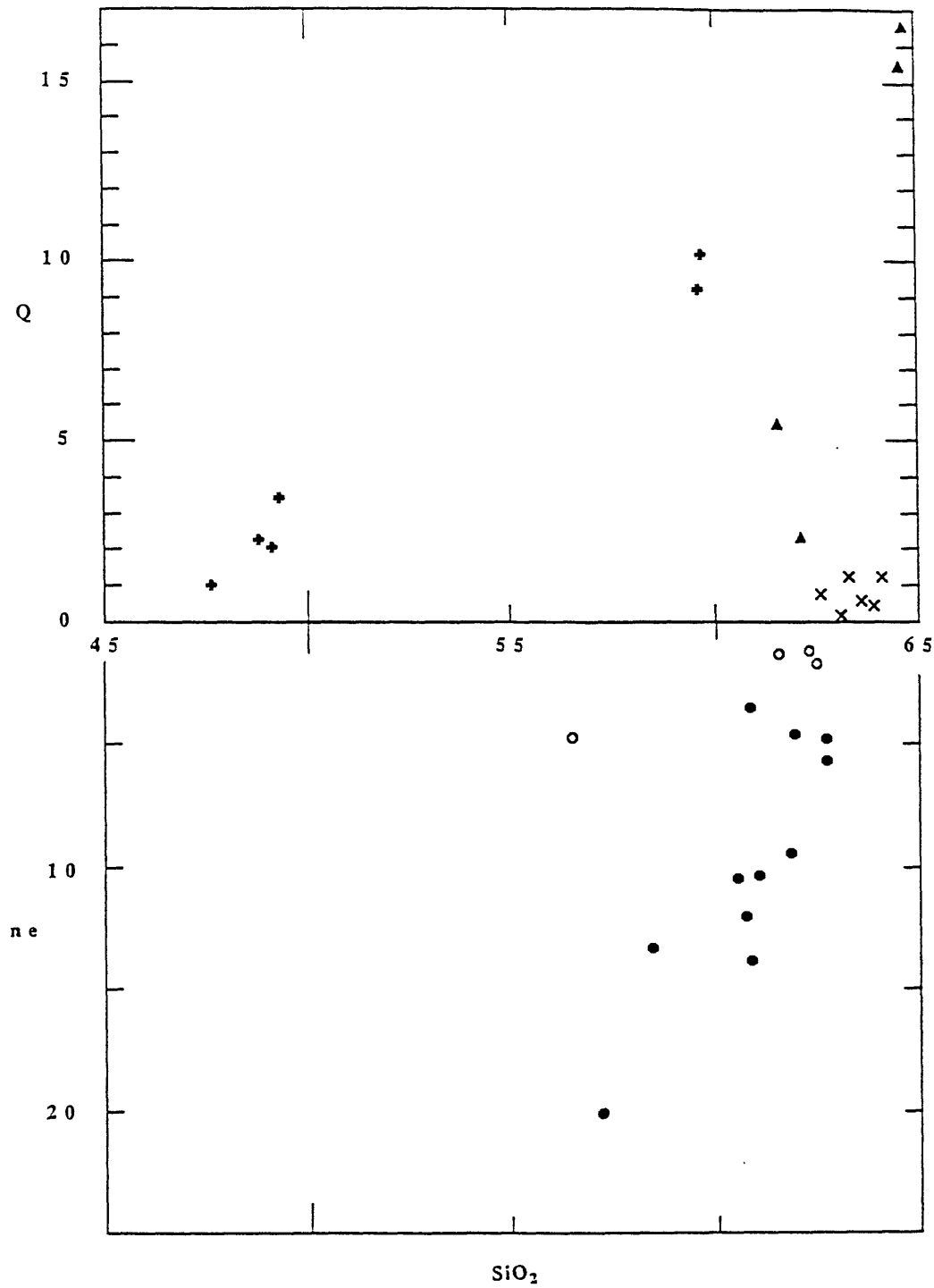

Figure 4. Plots of normative nepheline or quartz versus silica. Solid circles are nepheline syenite, open circles are foid- less syenite, X's are amphibole syenite, filled triangles are quartz syenite, and crosses are monzogabbro.

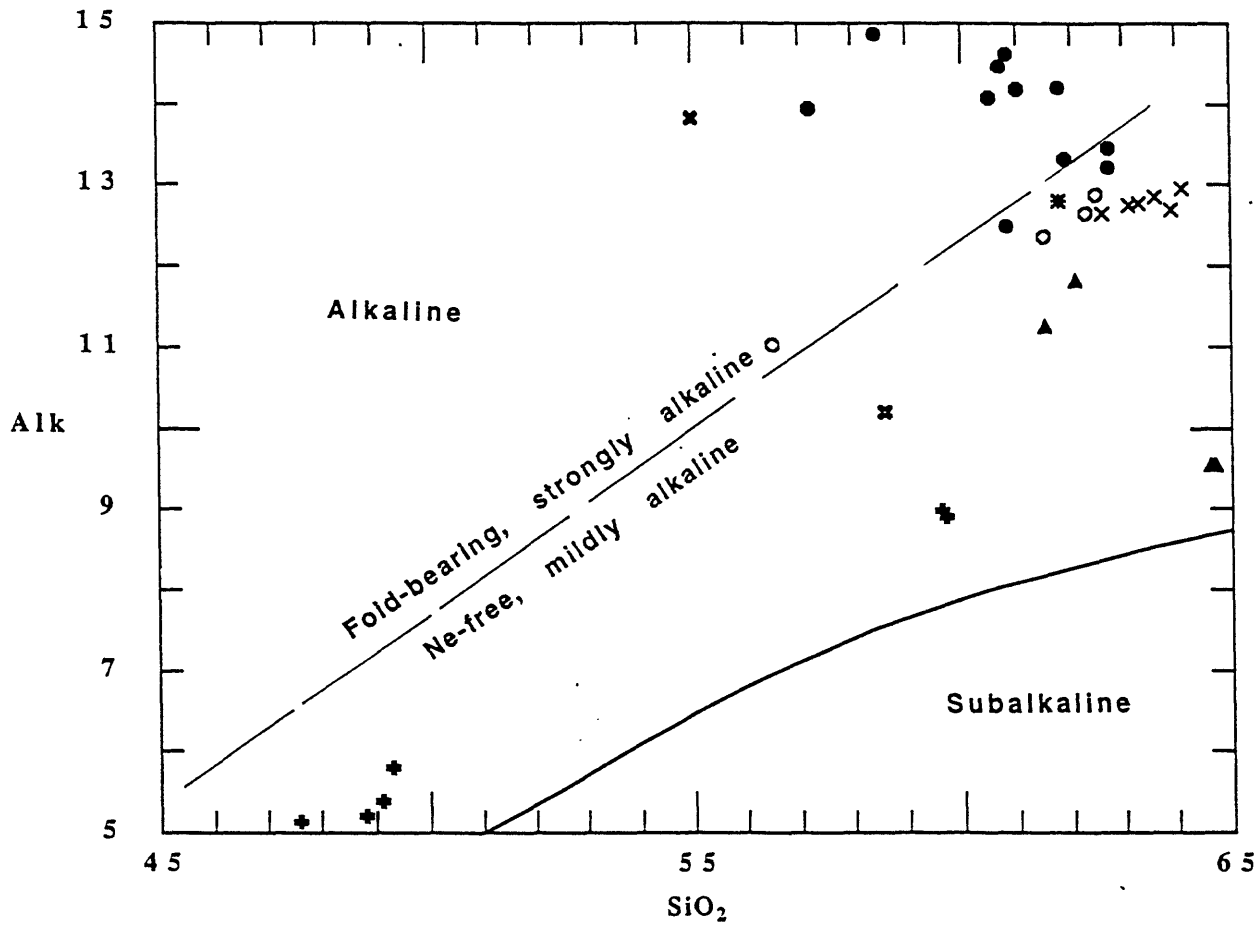

Figure 5. Plots of alkalies versus silica. Curved line after Miyashiro (1978); straight line after Saggerson and Williams (1964). Solid circles are nepheline syenite, open circles are foid-less syenite, X's are amphibole syenite, filled triangles are quartz syenite, and crosses are monzogabbro.

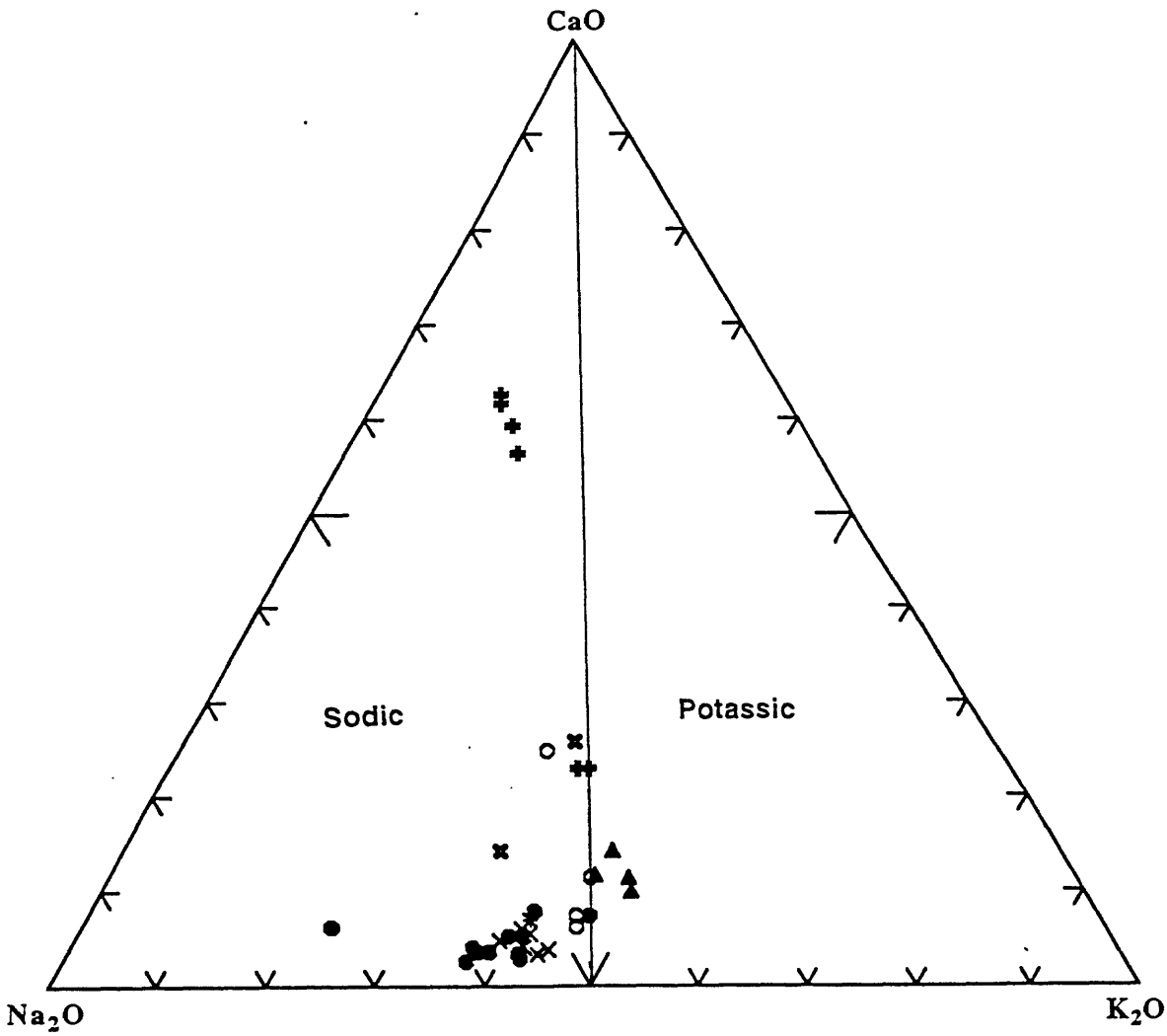

Figure 6. Plots of CaO-Na_2O-K_2O. Solid circles are nepheline syenite, open circles are foid-less syenite, X's are amphibole syenite, filled triangles are quartz syenite, and crosses are monzogabbro.

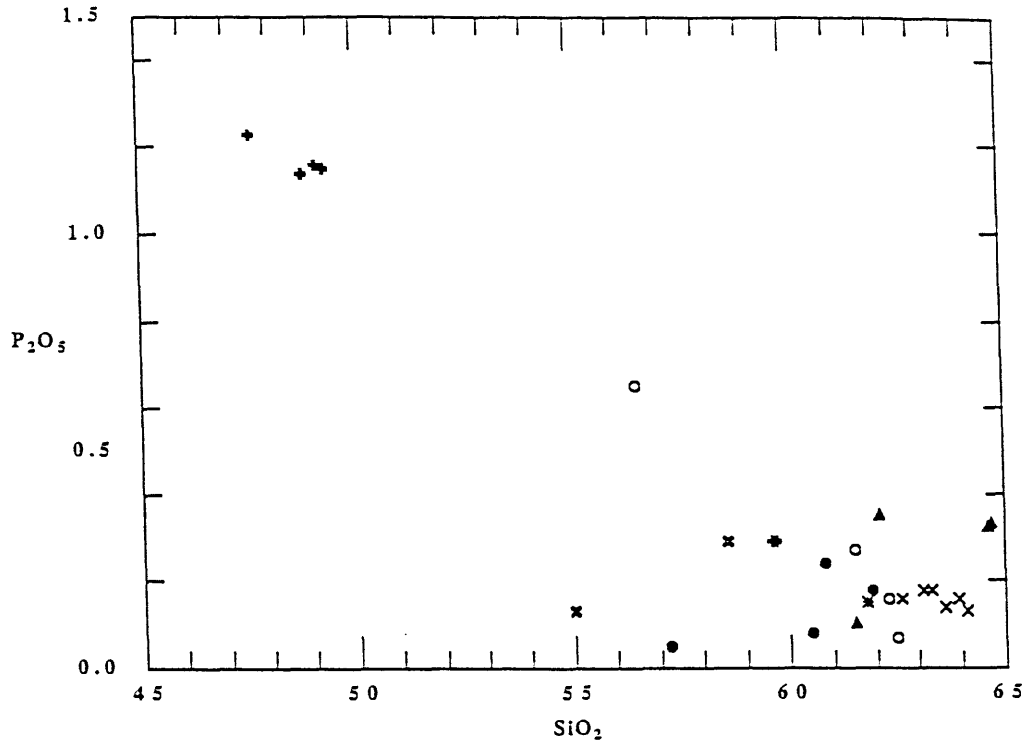

Figure 7. Harker diagram plotting major oxides versus silica. Solid circles are nepheline syenite, open circles are foid-less syenite, X's are amphibole syenite, filled triangles are quartz syenite, and crosses are monzogabbro.

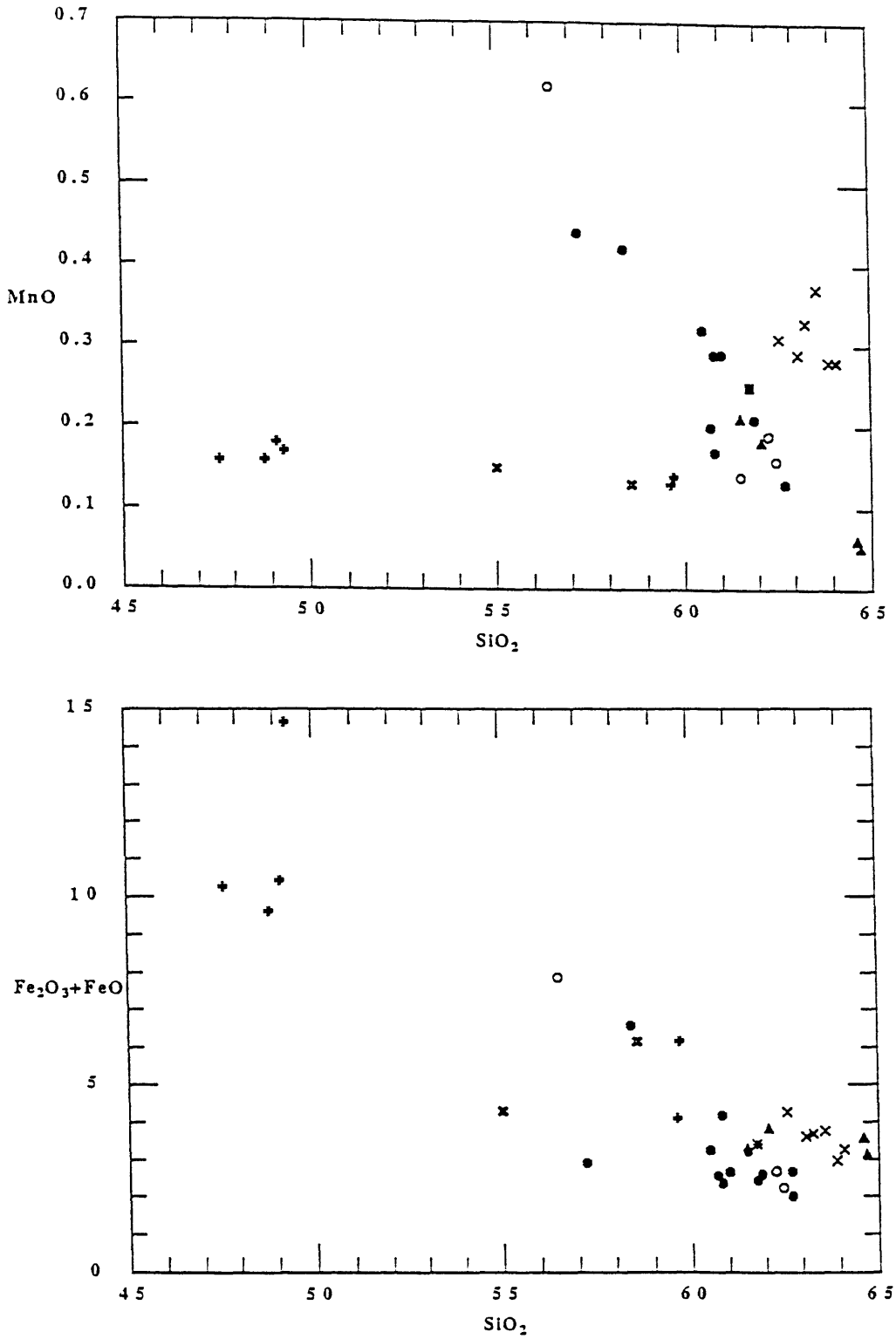

Figure 7. continued

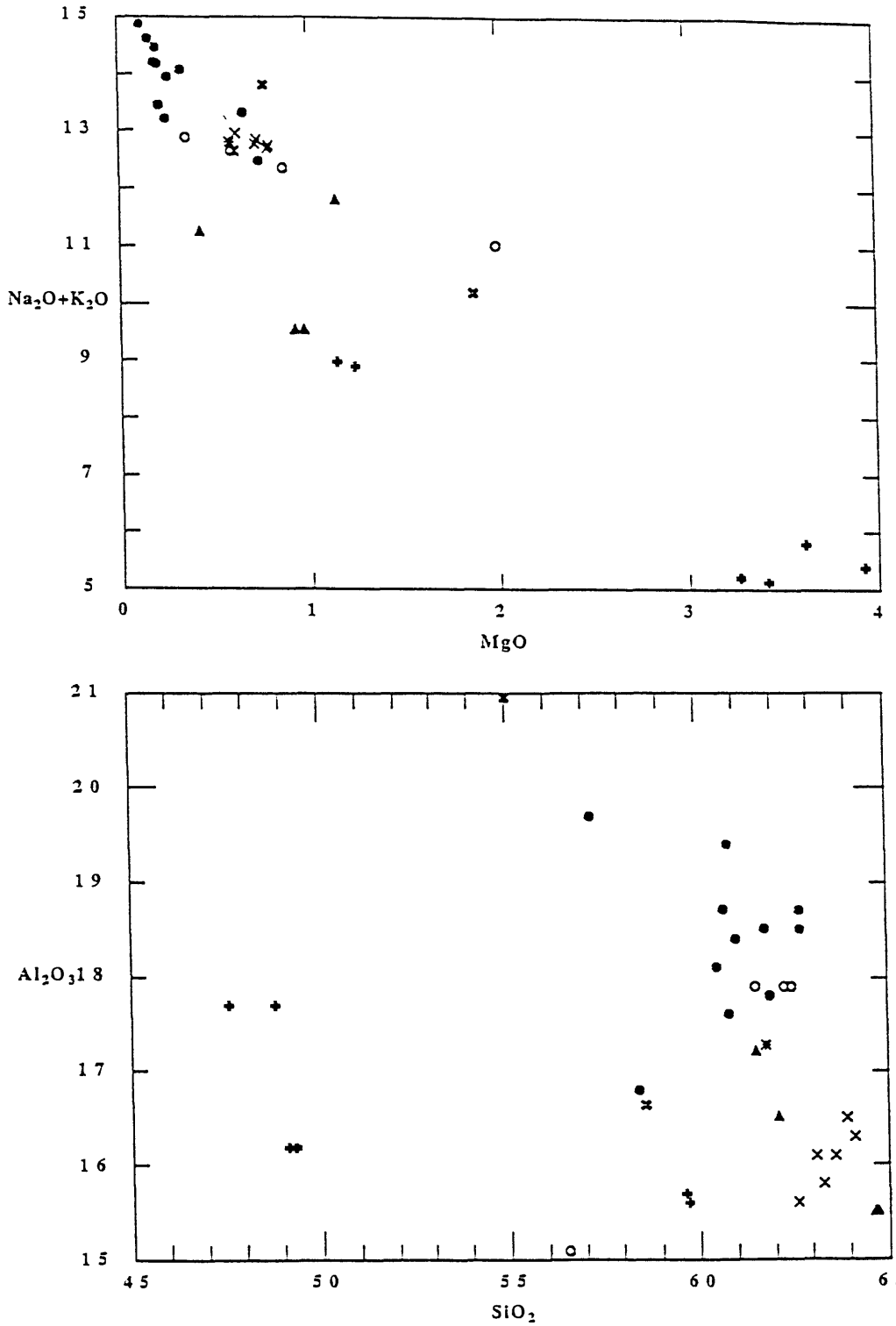

Figure 7. continued

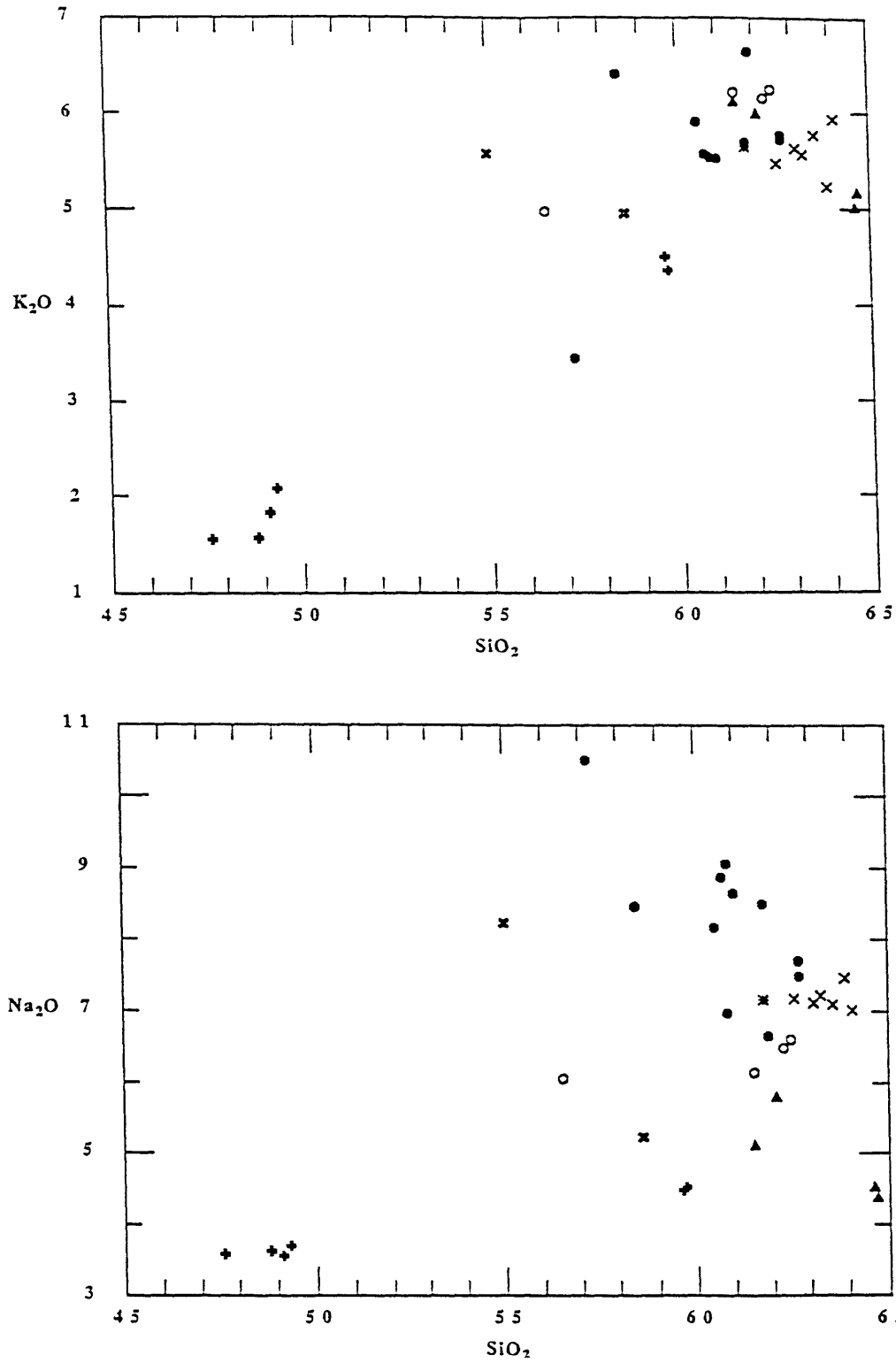

Figure 7. continued

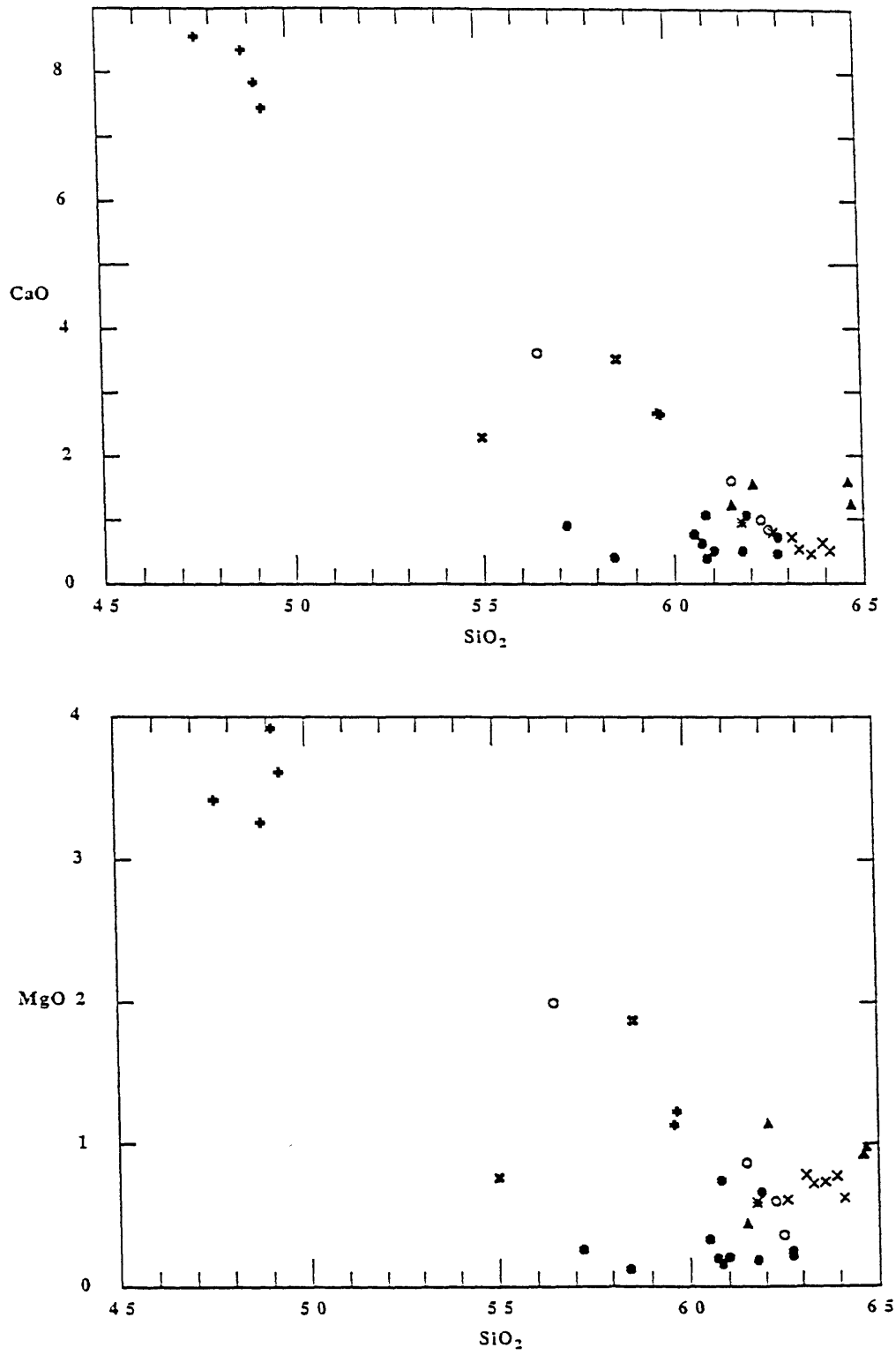

Figure 7. continued

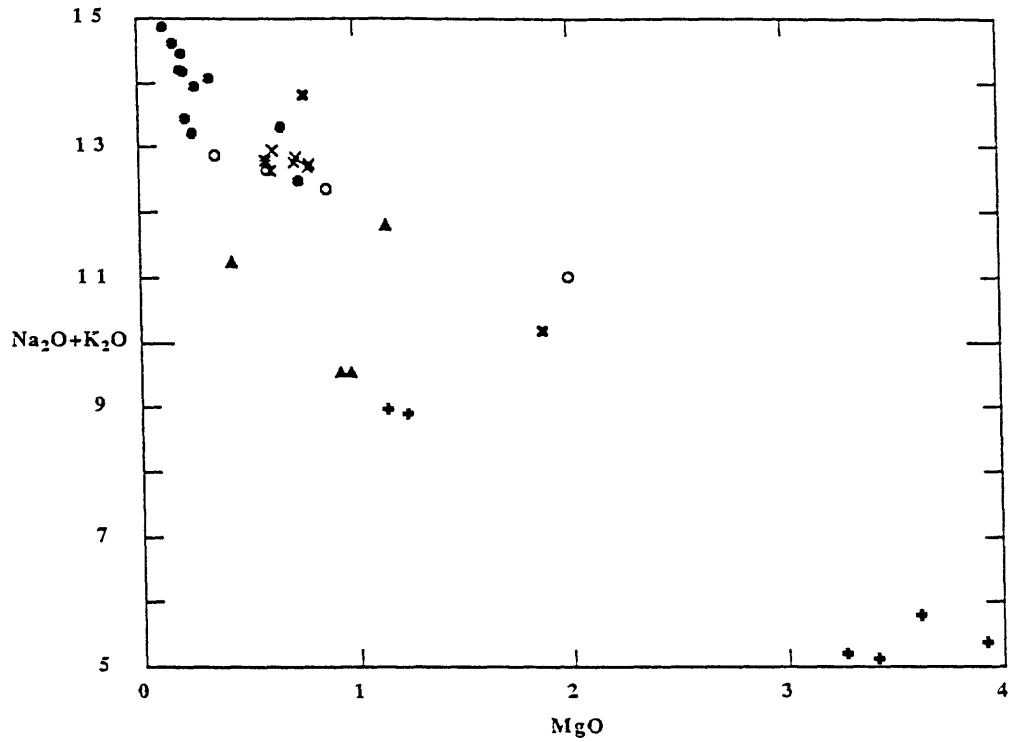

Figure 8. Plots of major oxides versus MgO. Solid circles are foid-bearing syenite, open circles are foid-less syenite, X's are amphibole syenite, filled triangles are quartz syenite, and crosses are monzogabbro.

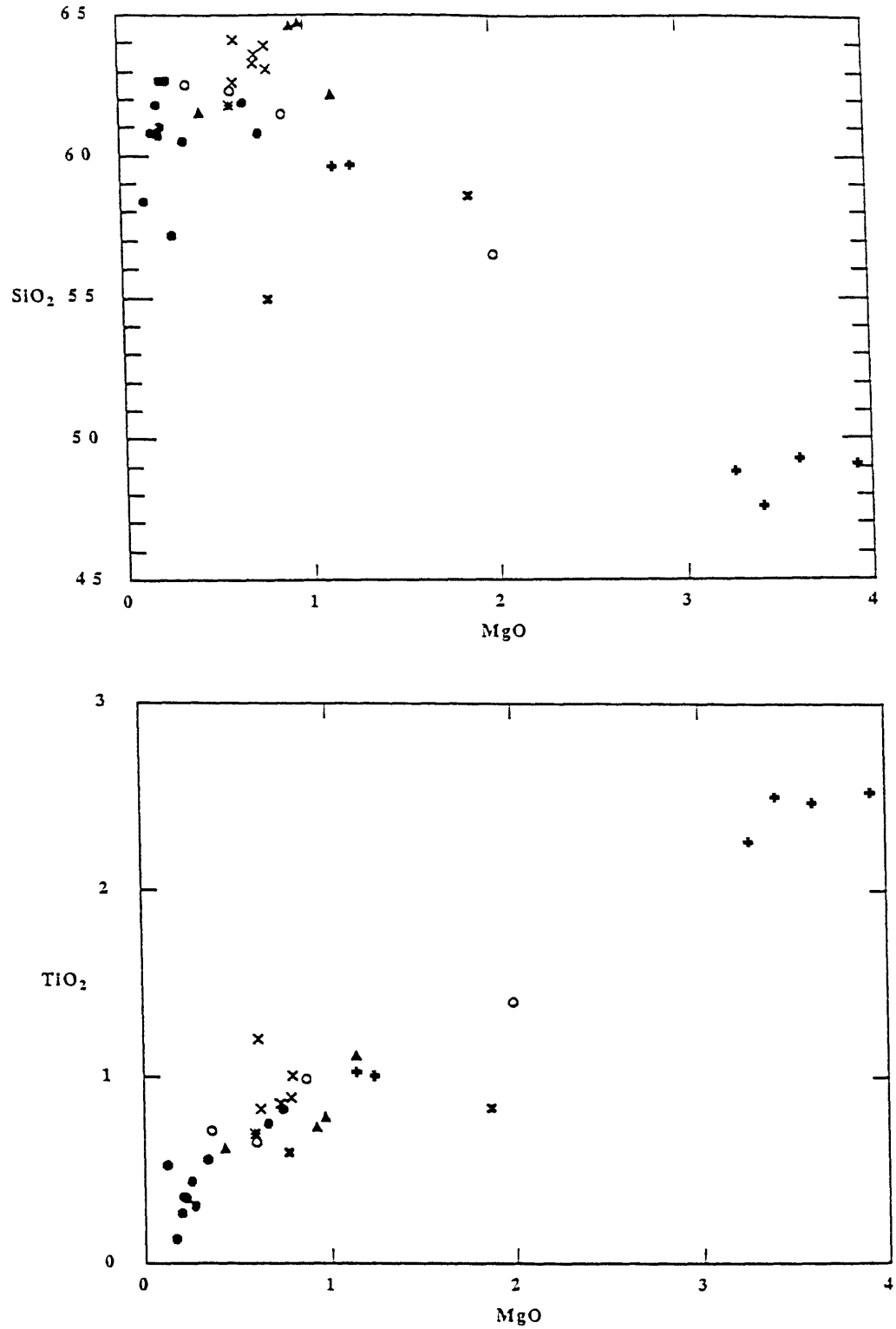

Figure 8. continued

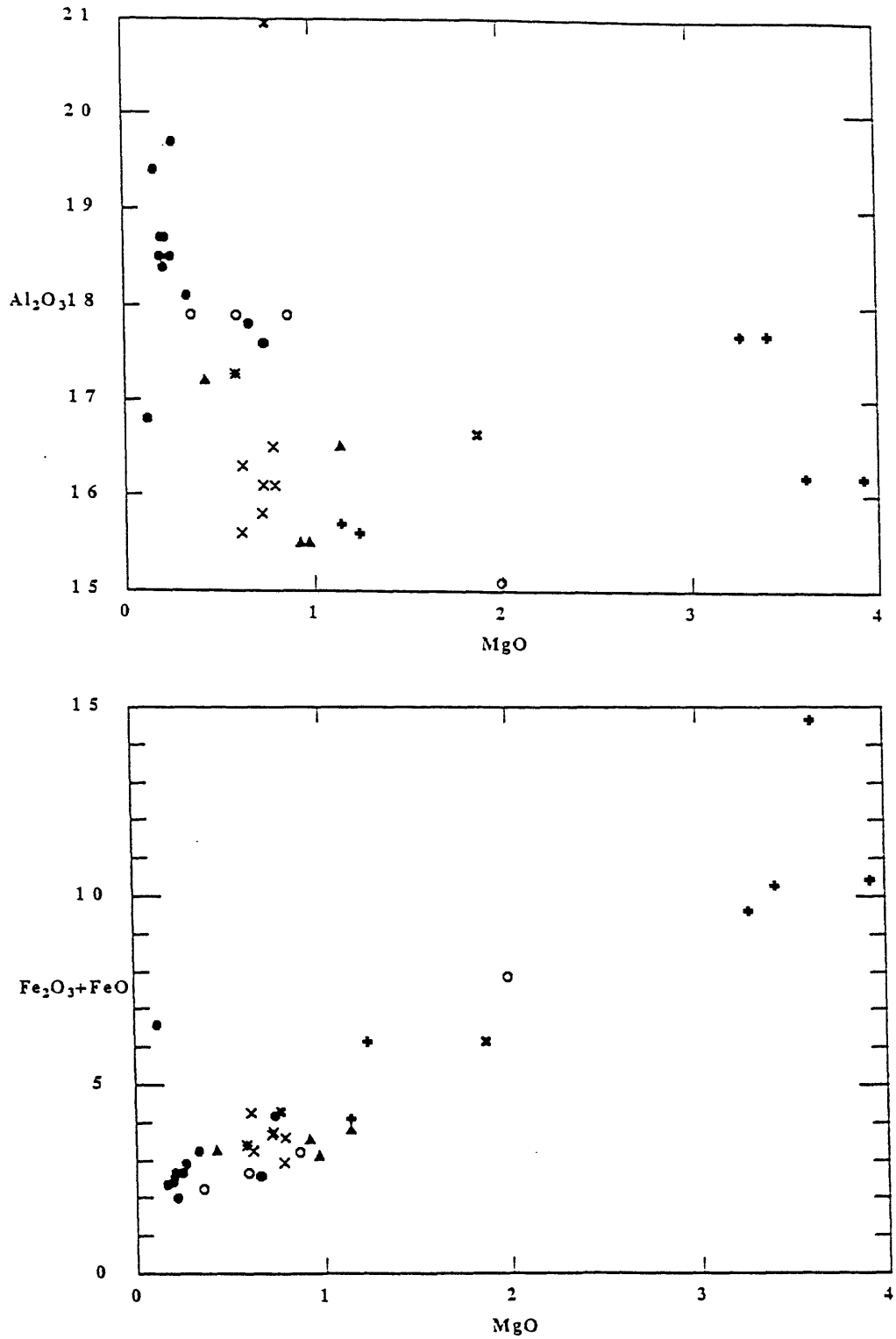

Figure 8. continued

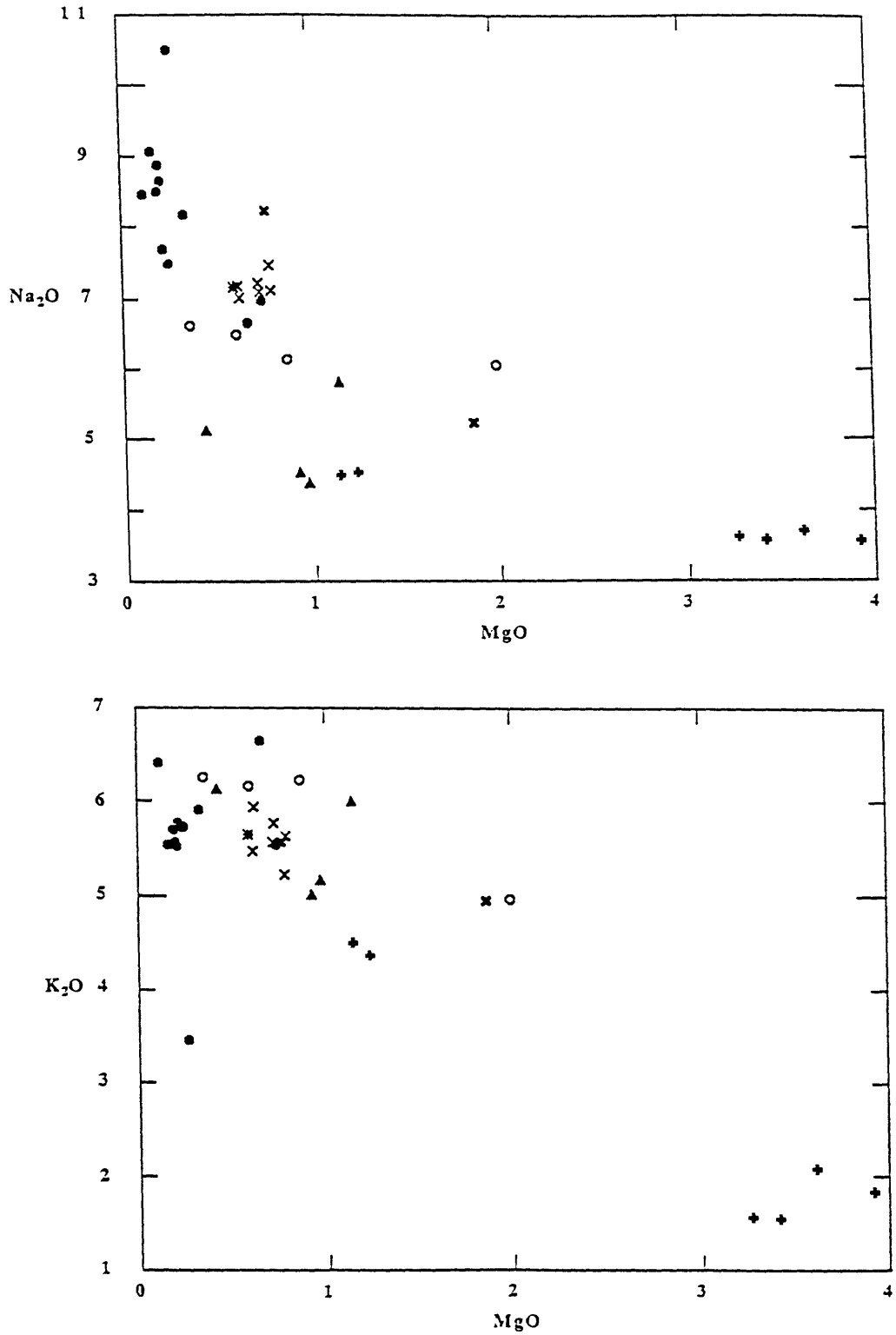

Figure 8. continued

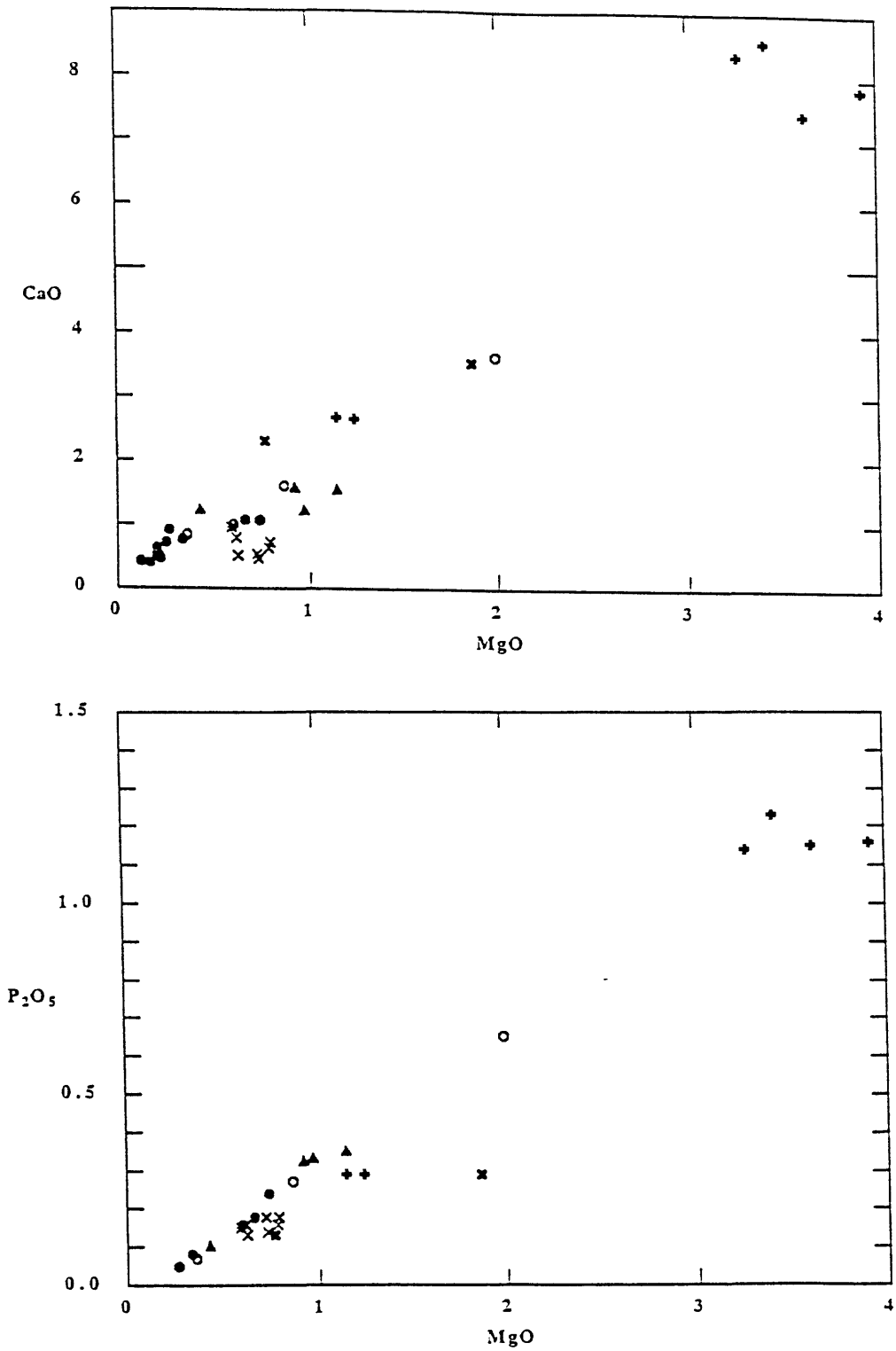

Figure 8. continued

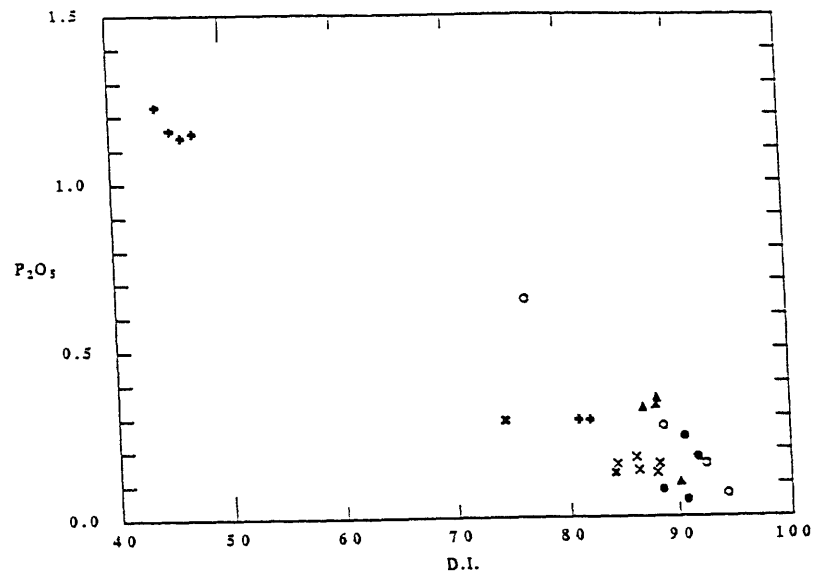

Figure 9. Plots of differentiation indexes (D.I.) versus major oxides. Solid circles are nepheline syenite, open circles are foid-less syenite, X's are amphibole syenite, filled triangles are quartz syenite, and crosses are monzogabbro.

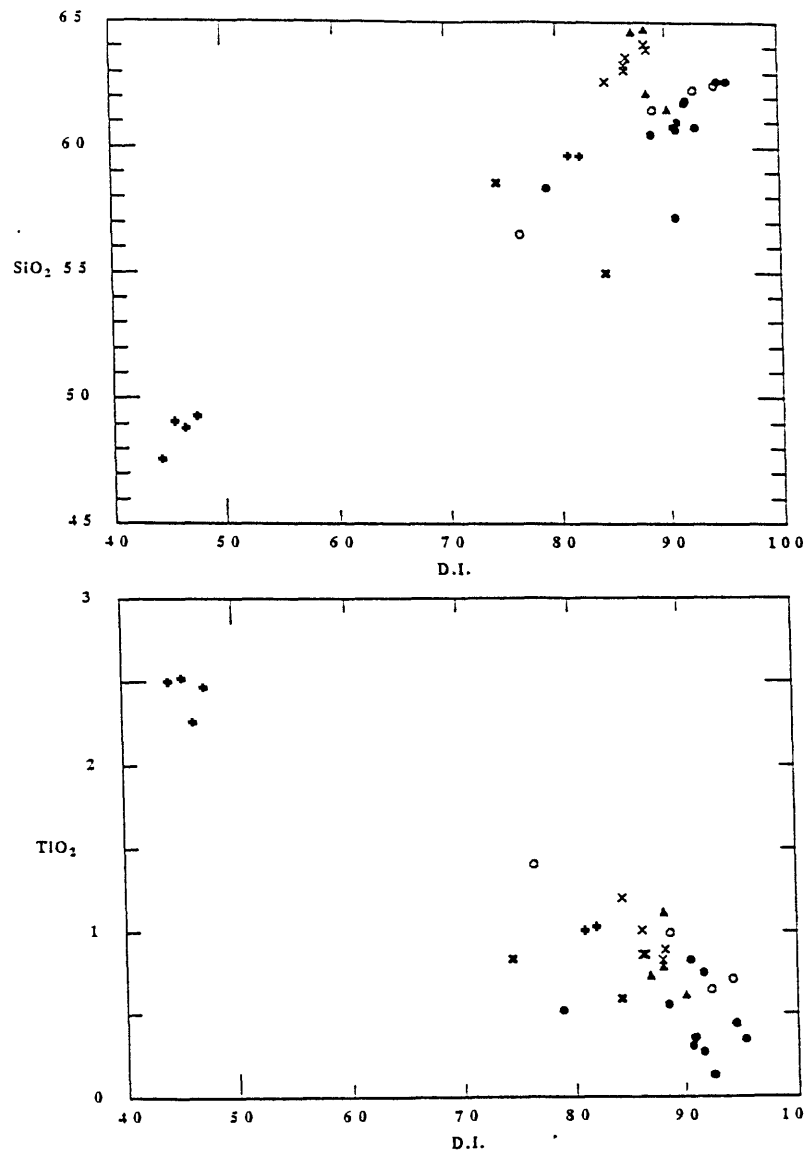

Figure 9. continued

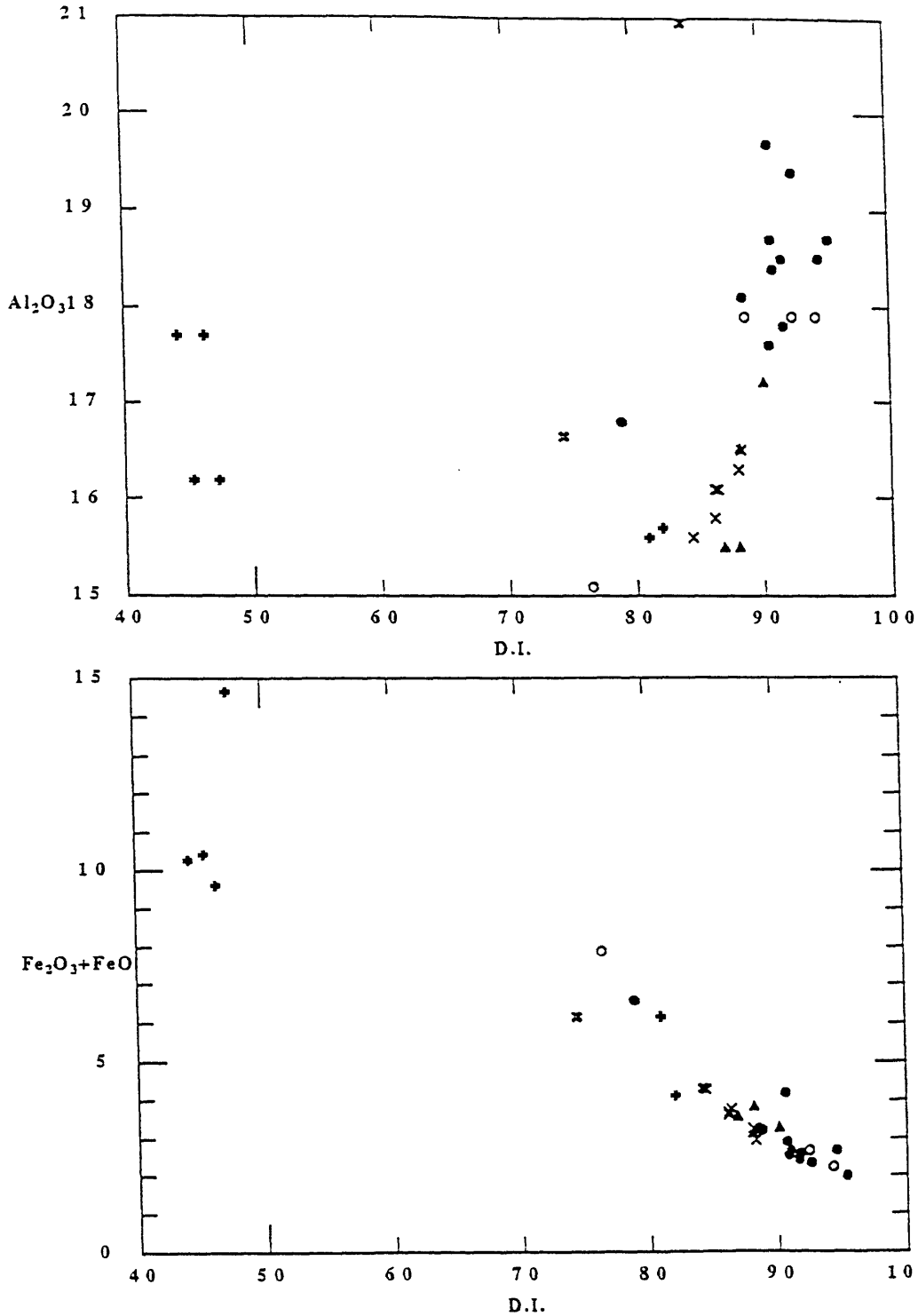

Figure 9. continued

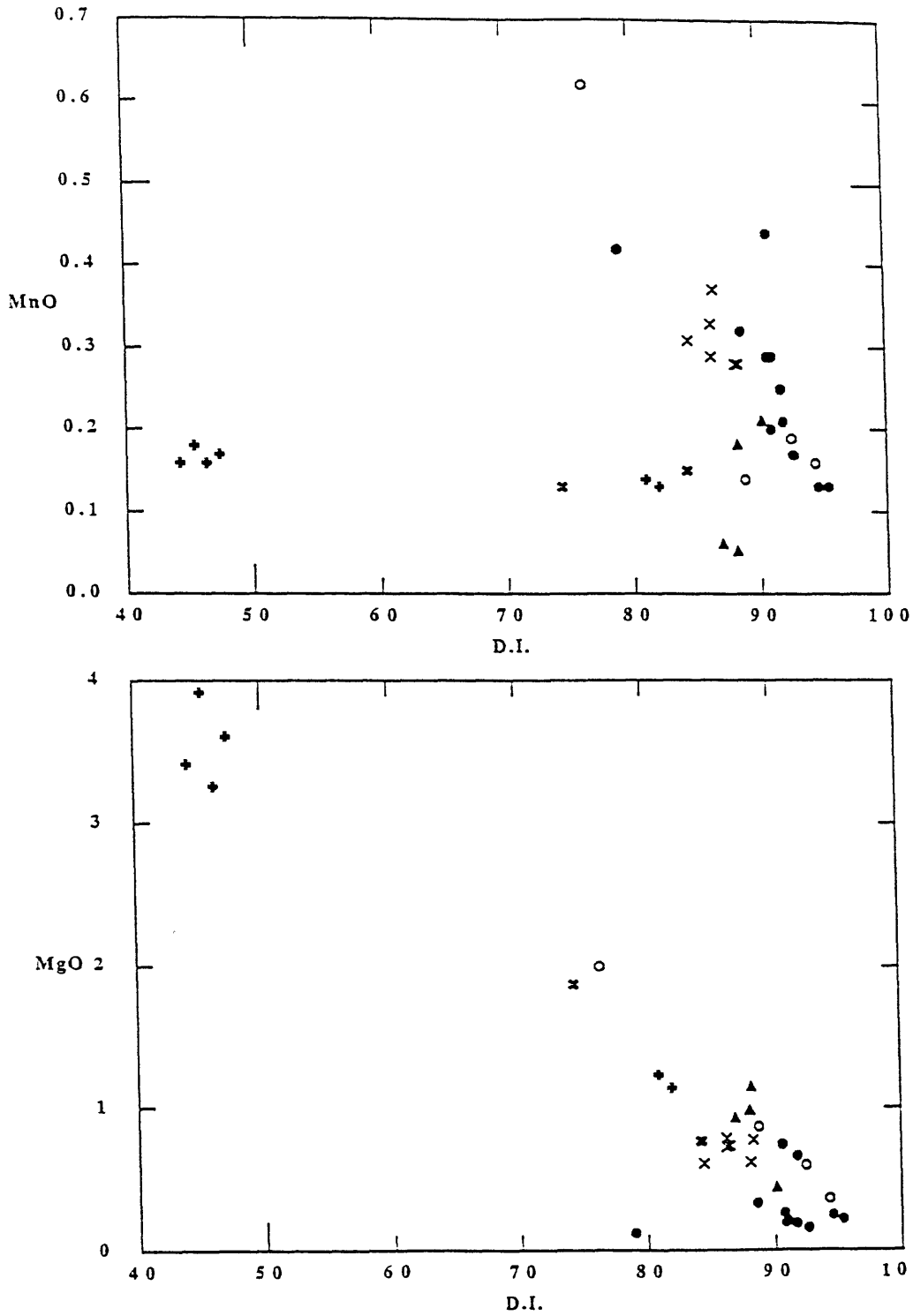

Figure 9. continued

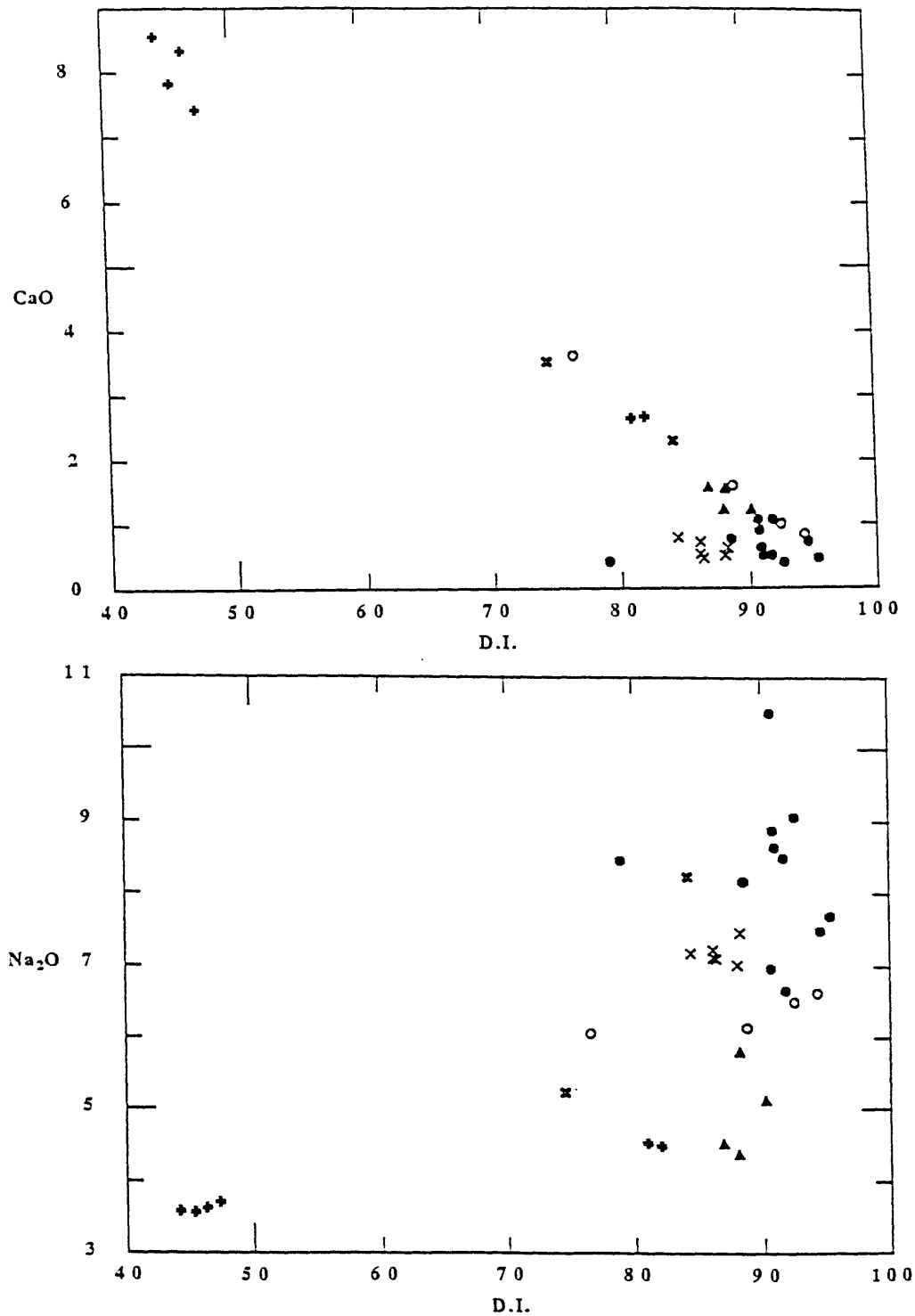

Figure 9. continued

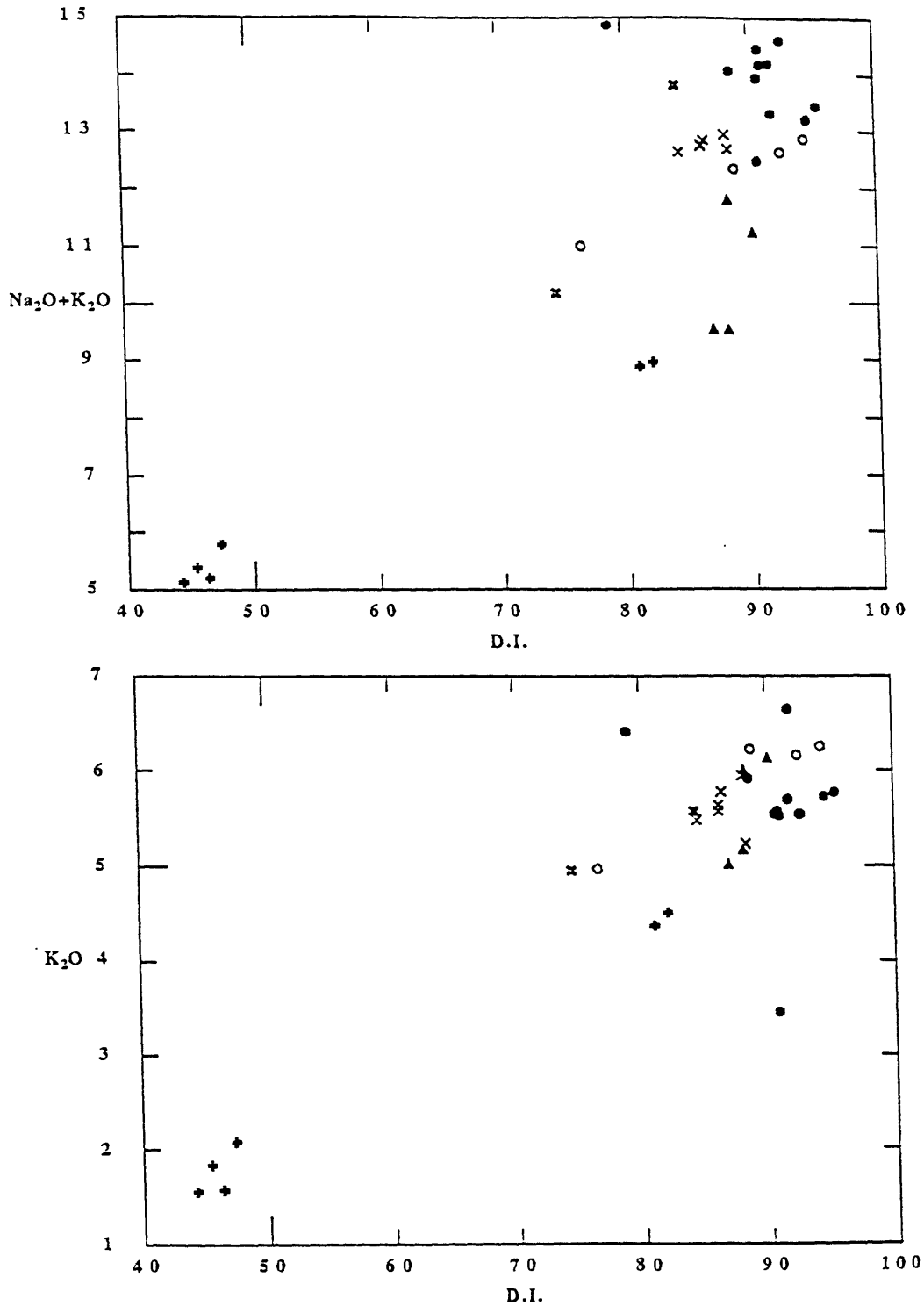

Figure 9. continued

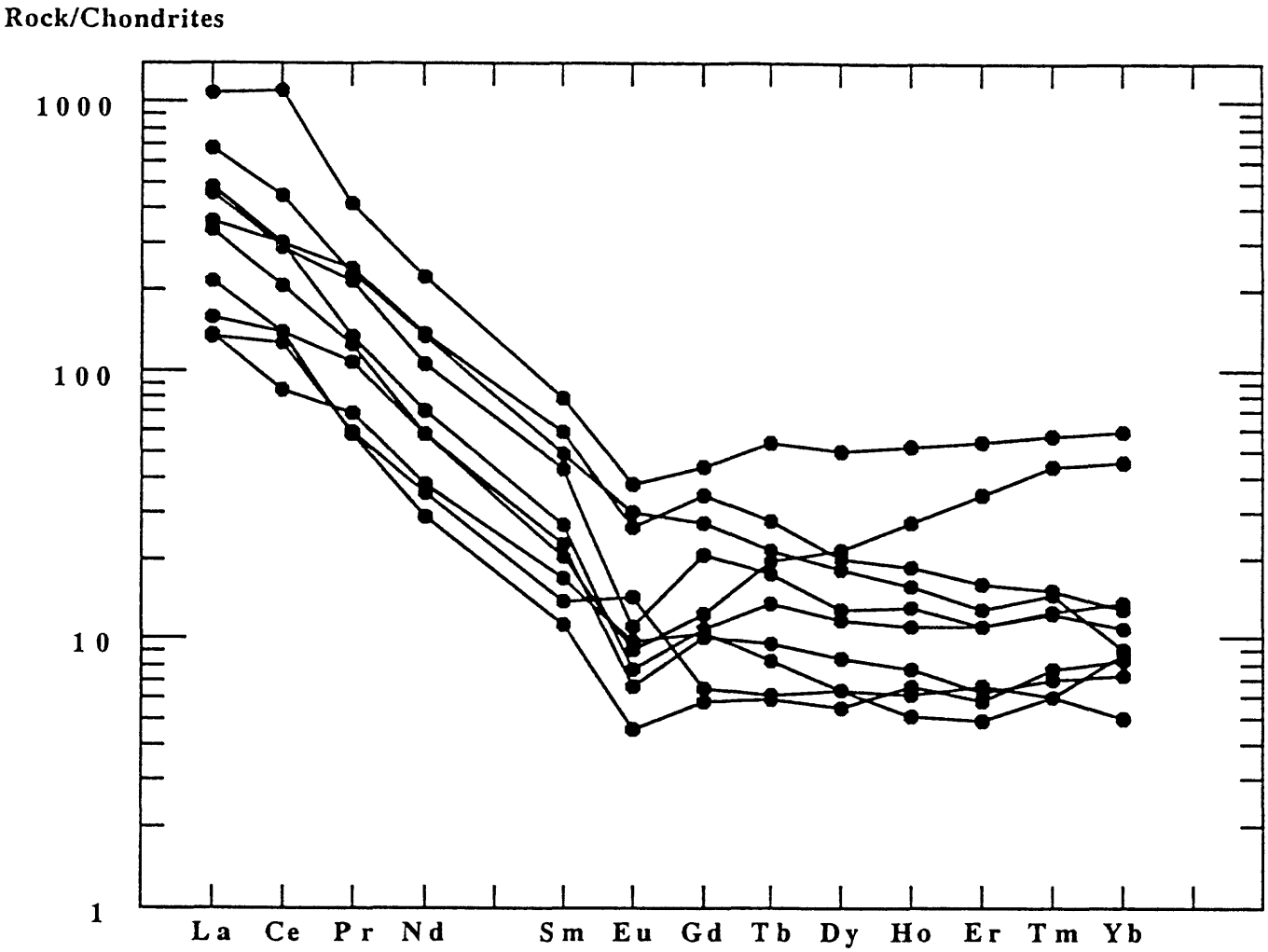

Figure 10. Chondrite-normalized rare-earth element (REE) diagrams. Solid circles are nepheline syenite, open circles are foid-less syenite, X's are amphibole syenite, filled triangles are quartz syenite, and crosses are monzogabbro. Normalizing values taken from Nakamura (1974).

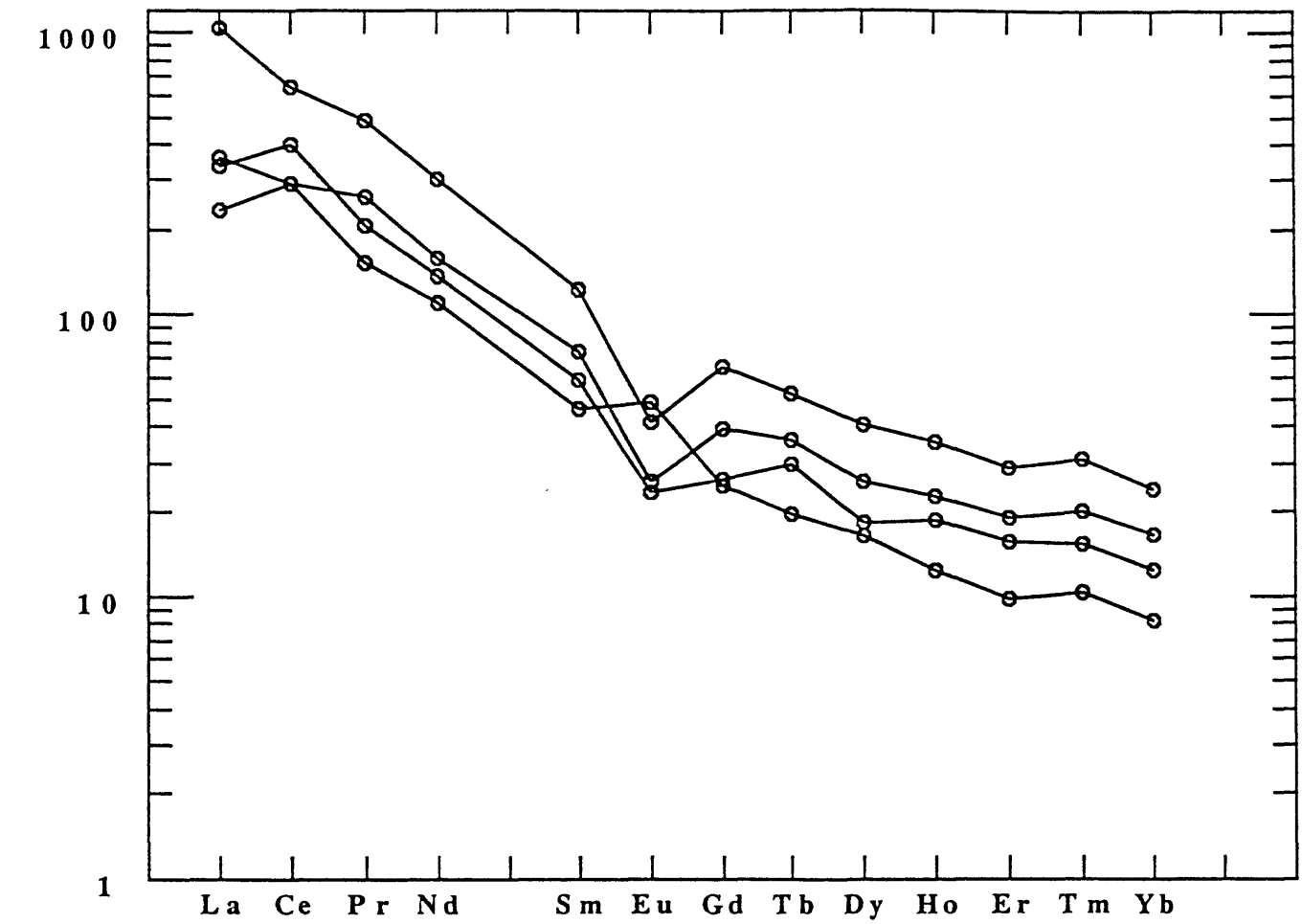

Figure 10. continued

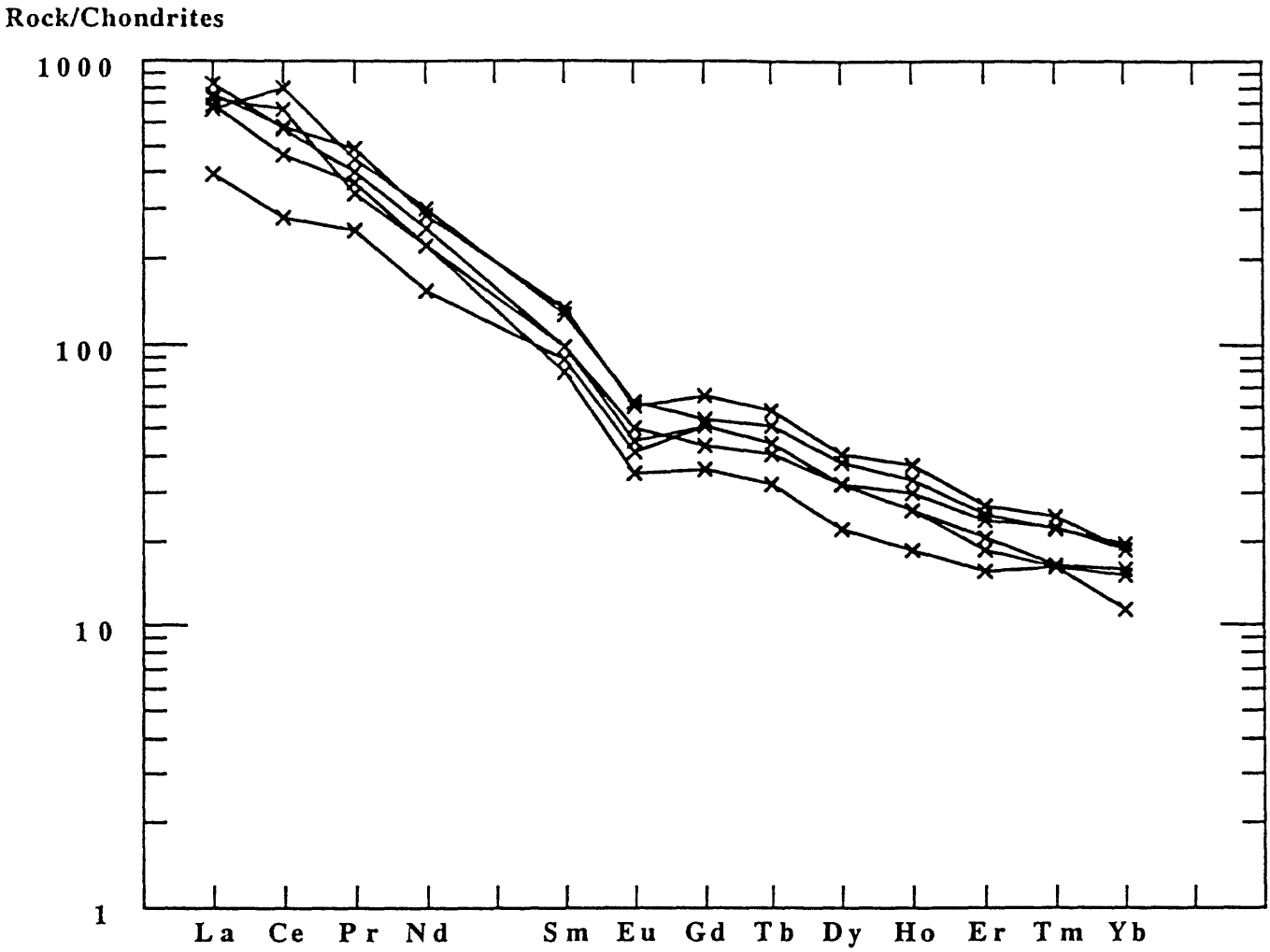

Figure 10. continued

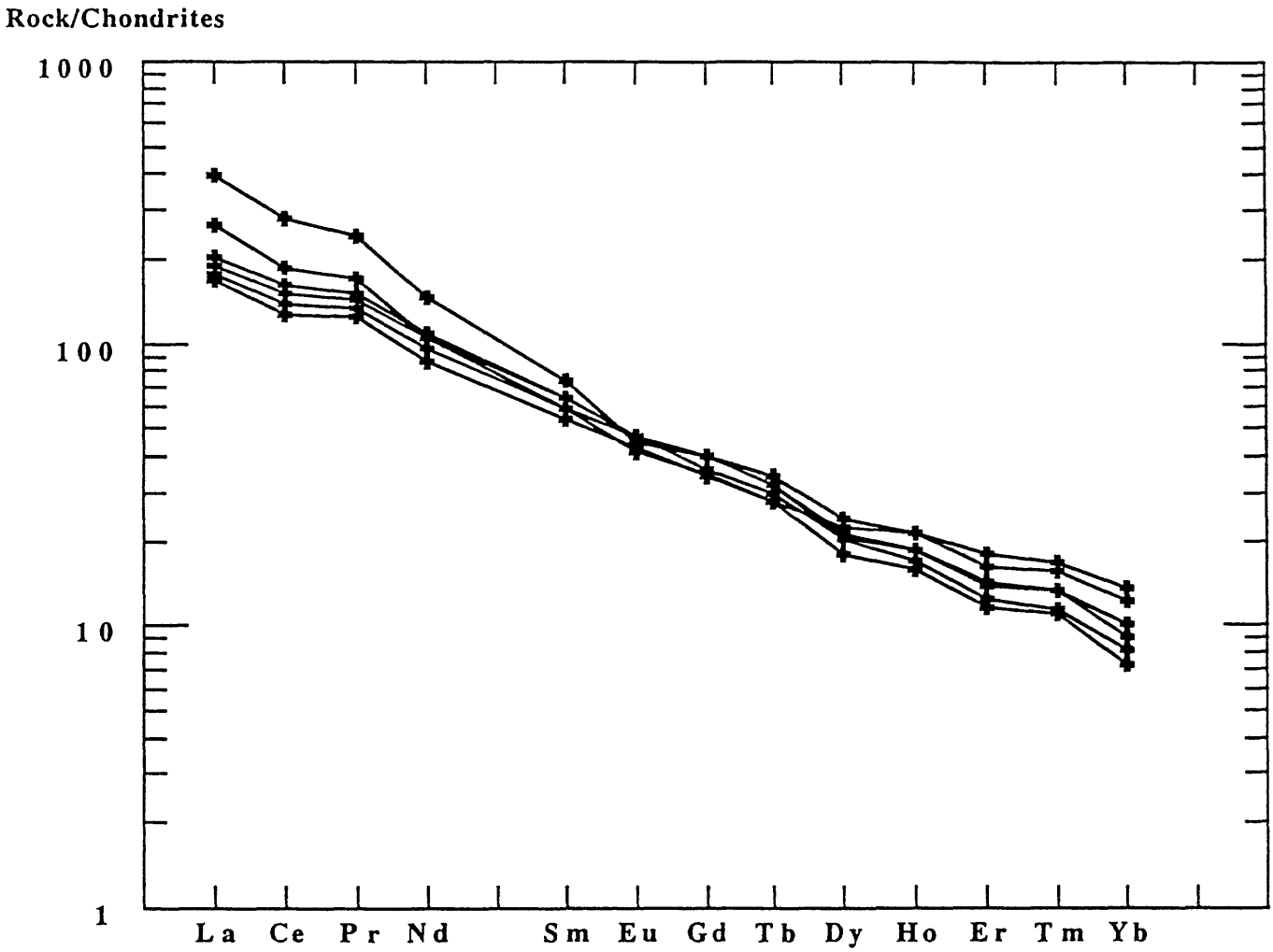

Figure 10. continued

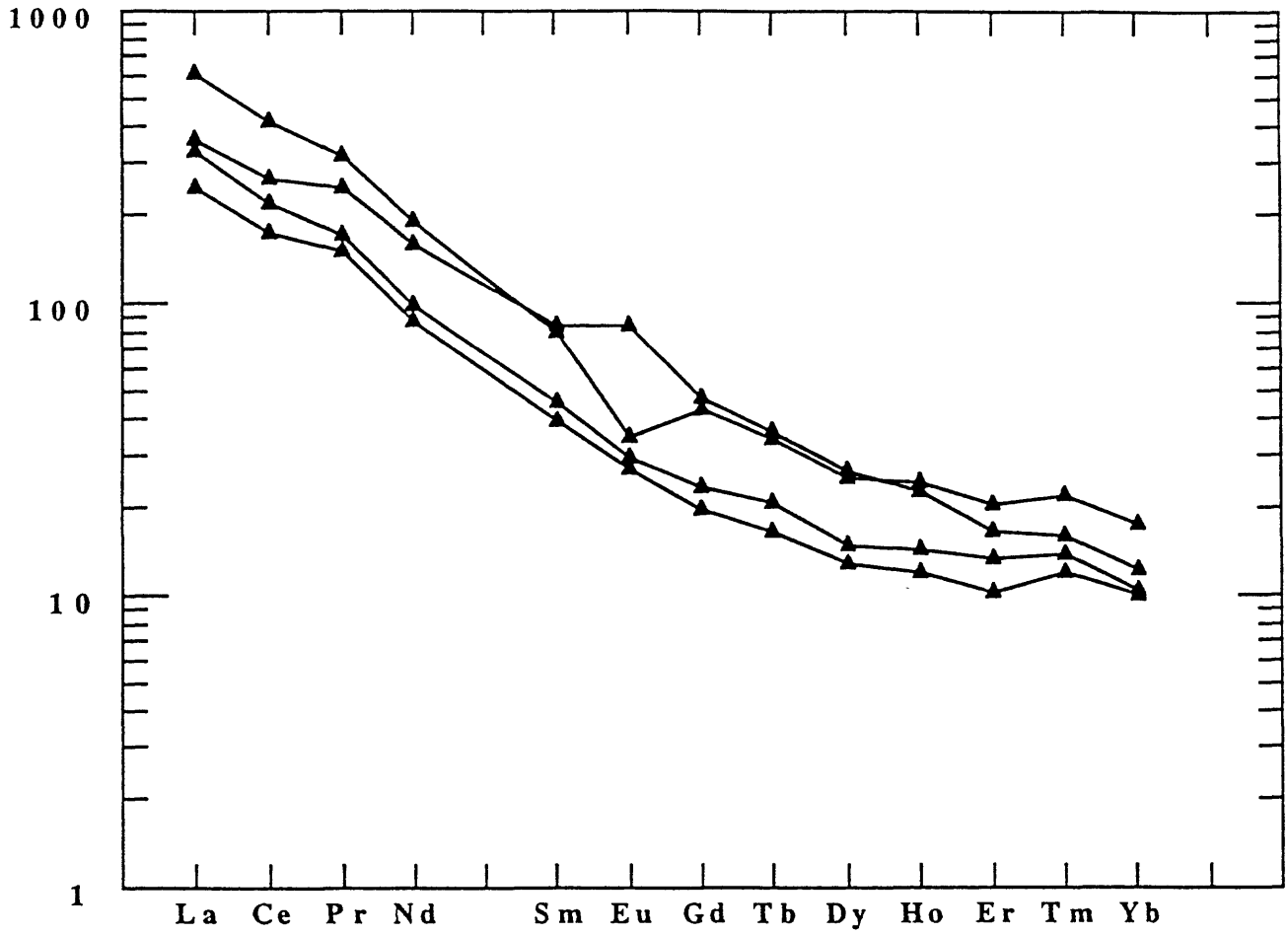

Figure 10. continued

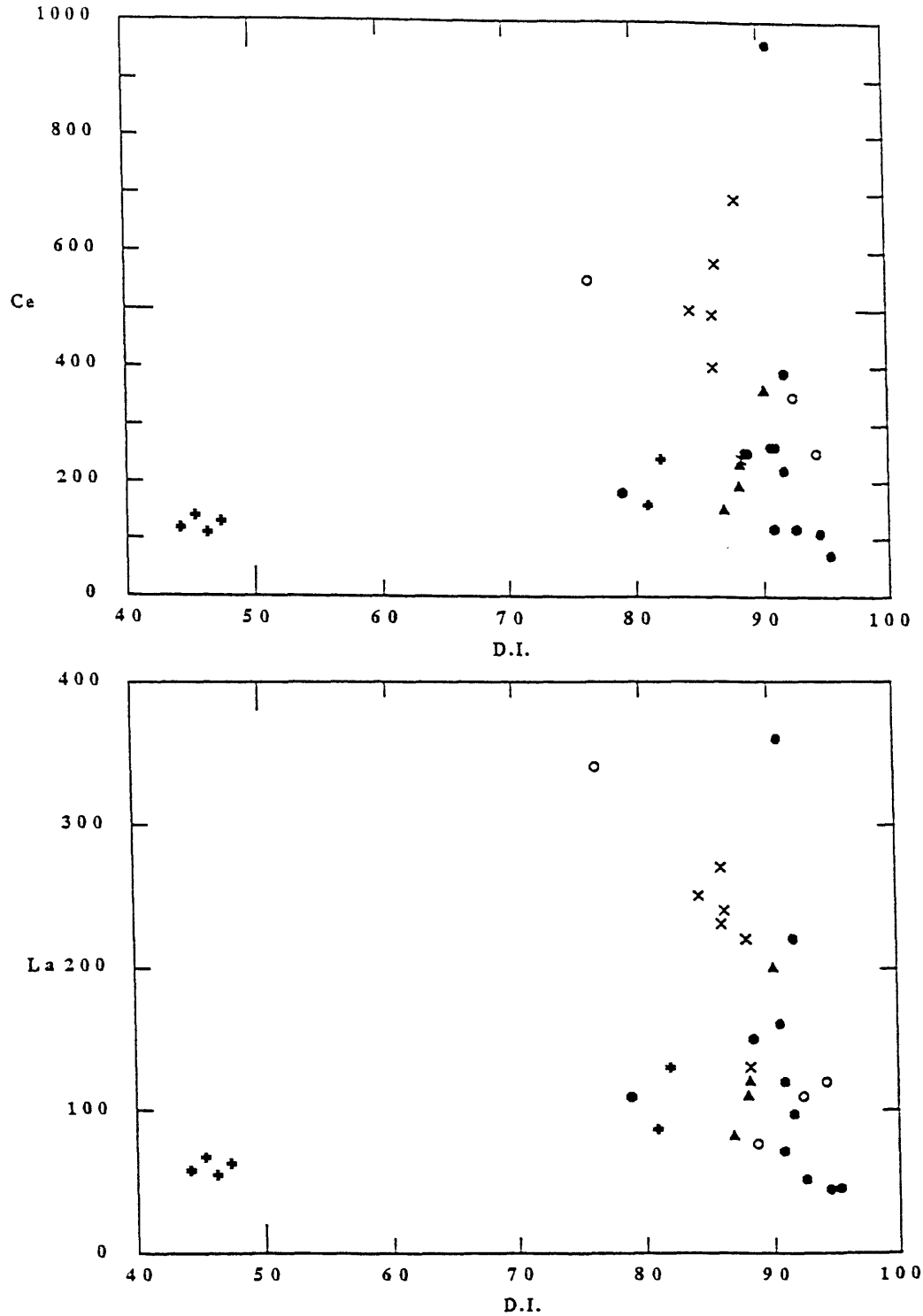

Figure 11. Differentiation index versus minor and trace elements. Solid circles are nepheline syenite, open circles are foid-less syenite, X's are amphibole syenite, filled triangles are quartz syenite, and crosses are monzogabbro.

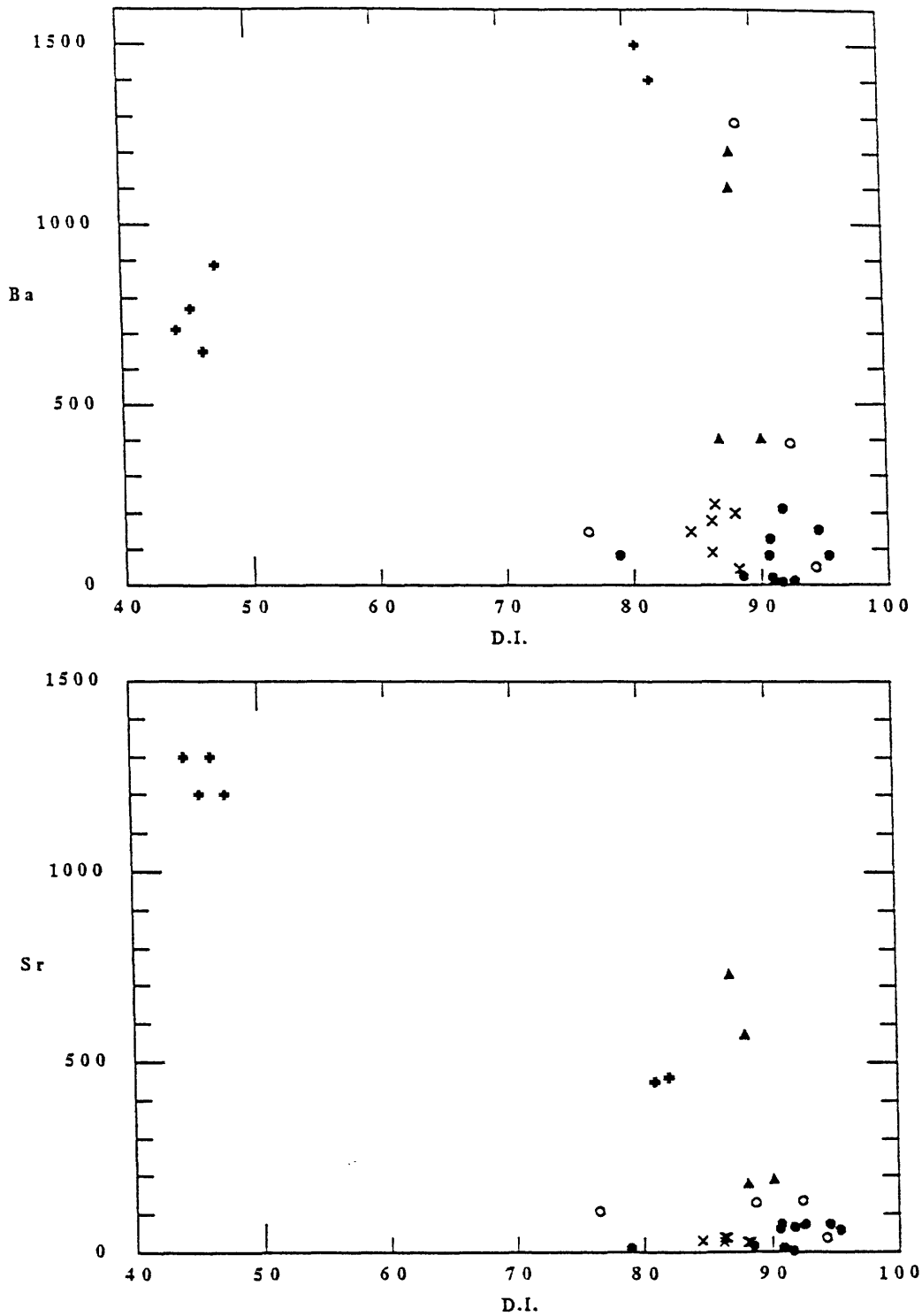

Figure 11. continued

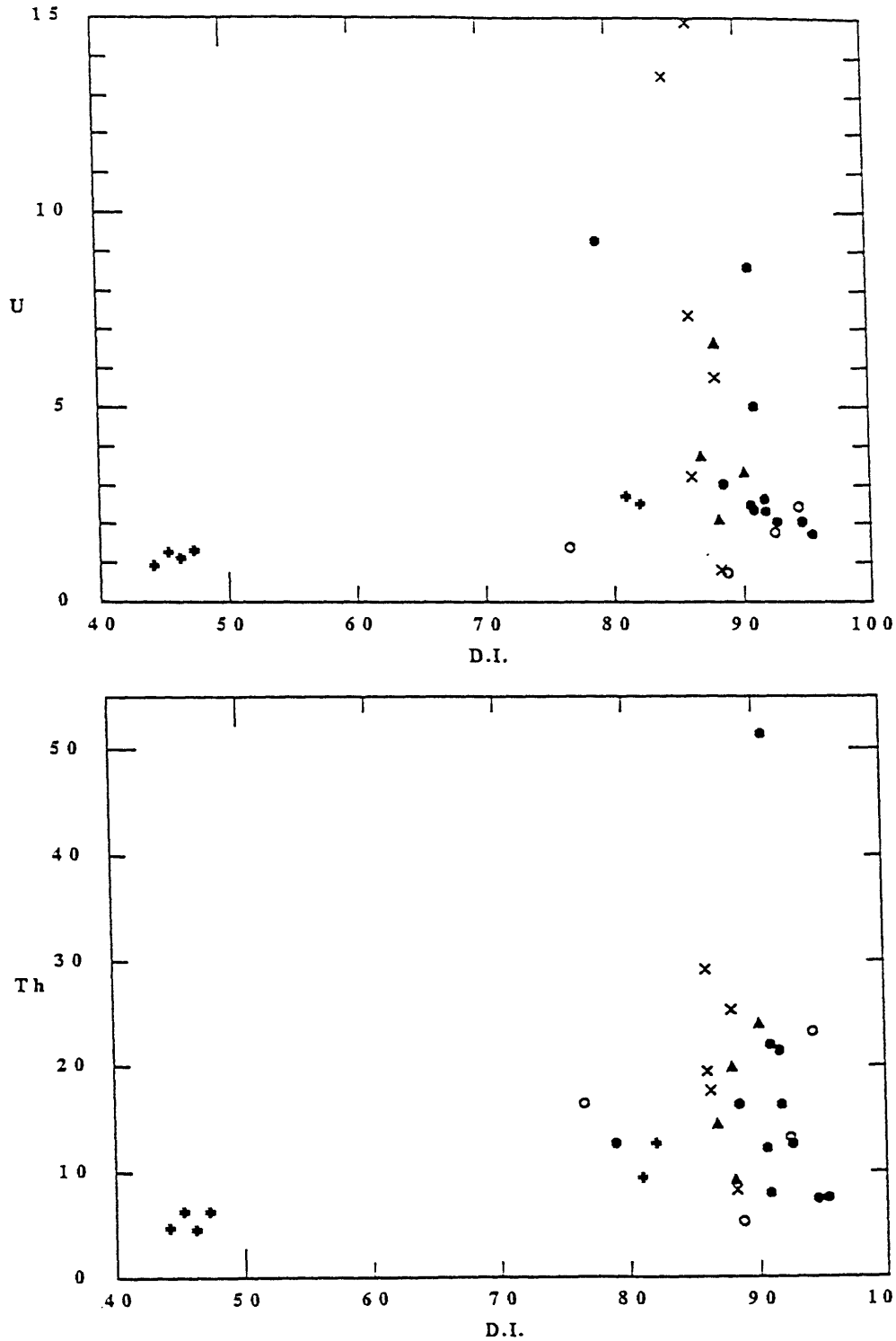

Figure 11. continued

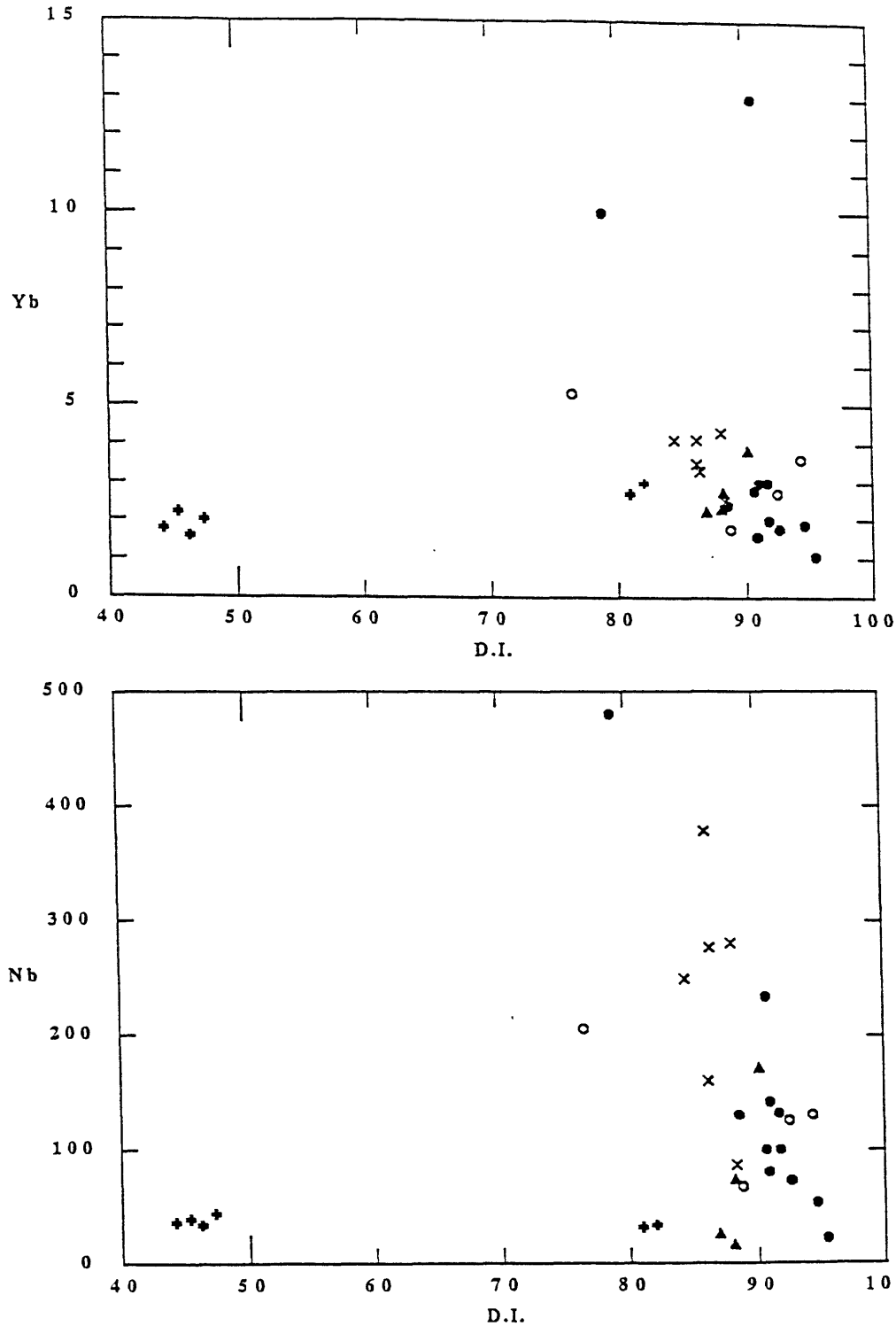

Figure 11. continued

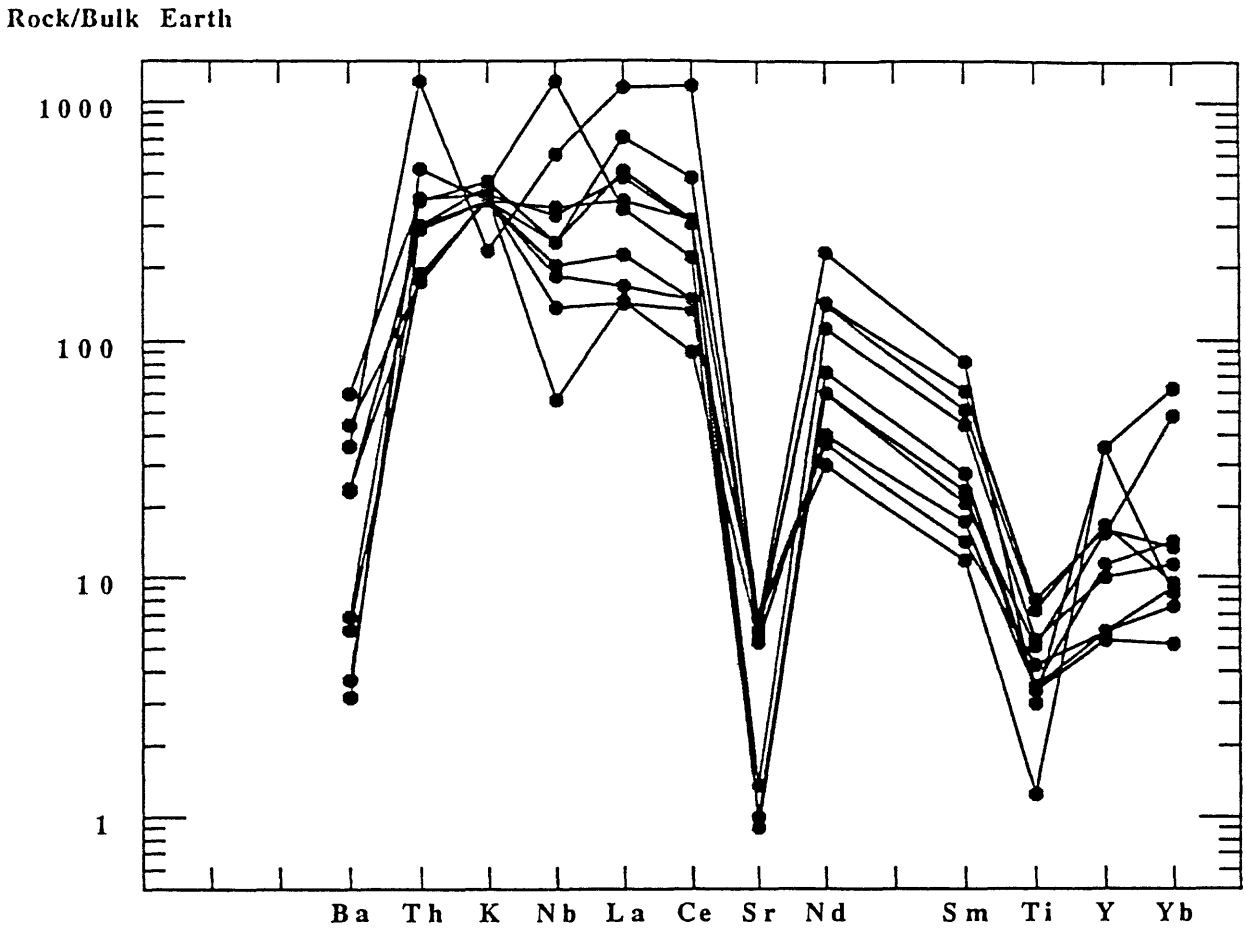

Figure 12. Spider diagrams. Solid circles are nepheline syenite, open circles are foid-less syenite, X's are amphibole syenite, filled triangles are quartz syenite, and crosses are monzogabbro. Normalized values from Hickey and others (1986).

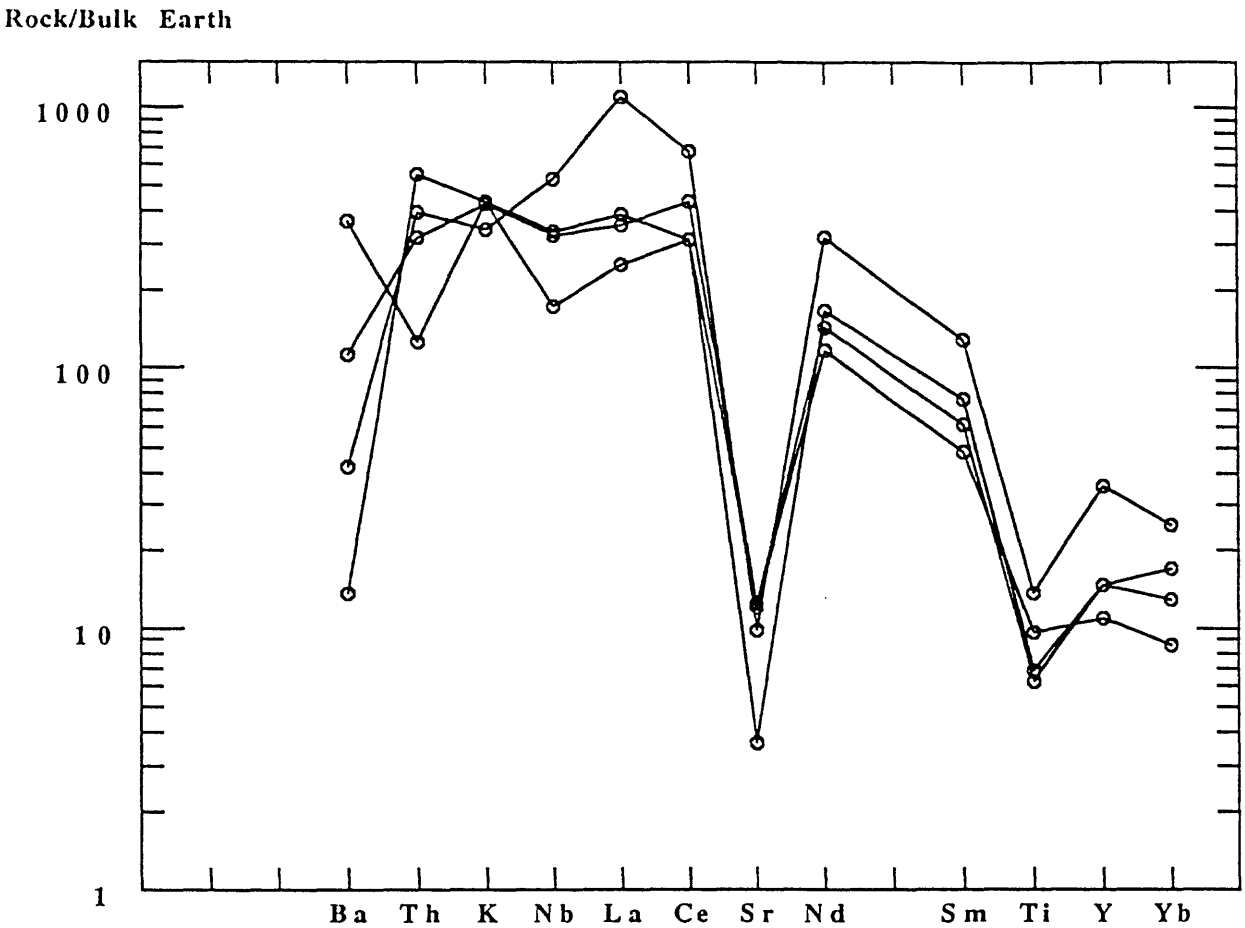

Figure 12. continued

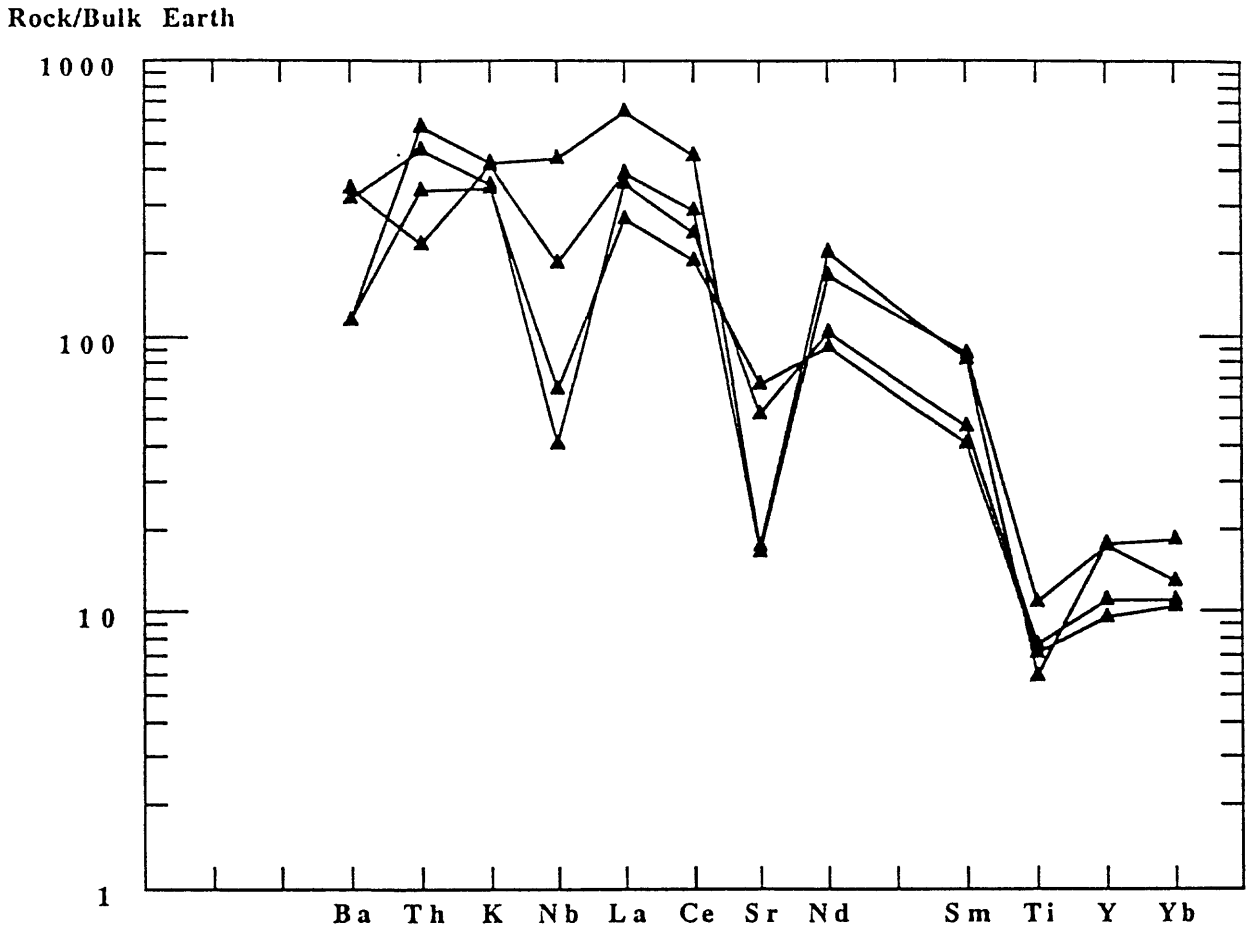

Figure 12. continued

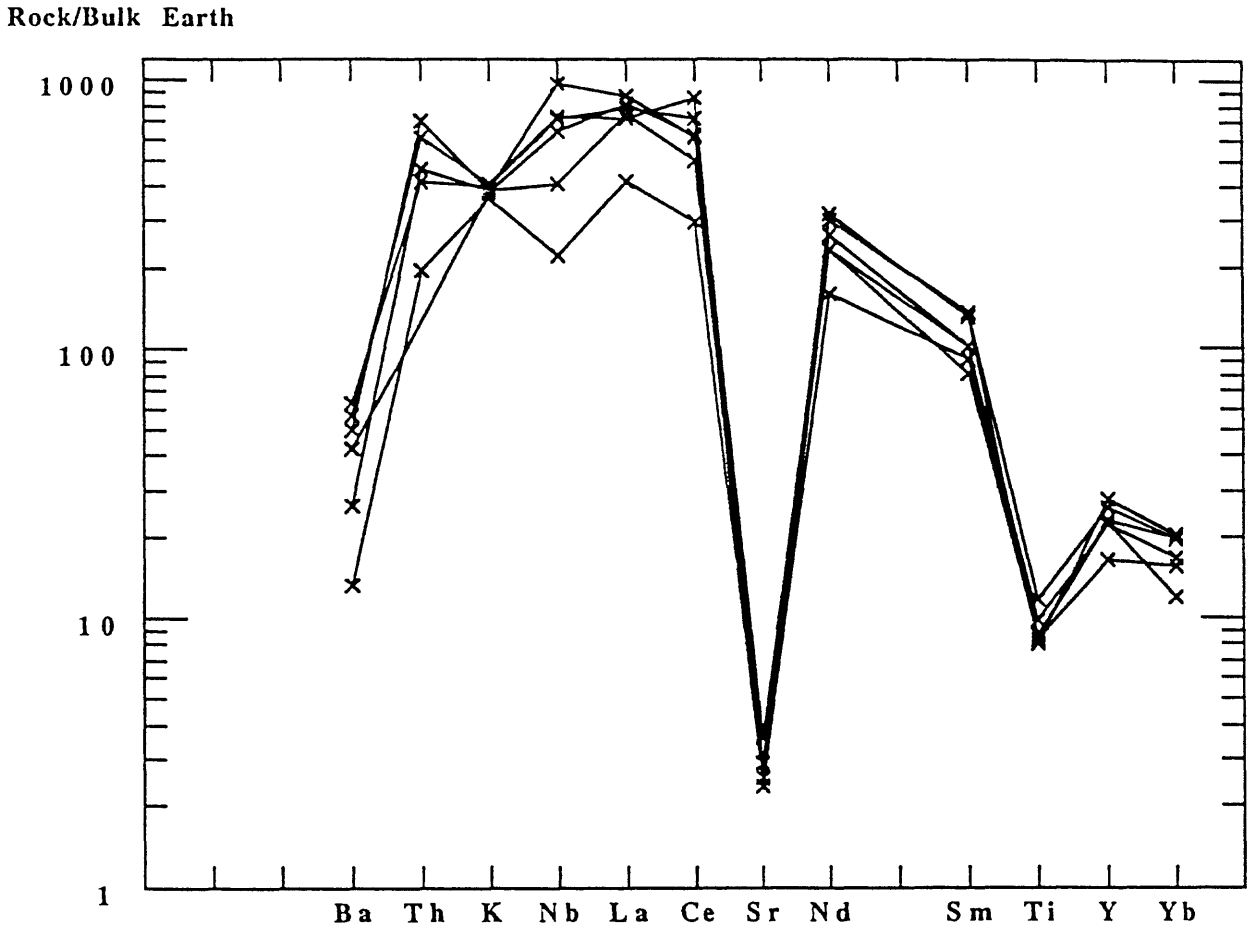

Figure 12. continued

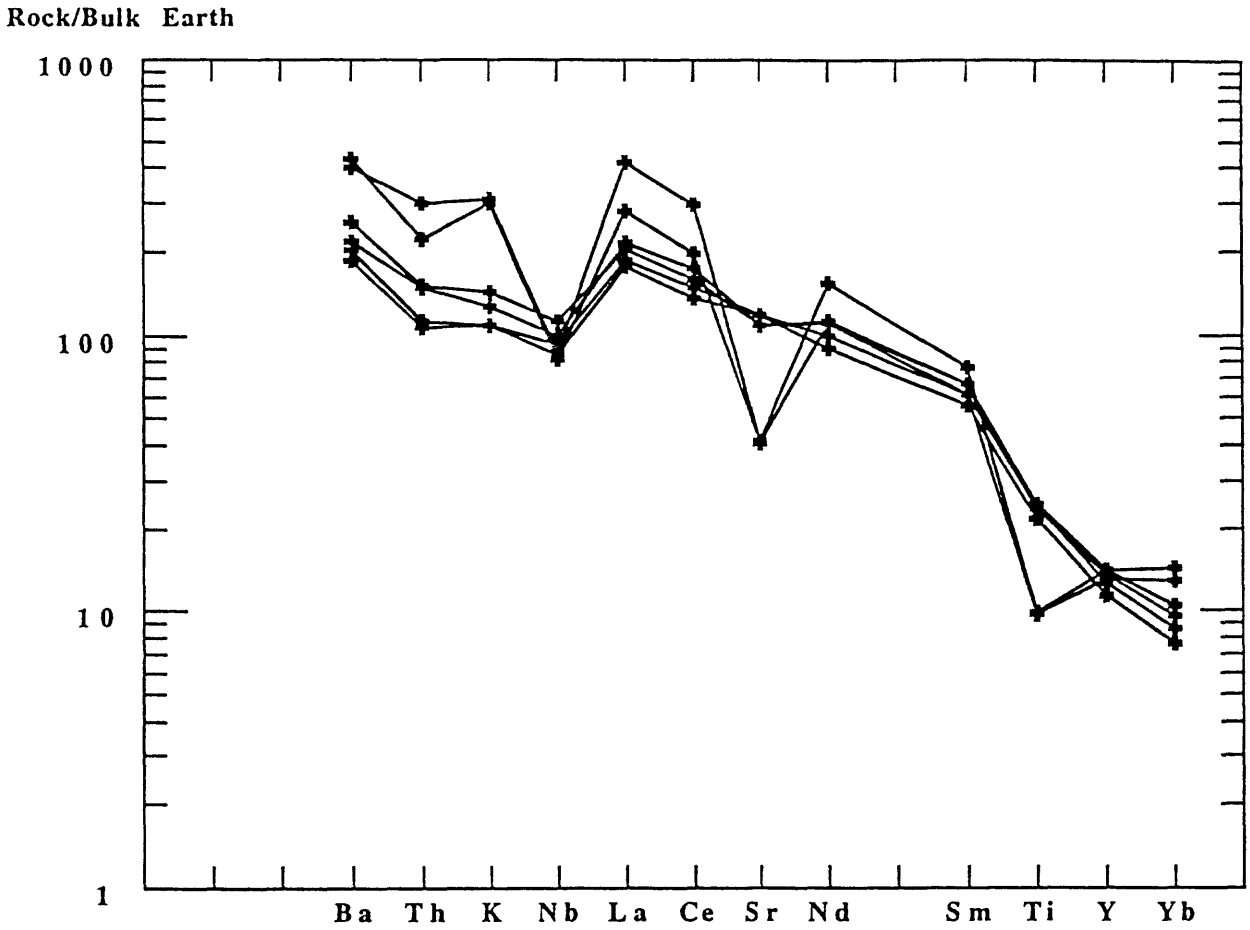

Figure 12. continued

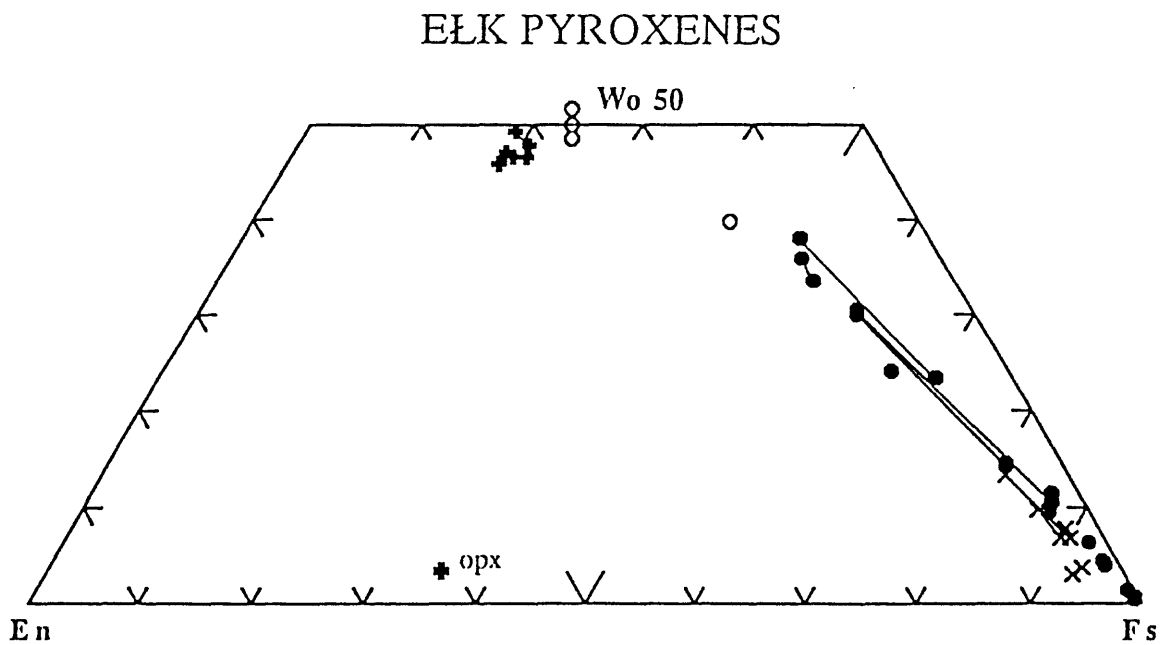

Figure 13. Quadrilateral (Mg-Ca-∑Fe+Mn) plot of pyroxene compositions. Tie lines connect core-rim compositions of zoned pyroxene crystals. Solid circles are foid-bearing syenite, open circles are foid-less syenite, X's are amphibole syenite, filled triangles are quartz.

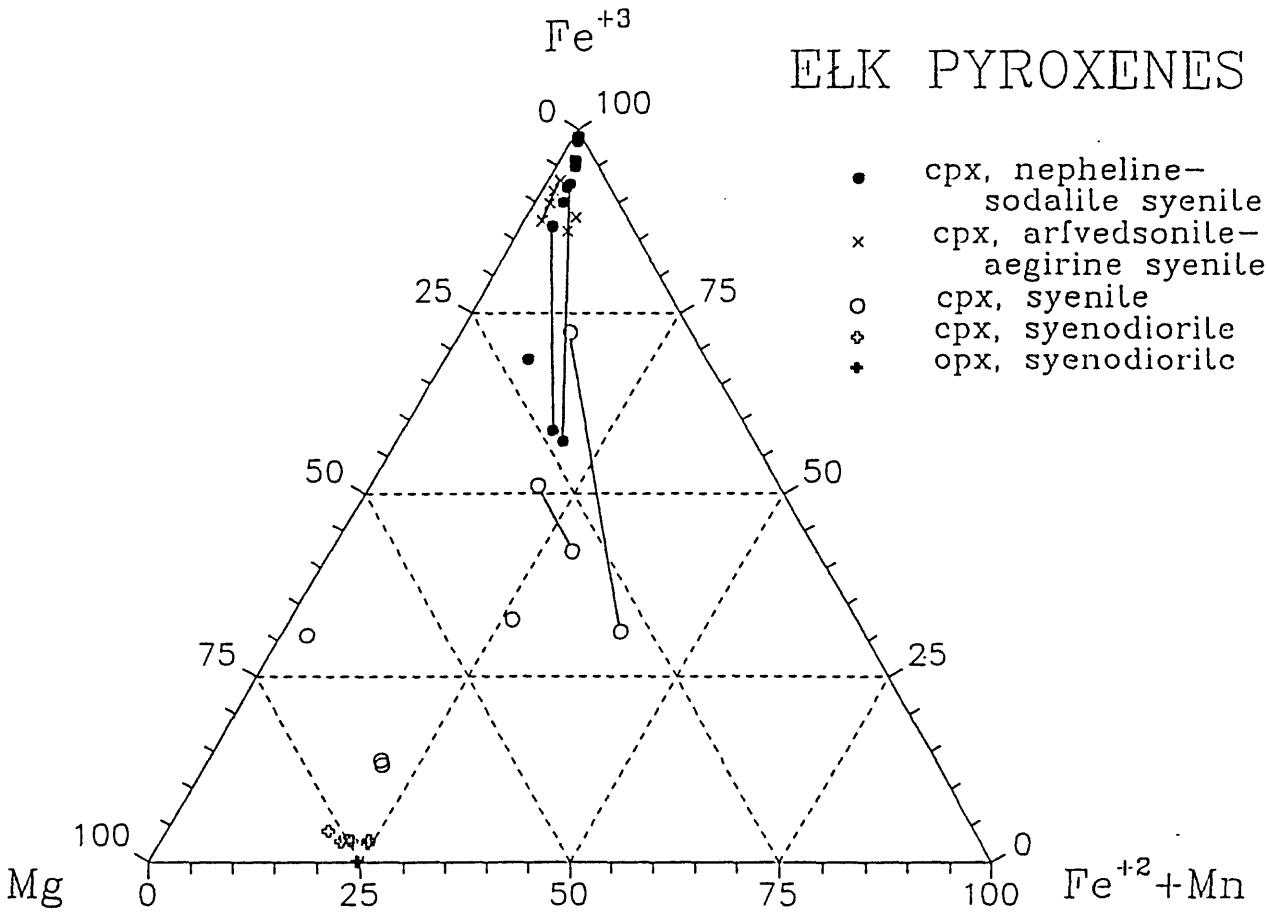

Figure 14. Ternary (Mg-Fe^{+3}-Fe^{+2}+Mn) plot of pyroxene compositions. Tie lines connect core-rim compositions of zoned pyroxene crystals. Solid circles are foid-bearing syenite, open circles are foid-less syenite, X's are amphibole syenite, filled triangles are quartz syenite, and crosses are monzogabbro.

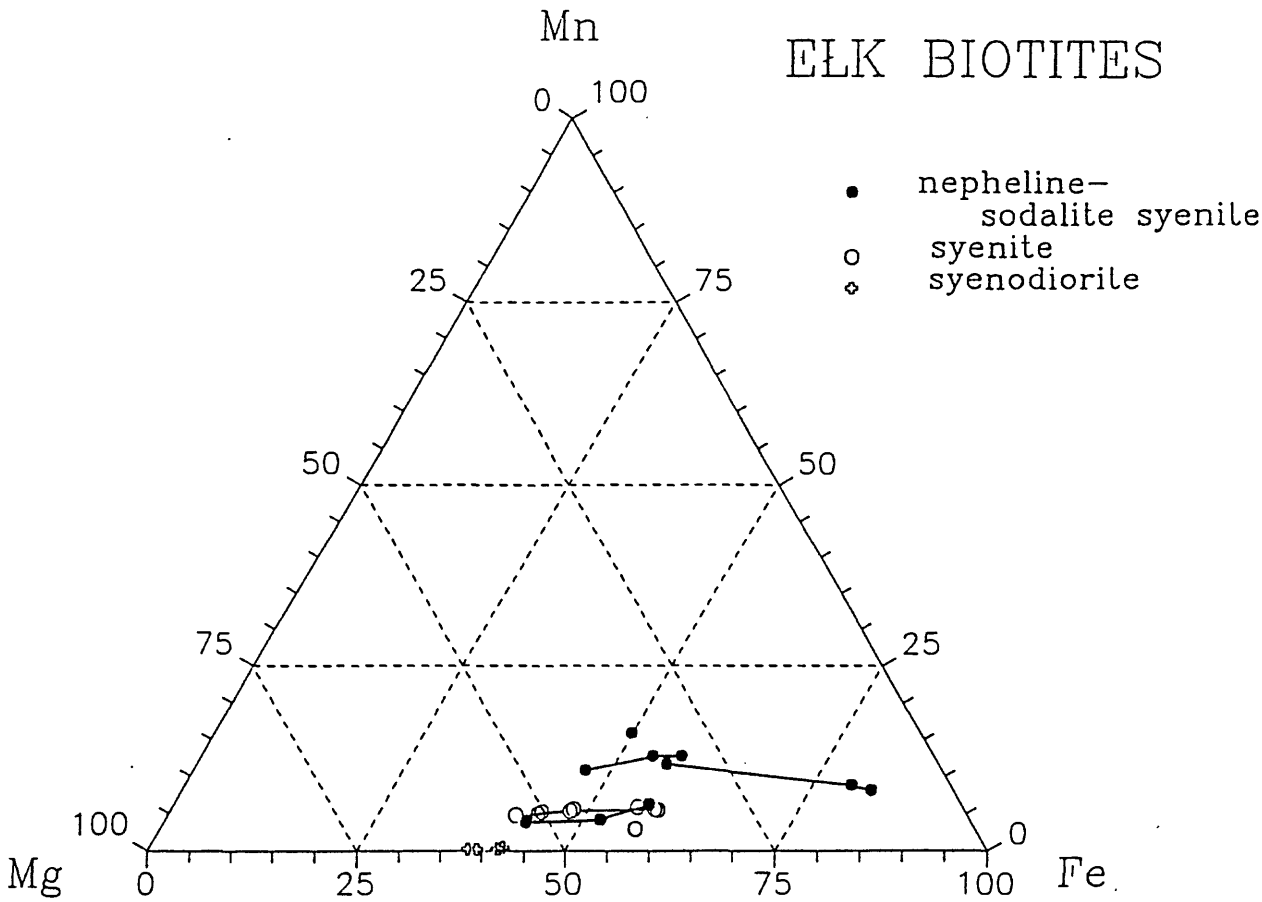

Figure 15. Ternary (Mg-Mn-ΣFe) plot of biotite compositions. Tie lines connect compositions of biotite grains within the same rock. Solid circles are nepheline syenite, open circles are foid-less syenite, X's are amphibole syenite, filled triangles are quartz syenite, and crosses are monzogabbro.

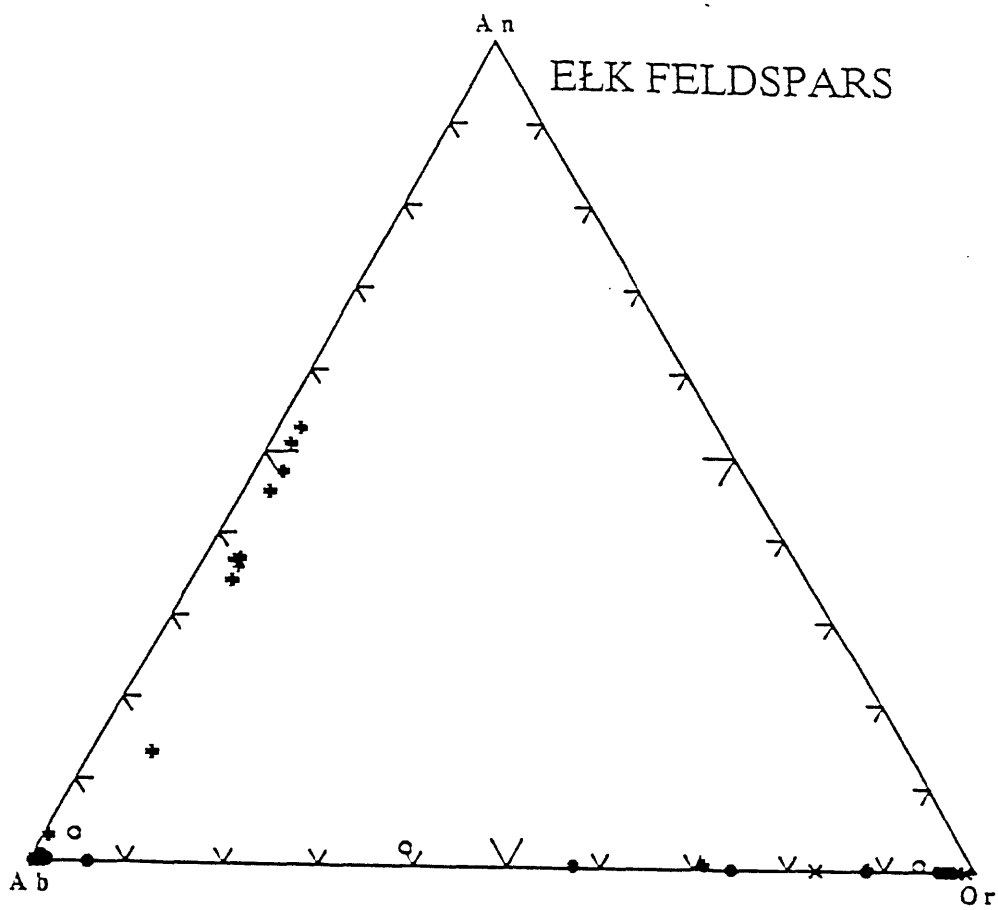

Figure 16. Ternary (Na-Ca-K) plot of feldspar compositions. Solid circles are nepheline syenite, open circles are foid-less syenite, X's are amphibole syenite, filled triangles are quartz syenite, and crosses are monzogabbro.

Table 1. Chemical data for rocks from the Elk complex

	A	B	C	D	E	F	G	H	I	J
1	Sample	E2-1844	E2-1850	E2-1856	E2-1859	E3-1810	E3-1286.5	E3-2013.5	E3-1230	E3-1019
2						Major elements (in percent)				
3	SiO2	57.2	60.8	61	61.8	62.7	56.5	61.9	61.5	62.3
4	Al2O3	19.7	19.4	18.4	18.5	18.5	15.1	17.8	17.9	17.9
5	Fe2O3	1.32	1.78	2.12	1.99	1.56	4.13	1.39	1.49	1.48
6	FeO	1.58	0.57	0.57	0.46	1.1	3.72	1.19	1.71	1.18
7	MgO	0.26	0.16	0.21	0.19	0.25	1.99	0.66	0.87	0.6
8	CaO	0.91	0.4	0.52	0.51	0.73	3.63	1.07	1.6	1.01
9	Na2O	10.5	9.05	8.65	8.49	7.49	6.06	6.66	6.14	6.49
10	K2O	3.45	5.55	5.53	5.7	5.73	4.97	6.65	6.22	6.17
11	TiO2	0.31	0.13	0.36	0.27	0.44	1.4	0.75	0.99	0.65
12	P2O5	0.05	0	0	0	0	0.65	0.18	0.27	0.16
13	MnO	0.44	0.17	0.29	0.25	0.13	0.62	0.21	0.14	0.19
14	H2O+	1.02	0.3	0.28	0.28	0.26	0.37	0.26	0.24	0.4
15	H2O-	0.11	0.1	0.11	0.08	0.09	0.08	0.07	0.04	0.14
16	CO2	1.26	0.42	0.45	0.42	0.27	0.18	0.35	0.07	0.28
17	Total	98.11	98.83	98.49	98.94	99.25	99.4	99.14	99.18	98.95
18										
19						Rare-earth elements (in parts per million)				
20	La	360	52	120	97	44	340	220	77	110
21	Ce	960	120	260	220	110	550	390	250	350
22	Pr	47	6.4	15	12	606	55	26	17	23
23	Nd	140	18	44	36	22	190	85	70	86
24	Sm	16	2.3	5.4	4.4	208	25	10	9.4	12
25	Eu	2.9	0.35	0.59	0.65	1.1	3.2	2.3	3.8	1.8
26	Gd	12	1.6	3	3.3	1.8	18	7.5	6.8	7.2
27	Tb	2.5	0.28	0.63	0.62	0.29	2.5	1	0.93	1.4
28	Dy	17	1.9	4	3.9	2.2	14	6.2	5.6	6.3
29	Ho	3.6	0.46	0.77	0.77	0.43	2.5	1.1	0.86	1.3
30	Er	12	1.3	2.5	2.5	1.5	6.5	2.9	2.2	3.5
31	Tm	1.7	0.23	0.38	0.28	0.18	0.93	0.44	0.31	0.46
32	Yb	13	1.8	3	3	1.9	5.3	2	1.8	2.7
33	REE total	1587.7	206.62	459.27	384.42	999.4	1212.93	754.44	445.7	605.66
34										
35						Trace and minor elements (in parts per million)				
36	Ba	127	13	11	9	154	147	211	1280	393
37	Be	12	3	5	5	4	4	4	2	4
38	Co	0	0	0	0	0	2	0	2	1
39	Cu	6	2	2	5	2	4	4	2	4
40	Ga	34	27	26	26	31	33	29	22	30
41	Li	28	12	17	13	6	25	26	8	15

Table 1. Chemical data for rocks from the Elk complex (continued)

	A	B	C	D	E	F	G	H	I	J
42	Mo	8	0	3	2	0	4	3	0	0
43	Nb	234	72	142	132	53	206	100	67	125
44	Pb	17	15	20	11	8	5	7	6	11
45	Sc	0	0	0	0	0	24	5	6	4
46	Sr	73	73	11	5	74	108	67	131	137
47	Y	77	77	25	23	13	78	37	24	32
48	Zn	151	151	91	87	74	264	91	80	114
49	U	8.61	2.06	5.05	2.64	2.05	1.41	2.34	0.74	1.78
50	Th	51.4	12.6	22.01	21.5	7.33	6.5	16.3	5.26	13.2
51										
52		Sample descriptions								
53		E2-1844, Nepheline syenite			G1-1394.5, Monzogabbro					
54		E2-1850, Nepheline syenite			G1-1411.3, Monzogabbro					
55		E2-1856, Nepheline syenite			G1-1982.7, Monzogabbro					
56		E2-1859, Nepheline syenite			G1-2000, Monzogabbro					
57		E3-1810, Nepheline syenite			K1-965.3, Quartz syenite (altered)					
58		E3-1286.5, Foid-less syenite			P1-974.2, Quartz syenite (altered)					
59		E3-2013.5, Nepheline syenite			P2-997.5, Quartz syenite					
60		E3-1230, Foid-less syenite			P2-1011.3, Quartz syenite					
61		E3-1019, Foid-less syenite			E2-1621.6, Nepheline syenite					
62		E4-1074, Amphibole syenite			E2-2001.4, Nepheline syenite					
63		E4-1129, Amphibole syenite			E3-950.0, Foid-less syenite					
64		E4-1256, Amphibole syenite			E3-1259.4, Nepheline syenite					
65		G1-829.7, Monzogabbro (altered)			E3-1263.2, Nepheline syenite					
66		G1-845.6, Monzogabbro (altered)			E3-2005.7, Nepheline syenite					
67					E4-950.2, Amphibole syenite					
68					E4-1267.7, Amphibole syenite					
69					E4-1639.1, Amphibole syenite					
70										
71										
72										
73										

Table 1. Chemical data for rocks from the Elk complex (continued)

	A	K	L	M	N	O	P	Q	R	S
1	Sample	E4-1074	E4-1129	E4-1256	G1-829.7	G1-845.6	G1-1394.5	G1-1411.3	G1-1982.7	G1-2000
2										
3	SiO2	64.1	63.1	63.6	59.6	59.7	49.3	49.1	47.6	48.8
4	Al2O3	16.3	16.1	16.1	15.7	15.6	16.2	16.2	17.7	17.7
5	Fe2O3	2.75	2.62	2.82	1.55	3.63	8.92	4.27	4.52	4.27
6	FeO	0.51	0.99	0.94	2.54	2.54	5.73	6.15	5.74	5.34
7	MgO	0.62	0.79	0.73	1.14	1.23	3.61	3.92	3.41	3.26
8	CaO	0.52	0.73	0.46	2.67	2.65	7.45	7.83	8.55	8.35
9	Na2O	7.01	7.12	7.09	4.48	4.54	3.7	3.56	3.57	3.62
10	K2O	5.95	5.64	5.77	4.51	4.36	2.09	1.84	1.56	1.58
11	TiO2	0.83	1.01	0.86	1.03	1.01	2.47	2.53	2.5	2.26
12	P2O5	0.13	0.18	0.14	0.29	0.29	1.15	1.16	1.23	1.14
13	MnO	0.28	0.29	0.37	0.13	0.14	0.17	0.18	0.16	0.16
14	H2O+	0.16	0.07	0.17	0.72	0.71	1.6	1.63	0.77	0.7
15	H2O-	0.04	0.1	0.07	0.22	0.18	0.14	0.1	0.13	0.16
16	CO2	0.1	0.03	0.03	4.33	4.36	0.7	0.91	1.61	1.68
17	Total	99.3	98.77	99.15	98.91	100.94	103.23	99.38	99.05	99.02
18										
19										
20	La	220	270	240	130	87	63	67	58	55
21	Ce	690	490	580	240	160	130	140	120	110
22	Pr	50	45	38	27	19	16	17	15	14
23	Nd	190	160	140	92	66	66	68	60	54
24	Sm	26	20	16	15	12	13	13	12	11
25	Eu	4.8	3.9	2.7	3.4	3.2	3.6	3.6	3.6	3.3
26	Gd	15	12	10	11	9.6	11	11	10	9.5
27	Tb	2.4	1.9	1.5	1.6	1.3	1.5	1.5	1.4	1.3
28	Dy	13	11	7.6	8.3	7.7	7.1	7.3	7	6.1
29	Ho	2.3	1.8	1.3	1.5	1.5	1.3	1.3	1.2	1.1
30	Er	5.6	4.6	3.5	4	3.6	3.1	3.2	2.8	2.6
31	Tm	0.66	0.49	0.48	0.5	0.47	0.4	0.4	0.34	0.33
32	Yb	4.3	3.5	3.3	3	2.7	2	2.2	1.8	1.6
33	REE total	1224.06	1024.19	1044.38	537.3	374.07	318	335.5	293.14	269.83
34										
35										
36	Ba	200	176	223	1400	1500	890	770	710	650
37	Be	5	5	6	3	3	2	2	2	2
38	Co	0	0	0	5	4	23	22	20	20
39	Cu	7	7	5	2	0	10	12	10	10
40	Ga	39	39	44	25	24	27	27	26	25
41	Li	46	46	57	15	14	15	18	13	12

Table 1. Chemical data for rocks from the Elk complex (continued)

	A	K	L	M	N	O	P	Q	R	S
42	Mo	0	0	0	3	2	0	0	0	0
43	Nb	281	379	227	34	32	44	39	36	33
44	Pb	5	0	0	18	15	8	8	8	8
45	Sc	6	7	5	7	7	16	17	14	12
46	Sr	28	39	40	460	450	1200	1200	1300	1300
47	Y	61	49	36	31	29	30	31	28	25
48	Zn	160	224	158	130	74	120	120	120	110
49	U	5.77	7.37	14.9	2.51	2.7	1.33	1.27	0.93	1.12
50	Th	25.3	29.2	17.6	12.6	9.39	6.3	6.2	4.76	4.5
51										
52										
53										
54										
55										
56										
57										
58										
59										
60										
61										
62										
63										
64										
65										
66										
67										
68										
69										
70										
71										
72										
73										

Table 1. Chemical data for rocks from the Elk complex (continued)

	A	T	U	V	W	X	Y	Z	AA	AB
1	Sample	K1-965.3	P1-974.2	P2-997.5	P2-1011.3	E2-1621.6	E2-2001.4	E3-950.0	E3-1259.4	E3-1263.2
2										
3	SiO2	62.1	61.5	64.6	64.7	60.7	60.5	62.5	62.7	60.8
4	Al2O3	16.5	17.2	15.5	15.5	18.7	18.1	17.9	18.7	17.6
5	Fe2O3	2.22	2.81	2.58	2.45	1.97	2.41	1.38	1.28	2.19
6	FeO	1.58	0.46	0.94	0.66	0.59	0.84	0.86	0.72	1.99
7	MgO	1.14	0.43	0.92	0.97	0.2	0.33	0.36	0.22	0.74
8	CaO	1.54	1.22	1.56	1.2	0.63	0.77	0.84	0.47	1.07
9	Na2O	5.8	5.11	4.51	4.36	8.88	8.16	6.62	7.69	6.96
10	K2O	5.99	6.11	5	5.16	5.58	5.91	6.26	5.77	5.54
11	TiO2	1.11	0.61	0.73	0.78	0.36	0.56	0.71	0.35	0.83
12	P2O5	0.35	0.1	0.32	0.33	0	0.08	0.07	0	0.24
13	MnO	0.18	0.21	0.06	0.05	0.2	0.32	0.16	0.13	0.29
14	H2O+	0.33	0.87	0.64	0.75	0.24	0.26	0.64	0.39	0.4
15	H2O-	0.05	0.15	0.15	0.51	0.05	0	0.08	0	0
16	CO2	0.03	1.52	0.46	0.4	0.11	0.22	0.52	0.16	0.22
17	Total	98.92	98.3	97.97	97.82	98.21	98.46	98.9	98.58	98.87
18										
19										
20	La	120	200	82	110	71	150	120	45	160
21	Ce	230	360	150	190	120	250	250	73	260
22	Pr	28	36	17	19	12	24	29	7.7	27
23	Nd	100	120	55	62	36	67	99	24	86
24	Sm	17	16	8	9.2	4.6	8.7	15	3.4	12
25	Eu	6.4	2.7	2.1	2.3	0.51	0.85	2	0.75	2
26	Gd	13	12	5.4	6.5	2.8	5.7	11	2.9	9.5
27	Tb	1.7	1.6	0.77	0.97	0.45	0.82	1.7	0.39	1.3
28	Dy	9.2	8.7	4.4	5.1	2.9	4.4	8.9	2.2	6.8
29	Ho	1.6	1.7	0.84	1	0.54	0.92	1.6	0.36	1.3
30	Er	3.7	4.6	2.3	3	1.4	2.5	4.3	1.1	3.6
31	Tm	0.48	0.66	0.36	0.41	0.21	0.37	0.6	0.18	0.45
32	Yb	2.7	3.8	2.2	2.3	1.6	2.4	3.6	1.1	2.8
33	REE total	533.78	767.76	330.37	411.78	254.01	517.66	546.7	162.08	572.75
34										
35										
36	Ba	1200	400	400	1100	21	24	48	84	84
37	Be	2	3	4	4	2	3	6	3	4
38	Co	2	0	6	8	0	0	0	0	1
39	Cu	0	2	53	42	1	1	6	0	0
40	Ga	30	26	19	18	25	27	33	24	35
41	Li	11	6	27	24	9	19	21	9	25

Table 1. Chemical data for rocks from the Elk complex (continued)

	A	T	U	V	W	X	Y	Z	AA	AB
42	Mo	0	0	13	4	0	0	0	4	5
43	Nb	72	170	25	16	80	130	130	22	100
44	Pb	15	20	19	24	15	7	13	0	8
45	Sc	7	2	4	4	0	2	2	0	5
46	Sr	180	190	730	570	11	15	40	59	61
47	Y	38	39	21	24	13	22	32	12	35
48	Zn	130	70	27	37	55	95	130	58	160
49	U	2.08	3.3	3.72	6.61	2.36	3.01	2.43	1.75	2.48
50	Th	9.08	23.9	14.3	19.7	7.91	16.4	23.3	7.54	12.2
51										
52										
53										
54										
55										
56										
57										
58										
59										
60										
61										
62										
63										
64										
65										
66										
67										
68										
69										
70										
71										
72										
73										

Table 1. Chemical data for rocks from the Elk complex (continued)

	A	AC	AD	AE	AF
1	Sample	E3-2005.7	E4-950.2	E4-1267.7	E4-1639.1
2					
3	SiO2	58.4	63.3	62.6	63.9
4	Al2O3	16.8	15.8	15.6	16.5
5	Fe2O3	6.16	2.96	3.25	2.14
6	FeO	0.42	0.73	1.02	0.82
7	MgO	0.12	0.72	0.61	0.78
8	CaO	0.42	0.53	0.79	0.62
9	Na2O	8.45	7.22	7.18	7.47
10	K2O	6.41	5.57	5.48	5.23
11	TiO2	0.53	0.86	1.2	0.89
12	P2O5	0	0.18	0.16	0.16
13	MnO	0.42	0.33	0.31	0.28
14	H2O+	0.07	0.23	0.17	0.15
15	H2O-	0	0	0	0.05
16	CO2	0.01	0	0	0
17	Total	98.21	98.43	98.37	98.99
18					
19					
20	La	110	230	250	130
21	Ce	180	400	500	240
22	Pr	14	41	55	28
23	Nd	36	140	180	97
24	Sm	4.1	20	27	18
25	Eu	0.69	3.5	4.6	3.2
26	Gd	3.4	14	18	14
27	Tb	0.91	2.1	2.7	2.1
28	Dy	7.3	11	14	11
29	Ho	1.9	2.1	2.6	1.8
30	Er	7.7	5.3	6	4.2
31	Tm	1.3	0.67	0.73	0.48
32	Yb	10	4.1	4.1	2.5
33	REE total	377.3	873.77	1064.73	552.28
34					
35					
36	Ba	82	92	150	46
37	Be	4	7	4	6
38	Co	0	0	0	0
39	Cu	7	3	5	0
40	Ga	57	47	46	44
41	Li	2	50	40	0

Table 1. Chemical data for rocks from the Elk complex (continued)

	A	AC	AD	AE	AF
42	Mo	0	0	0	0
43	Nb	480	160	250	86
44	Pb	0	11	0	4
45	Sc	0	7	6	7
46	Sr	10	26	32	26
47	Y	34	51	57	50
48	Zn	370	210	150	95
49	U	9.25	3.21	13.5	0.8
50	Th	12.7	19.4	0	8.24
51					
52					
53					
54					
55					
56					
57					
58					
59					
60					
61					
62					
63					
64					
65					
66					
67					
68					
69					
70					
71					
72					
73					

Table 2. Rock types and mineral phases analyzed via electron microprobe.

Drill hole and depth	*Rock type*	*Mineral analyses given in this paper*	*Notes on other mineral phases present*
E2-1844	Nepheline-sodalite syenite	Aegirine, biotite, sanidine, albite	Nepheline, sodalite, cancrinite, natrolite
E2-1850	Nepheline-sodalite syenite	Aegirine-augite, biotite, orthoclase, albite	Nepheline, sodalite, cancrinite, analcime, ilmenite, magnetite
E2-1856	Nepheline-sodalite syenite	Aegirine-augite, biotite, orthoclase, albite	Sodalite, cancrinite, nepheline
E3-2005.7	Nepheline-sodalite syenite	Aegirine, orthoclase, albite	Nepheline, sodalite, amphibole, pyrophanite
E3-2013.5	Nepheline-sodalite syenite	Biotite	Aegirine-augite, orthoclase, albite, cancrinite, sodalite, nepheline
E4-950.2	Arfvedsonite syenite	Aegirine, arfvedsonite, orthoclase, albite	Ilmenite
E4-1074	Arfvedsonite syenite	Aegirine, arfvedsonite, orthoclase, albite	-
E4-1256	Arfvedsonite syenite	Arfvedsonite	Aegirine, orthoclase, albite, ilmenite, chlorite
E3-1230	Syenite with trace feldspathoids	Aegirine-augite, biotite, sanidine, albite	Ilmenite, magnetite, titanite, apatite
E3-1286.5	Syenite with trace feldspathoids	Aegirine-augite, biotite, orthoclase, albite	Sodalite, titanite
E3-1810	Syenite with minor feldspathoids	Aegirine-augite, biotite, orthoclase, albite	Cancrinite, magnetite
G1-1394.5	Syenodiorite	Augite, biotite, hornblende, plagioclase, albite	Magnetite, ilmenite, quartz, chlorite, pyrite, apatite, calcite
G1-1408.0	Syenodiorite	Biotite, hornblende, plagioclase, sanidine	Quartz, augite, albite, magnetite, ilmenite, pyrite
G1-2000.0	Syenodiorite	Augite, biotite, hornblende, hypersthene, plagioclase	-

Table 3. Microprobe analyses of pyroxenes.
[Analyses in weight percent; Fe_2O_3 is computed assuming atomic Fe^{3+} = Na, or all Fe as Fe^{3+} if Na>Fe.]

	#1 E2-1844 Grain A	#2 E2-1844 Grain B	#3 E2-1844 Grain C	#4 E2-1850 Grain A	#5 E2-1850 Grain B	#6 E2-1850 Grain C
Na_2O	13.79	13.32	12.47	9.09	12.35	13.20
K_2O	0.01	0.04	0.15	0.01	0.01	0.01
MgO	0.07	0.14	1.14	3.70	0.78	0.42
CaO	0.14	0.37	3.02	8.76	3.72	1.18
MnO	0.18	0.23	0.97	1.80	0.85	0.52
FeO	-	-	-	1.29	-	-
Fe_2O_3	29.36	29.77	29.78	23.42	30.64	30.95
Al_2O_3	1.17	1.11	1.43	1.29	1.16	1.30
TiO_2	0.20	0.22	0.74	0.52	0.59	0.46
SiO_2	50.63	50.68	52.90	50.25	52.06	53.76
Σ	95.55	95.88	102.60	100.13	102.16	101.80
atomic proportions (normalized to 6 oxygens)						
Na	1.066	1.026	0.901	0.676	0.901	0.956
K	0.001	0.002	0.007	0.000	0.000	0.000
Mg	0.004	0.008	0.063	0.212	0.044	0.023
Ca	0.006	0.016	0.121	0.360	0.150	0.047
Mn	0.006	0.008	0.031	0.059	0.027	0.016
Fe^{2+}	-	-	-	0.041	-	-
Fe^{3+}	0.881	0.890	0.835	0.676	0.867	0.870
Al	0.055	0.052	0.063	0.058	0.051	0.057
Ti	0.006	0.007	0.021	0.015	0.017	0.013
Si	2.018	2.014	1.971	1.929	1.958	2.009
Σ cations	4.042	4.023	4.013	4.027	4.016	3.993
Σ oxygens	6.000	6.000	6.000	6.000	6.000	6.000
Q	0.010	0.024	0.184	0.613	0.194	0.071
J	2.131	2.052	1.802	1.353	1.802	1.913
J/(Q+J)	0.995	0.988	0.907	0.688	0.903	0.964
Ca(QUAD)	0.007	0.017	0.115	0.267	0.138	0.049
Mg(QUAD)	0.005	0.009	0.060	0.157	0.040	0.024
Fe(QUAD)	0.989	0.974	0.825	0.576	0.822	0.926
Fe^{3+}	0.989	0.982	0.899	0.684	0.924	0.957
$Fe^{2+}+Mn^{2+}$	0.007	0.009	0.033	0.101	0.029	0.018
Mg	0.004	0.009	0.068	0.215	0.047	0.025

#1-3 = aegirine; nepheline-sodalite syenite, drill hole E2, depth 1844 m.
#4-6 = aegirine-augite to aegirine; nepheline-sodalite syenite, drill hole E2, depth 1850 m.

Table 3. Microprobe analyses of pyroxenes (continued).

	#7 E2-1850 Grain D	#8 E2-1856 Grain A core	#9 E2-1856 Grain A rim	#10 E2-1856 Grain B core	#11 E2-1856 Grain B rim	#12 E3-2005.7 Grain A
Na_2O	14.18	7.52	11.66	7.29	12.30	13.01
K_2O	0.01	0.00	0.00	0.00	0.00	0.00
MgO	0.09	3.93	1.57	3.82	0.88	0.37
CaO	0.20	11.24	4.73	11.56	3.34	1.31
MnO	0.15	2.02	1.08	1.81	0.81	0.53
FeO	-	3.38	-	4.09	-	-
Fe_2O_3	32.91	19.38	28.01	18.78	29.93	29.46
Al_2O_3	1.41	1.18	1.08	0.92	0.91	0.95
TiO_2	0.11	0.44	0.66	0.42	0.56	0.79
SiO_2	50.28	52.47	51.12	51.71	53.05	53.61
Σ	99.34	101.56	99.91	100.40	101.78	100.03
atomic proportions (normalized to 6 oxygens)						
Na	1.067	0.549	0.867	0.540	0.895	0.956
K	0.000	0.000	0.000	0.000	0.000	0.000
Mg	0.005	0.221	0.090	0.218	0.049	0.021
Ca	0.008	0.454	0.194	0.473	0.134	0.053
Mn	0.005	0.064	0.035	0.059	0.026	0.017
Fe^{2+}	-	0.106	-	0.131	-	-
Fe^{3+}	0.961	0.549	0.809	0.540	0.845	0.840
Al	0.064	0.052	0.049	0.041	0.040	0.042
Ti	0.003	0.012	0.019	0.012	0.016	0.023
Si	1.951	1.976	1.961	1.976	1.991	2.031
Σ cations	4.066	3.985	4.025	3.991	3.998	3.983
Σ oxygens	6.000	6.000	6.000	6.000	6.000	6.000
Q	0.014	0.781	0.284	0.822	0.184	0.074
J	2.134	1.098	1.735	1.080	1.790	1.911
J/(Q+J)	0.994	0.585	0.859	0.568	0.907	0.963
Ca(QUAD)	0.008	0.325	0.172	0.333	0.127	0.057
Mg(QUAD)	0.005	0.158	0.080	0.153	0.047	0.022
Fe(QUAD)	0.986	0.516	0.748	0.514	0.826	0.920
Fe^{3+}	0.990	0.584	0.866	0.570	0.919	0.957
$Fe^{2+}+Mn^{2+}$	0.005	0.181	0.038	0.200	0.028	0.019
Mg	0.005	0.235	0.096	0.230	0.053	0.024

#7 = aegirine; nepheline-sodalite syenite, drill hole E2, depth 1850 m.
#8-11 = zoned aegrine to aegirine-augite; nepheline-sodalite syenite, drill hole E2, depth 1856 m.
#12 = aegirine; nepheline-sodalite syenite, drill hole E3, depth 2005.7 m.

Table 3. Microprobe analyses of pyroxenes (continued).

	#13 E3-2005.7 Grain B	#14 E4-950.2 Grain A core	#15 E4-950.2 Grain A rim	#16 E4-950.2 Grain B core	#17 E4-950.2 Grain B rim	#18 E4-1074 Grain A
Na_2O	13.03	12.26	13.25	11.89	13.11	12.83
K_2O	0.00	0.00	0.00	0.00	0.00	0.00
MgO	0.45	1.39	1.14	1.75	0.91	0.91
CaO	1.84	3.08	2.05	4.41	2.08	2.39
MnO	0.59	0.53	0.40	0.64	0.40	0.44
FeO	-	-	-	-	-	-
Fe_2O_3	28.58	29.35	29.17	28.99	30.04	29.82
Al_2O_3	0.98	0.58	0.49	0.32	0.40	0.20
TiO_2	1.99	0.74	0.87	0.64	1.07	1.12
SiO_2	53.29	52.22	52.46	52.54	53.25	52.30
Σ	100.75	100.15	99.83	101.18	101.26	100.01
	atomic proportions (normalized to 6 oxygens)					
Na	0.951	0.906	0.981	0.871	0.957	0.951
K	0.000	0.000	0.000	0.000	0.000	0.000
Mg	0.025	0.079	0.065	0.099	0.051	0.052
Ca	0.074	0.126	0.084	0.179	0.084	0.042
Mn	0.019	0.017	0.013	0.020	0.013	0.014
Fe^{2+}	-	-	-	-	-	-
Fe^{3+}	0.810	0.842	0.838	0.825	0.851	0.857
Al	0.043	0.026	0.022	0.014	0.018	0.009
Ti	0.056	0.021	0.025	0.018	0.030	0.032
Si	2.007	1.990	2.004	1.986	2.005	1.998
Σ cations	3.986	4.007	4.032	4.012	4.009	4.011
Σ oxygens	6.000	6.000	6.000	6.000	6.000	6.000
Q	0.099	0.205	0.149	0.277	0.135	0.150
J	1.903	1.812	1.962	1.743	1.914	1.901
J/(Q+J)	0.950	0.898	0.930	0.863	0.934	0.927
Ca(QUAD)	0.080	0.118	0.084	0.159	0.084	0.096
Mg(QUAD)	0.027	0.074	0.065	0.088	0.051	0.051
Fe(QUAD)	0.893	0.807	0.851	0.753	0.865	0.853
Fe^{3+}	0.949	0.898	0.915	0.874	0.930	0.929
$Fe^{2+}+Mn^{2+}$	0.022	0.018	0.014	0.021	0.014	0.015
Mg	0.029	0.084	0.071	0.105	0.056	0.056

#13 = aegirine; nepheline-sodalite syenite, drill hole E3, depth 2005.7 m.
#14-17 = aegirine; arfvedsonite-aegirine syenite, drill hole E4, depth 950.2 m.
#18 = aegirine; arfvedsonite-aegirine syenite, drill hole E4, depth 1074 m.

Table 3. Microprobe analyses of pyroxenes (continued).

	#19 E4-1074 Grain B	#20 E4-1074 Grain C	#21 E3-1810 Grain A core	#22 E3-1810 Grain A rim	#23 E3-1810 Grain B core	#24 E3-1810 Grain B rim
Na_2O	13.94	14.13	4.30	9.69	5.51	6.63
K_2O	0.00	0.00	0.01	0.00	0.05	0.11
MgO	0.98	1.20	5.14	2.54	4.95	4.86
CaO	1.03	0.81	16.98	8.79	14.52	13.12
MnO	1.62	1.51	1.79	1.18	2.48	1.70
FeO	-	-	11.00	2.86	6.20	4.31
Fe_2O_3	27.27	25.05	11.08	24.97	14.20	17.08
Al_2O_3	0.10	0.03	0.58	0.56	1.28	1.04
TiO_2	3.05	5.33	0.33	0.23	0.62	0.50
SiO_2	52.94	52.96	51.51	52.19	49.53	51.22
Σ	100.93	101.02	102.72	103.01	99.33	100.57
atomic proportions (normalized to 6 oxygens)						
Na	1.021	1.028	0.317	0.705	0.417	0.491
K	0.000	0.000	0.000	0.000	0.002	0.005
Mg	0.055	0.067	0.291	0.142	0.288	0.277
Ca	0.042	0.033	0.692	0.353	0.607	0.537
Mn	0.052	0.048	0.058	0.038	0.082	0.055
Fe^{2+}	-	-	0.350	0.090	0.202	0.138
Fe^{3+}	0.775	0.707	0.317	0.705	0.417	0.491
Al	0.004	0.001	0.026	0.025	0.059	0.047
Ti	0.087	0.150	0.009	0.006	0.018	0.014
Si	1.999	1.987	1.959	1.958	1.931	1.956
Σ cations	4.035	4.022	4.019	4.023	4.022	4.009
Σ oxygens	6.000	6.000	6.000	6.000	6.000	6.000
Q	0.097	0.100	1.333	0.585	1.096	0.951
J	2.041	2.056	0.634	1.410	0.833	0.982
J/(Q+J)	0.955	0.954	0.322	0.707	0.432	0.508
Ca(QUAD)	0.045	0.038	0.405	0.266	0.380	0.359
Mg(QUAD)	0.060	0.079	0.171	0.107	0.180	0.185
Fe(QUAD)	0.895	0.883	0.424	0.627	0.439	0.457
Fe^{3+}	0.879	0.860	0.312	0.723	0.422	0.511
$Fe^{2+}+Mn^{2+}$	0.059	0.058	0.402	0.131	0.287	0.201
Mg	0.062	0.082	0.286	0.146	0.291	0.288

#19-20 = titaniferous aegirine; arfvedsonite-aegirine syenite, drill hole E4, depth 1074 m.
#21-24 = zoned aegirine-augite; syenite, drill hole E3, depth 1810 m.

Table 3. Microprobe analyses of pyroxenes (continued).

	#25 E3-1286.5 Grain A	#26 E3-1286.5 Grain B	#27 E3-1230 Grain A	#28 E3-1230 Grain B	#29 G1-1394.5 Grain A core	#30 G1-1394.5 Grain A rim
Na_2O	1.96	4.20	4.37	1.83	0.42	0.44
K_2O	0.02	0.02	0.00	0.04	0.03	0.02
MgO	12.17	6.78	8.22	11.98	14.00	14.10
CaO	21.69	15.79	16.46	22.57	21.53	21.41
MnO	1.53	2.08	0.67	0.97	0.21	0.40
FeO	5.14	5.70	-	5.74	7.05	8.02
Fe_2O_3	5.05	10.82	7.55	4.72	1.08	1.13
Al_2O_3	1.22	1.00	7.59	1.73	2.45	0.89
TiO_2	0.81	0.36	0.49	0.84	0.87	0.25
SiO_2	51.78	51.15	56.78	49.93	49.89	52.00
Σ	101.37	97.90	102.13	100.35	97.53	98.66
	atomic proportions (normalized to 6 oxygens)					
Na	0.141	0.316	0.297	0.134	0.031	0.032
K	0.001	0.001	0.000	0.002	0.001	0.001
Mg	0.674	0.393	0.430	0.674	0.797	0.795
Ca	0.863	0.657	0.619	0.913	0.881	0.867
Mn	0.048	0.068	0.020	0.031	0.007	0.013
Fe^{2+}	0.160	0.185	-	0.181	0.225	0.254
Fe^{3+}	0.141	0.316	0.199	0.134	0.031	0.032
Al	0.053	0.046	0.314	0.077	0.110	0.040
Ti	0.023	0.011	0.013	0.024	0.025	0.007
Si	1.923	1.987	1.993	1.884	1.906	1.966
Σ cations	4.028	3.980	3.886	4.054	4.015	4.007
Σ oxygens	6.000	6.000	6.000	6.000		
Q	1.697	1.235	1.049	1.768	1.903	1.916
J	0.282	0.633	0.595	0.268	0.062	0.065
J/(Q+J)	0.143	0.339	0.362	0.132	0.032	0.033
Ca(QUAD)	0.458	0.406	0.488	0.472	0.454	0.442
Mg(QUAD)	0.357	0.242	0.339	0.349	0.411	0.405
Fe(QUAD)	0.185	0.352	0.173	0.179	0.135	0.152
Fe^{3+}	0.138	0.328	0.307	0.131	0.029	0.029
$Fe^{2+}+Mn^{2+}$	0.203	0.263	0.031	0.208	0.219	0.244
Mg	0.659	0.409	0.662	0.661	0.752	0.727

#25-26 = augite to aegirine-augite; syenite, drill hole E3, depth 1286.5 m.
#27-28 = augite; syenite, drill hole E3, depth 1230 m.
#29-30 = diopsidic augite; syenodiorite, drill hole G1, depth 1394.5 m.

Table 3. Microprobe analyses of pyroxenes (continued).

	#31 G1-1394.5 Grain B	#32 G1-2000.0 Grain A	#33 G1-2000.0 Grain A	#34 G1-2000.0 Grain B	#35 G1-2000.0 Grain C Opx	#36 G1-2000.0 Grain C Opx
Na_2O	0.42	0.64	0.39	0.45	0.00	0.00
K_2O	0.02	0.11	0.01	0.02	0.00	0.00
MgO	15.04	15.01	14.42	15.05	26.76	26.75
CaO	20.74	19.55	20.86	20.88	1.55	1.50
MnO	0.30	0.21	0.38	0.41	0.53	0.57
FeO	7.23	6.44	8.26	7.65	15.03	15.00
Fe_2O_3	1.08	1.65	1.00	1.16	-	-
Al_2O_3	1.78	3.10	1.34	1.50	1.20	1.20
TiO_2	0.56	1.03	0.42	0.42	0.28	0.33
SiO_2	51.13	51.12	51.98	52.37	55.28	54.79
$\sum$	98.30	98.86	99.06	99.91	100.63	100.14
atomic proportions (normalized to 6 oxygens)						
Na	0.031	0.046	0.028	0.032	0.000	0.000
K	0.001	0.005	0.000	0.001	0.000	0.000
Mg	0.847	0.835	0.808	0.834	1.428	1.435
Ca	0.839	0.782	0.840	0.832	0.059	0.058
Mn	0.010	0.007	0.012	0.013	0.016	0.017
Fe^{2+}	0.228	0.201	0.260	0.238	0.450	0.451
Fe^{3+}	0.031	0.046	0.028	0.032	-	-
Al	0.079	0.136	0.059	0.066	0.051	0.051
Ti	0.016	0.029	0.012	0.012	0.008	0.009
Si	1.931	1.909	1.955	1.948	1.978	1.972
$\sum$ cations	4.013	3.997	4.004	4.008	3.989	3.994
$\sum$ oxygens	6.000	6.000	6.000	6.000	6.000	6.000
Q	1.915	1.818	1.908	1.904	1.937	1.945
J	0.062	0.093	0.057	0.065	0.000	0.000
J/(Q+J)	0.031	0.048	0.029	0.033	0.000	0.000
Ca(QUAD)	0.429	0.418	0.431	0.427	0.030	0.029
Mg(QUAD)	0.433	0.446	0.415	0.428	0.731	0.732
Fe(QUAD)	0.137	0.136	0.154	0.145	0.239	0.243
Fe^{3+}	0.028	0.042	0.025	0.029	0.000	0.000
$Fe^{2+}+Mn^{2+}$	0.213	0.191	0.246	0.225	0.246	0.246
Mg	0.759	0.767	0.729	0.746	0.754	0.754

#31 = diopsidic augite; syenodiorite, drill hole G1, depth 1394.5 m.
#32-34 = diopsidic augite; syenodiorite, drill hole G1, depth 2000.0 m.
#35-36 = orthopyroxene (bronzite); syenodiorite, drill hole G1, depth 2000.0 m.

Table 4. Microprobe analyses of biotite.
[Analyses in weight percent; na = not analyzed. All iron computed as FeO.]

	#1 E2-1844 Grain A	#2 E2-1850 Grain A	#3 E2-1850 Grain B	#4 E2-1850 Grain C	#5 E2-1856 Grain A	#6 E2-1856 Grain B
Na_2O	0.22	0.22	0.10	0.03	0.00	0.00
K_2O	8.77	9.53	9.40	9.03	9.27	9.22
MgO	7.53	2.24	8.12	2.78	7.77	7.02
CaO	0.03	0.00	0.02	0.00	0.00	0.00
SrO	0.01	na	na	na	na	na
BaO	0.00	na	na	na	na	na
MnO	6.14	3.31	5.16	3.68	5.22	5.26
FeO	19.51	33.99	25.22	33.89	22.45	24.03
Al_2O_3	10.67	9.94	10.96	10.64	9.96	10.14
TiO_2	1.68	2.54	2.22	2.43	2.59	2.78
SiO_2	35.75	34.76	38.09	36.46	38.01	37.17
F	na	0.85	2.05	0.69	na	na
Cl	0.02	0.02	0.02	0.00	na	na
$\sum$	90.33	97.40	101.36	99.63	95.27	95.62
O=F	-	0.36	0.86	0.29	-	-
O=Cl	0.00	0.00	0.00	0.00	-	-
$\sum'$	90.33	97.04	100.49	99.34	95.27	95.62
atomic proportions (normalized to 11 oxygens)						
Na	0.036	0.036	0.015	0.005	0.000	0.000
K	0.936	1.015	0.925	0.926	0.941	0.942
Mg	0.939	0.279	0.934	0.333	0.922	0.838
Ca	0.003	0.000	0.002	0.000	0.000	0.000
Sr	0.001	-	-	-	-	-
Ba	0.000	-	-	-	-	-
Mn	0.435	0.234	0.337	0.251	0.352	0.357
Fe^{2+}	1.365	2.373	1.627	2.279	1.494	1.609
Al	1.052	0.978	0.997	1.008	0.934	0.957
Ti	0.106	0.159	0.129	0.147	0.155	0.167
Si	2.991	2.902	2.939	2.932	3.025	2.977
F	-	0.224	0.500	0.175	0.000	0.000
Cl	0.003	0.003	0.003	0.000	0.000	0.000
$\sum$ cations	7.863	7.975	7.904	7.882	7.823	7.848
$\sum$ oxygens	11.000	11.000	11.000	11.000	11.000	11.000
Mg/(Mg+Fe)	0.408	0.105	0.365	0.128	0.382	0.342
Mg	0.343	0.097	0.322	0.116	0.333	0.299
Fe	0.498	0.822	0.561	0.796	0.540	0.574
Mn	0.159	0.081	0.116	0.088	0.127	0.127

#1 = biotite; nepheline-sodalite syenite, drill hole E2, depth 1844 m.
#2-4 = biotite; nepheline-sodalite syenite, drill hole E2, depth 1850 m.
#5-6 = biotite; nepheline-sodalite syenite, drill hole E2, depth 1856 m.

Table 4. Microprobe analyses of biotite (continued).

	#7 E2-1856 Grain C	#8 E3-1230 Grain A	#9 E3-1286.5 Grain A	#10 E3-1286.5 Grain B	#11 E3-1286.5 Grain C	#12 E3-1286.5 Grain D
Na_2O	0.22	0.35	0.27	0.31	0.34	0.35
K_2O	9.46	9.88	9.96	10.00	10.09	9.66
MgO	10.83	9.30	9.61	9.15	11.79	8.86
CaO	0.03	0.01	0.04	0.01	0.01	0.05
MnO	4.88	1.20	2.56	2.44	2.38	2.34
FeO	21.45	23.44	24.74	25.76	21.54	25.36
Al_2O_3	10.49	12.35	11.64	11.55	11.80	11.51
TiO_2	1.98	3.87	2.39	2.70	3.11	2.83
SiO_2	38.50	36.21	36.08	36.22	36.35	36.21
F	2.91	na	na	na	na	na
Cl	0.02	0.02	0.01	0.02	0.01	0.02
$\sum$	100.77	96.63	97.30	98.16	97.42	97.19
O=F	1.23	-	-	-	-	-
O=Cl	0.00	0.00	0.00	0.00	0.00	0.00
$\sum$'	99.54	96.63	97.30	98.16	97.42	97.19
atomic proportions (normalized to 11 oxygens)						
Na	0.033	0.053	0.041	0.047	0.051	0.053
K	0.928	0.982	0.997	0.996	0.993	0.968
Mg	1.242	1.080	1.124	1.065	1.356	1.038
Ca	0.002	0.001	0.003	0.001	0.001	0.004
Mn	0.318	0.079	0.170	0.161	0.155	0.156
Fe^{2+}	1.380	1.527	1.624	1.682	1.389	1.667
Al	0.951	1.134	1.077	1.063	1.073	1.066
Ti	0.115	0.227	0.141	0.159	0.180	0.167
Si	2.961	2.821	2.831	2.828	2.804	2.846
F	0.708	-	-	-	-	-
Cl	0.003	0.003	0.001	0.003	0.001	0.003
$\sum$ cations	7.929	7.903	8.008	8.003	8.002	7.965
$\sum$ oxygens	11.000	11.000	11.000	11.000	11.000	11.000
Mg/(Mg+Fe)	0.474	0.414	0.409	0.388	0.494	0.384
Mg	0.422	0.402	0.385	0.366	0.467	0.363
Fe	0.469	0.568	0.556	0.578	0.479	0.583
Mn	0.108	0.029	0.058	0.055	0.054	0.054

#7 = biotite; nepheline-sodalite syenite, drill hole E2, depth 1856 m.
#8 = biotite; syenite, drill hole E3, depth 1230 m.
#9-12 = biotite; syenite, drill hole E3, depth 1286.5 m.

Table 4. Microprobe analyses of biotite (continued).

	#13 E3-1810 syenite Grain A	#14 E3-1810 syenite Grain B	#15 E3-1810 syenite Grain C	#16 E3-1810 syenite Grain D	#17 E3-2013.5 ne.-sod.sy. Grain A	#18 E3-2013.5 ne.-sod.sy. Grain B
Na_2O	0.14	0.18	0.18	0.10	0.16	0.34
K_2O	10.35	10.37	10.32	10.57	9.80	9.04
MgO	13.23	12.87	11.73	14.03	12.99	10.64
CaO	0.10	0.12	0.03	0.01	0.03	0.01
MnO	2.28	2.34	2.51	2.23	1.67	1.82
FeO	20.49	20.30	21.80	19.37	18.93	22.55
Al_2O_3	10.96	10.98	11.71	11.37	11.00	10.90
TiO_2	1.65	1.76	1.92	1.51	1.99	2.19
SiO_2	37.31	37.06	35.44	37.97	38.86	37.97
F	na	na	na	na	na	na
Cl	na	0.01	0.01	0.01	0.01	na
Σ	96.51	95.99	95.65	97.17	95.44	95.46
O=F	-	-	-	-	-	-
O=Cl	-	0.00	0.00	0.00	0.00	-
Σ'	96.51	95.99	95.65	97.17	95.44	95.46
atomic proportions (normalized to 11 oxygens)						
Na	0.021	0.027	0.028	0.015	0.024	0.051
K	1.022	1.030	1.041	1.029	0.960	0.901
Mg	1.527	1.494	1.383	1.596	1.487	1.239
Ca	0.008	0.010	0.003	0.001	0.002	0.001
Mn	0.149	0.154	0.168	0.144	0.109	0.120
Fe^{2+}	1.326	1.322	1.442	1.236	1.216	1.473
Al	1.000	1.008	1.091	1.022	0.996	1.003
Ti	0.096	0.103	0.114	0.087	0.115	0.129
Si	2.888	2.886	2.803	2.897	2.985	2.965
F	-	-	-	-	-	-
Cl	-	0.001	0.001	0.001	0.001	-
Σ cations	8.038	8.035	8.072	8.027	7.894	7.881
Σ oxygens	11.000	11.000	11.000	11.000	11.000	11.000
Mg/(Mg+Fe)	0.535	0.531	0.490	0.564	0.550	0.457
Mg	0.508	0.503	0.462	0.536	0.529	0.437
Fe	0.442	0.445	0.482	0.415	0.432	0.520
Mn	0.050	0.052	0.056	0.048	0.039	0.043

#13-16 = biotite-phlogopite; syenite, drill hole E3, depth 1810 m.
#17-18 = biotite-phlogopite; nepheline-sodalite syenite, drill hole E3, depth 2013.5 m.

Table 4. Microprobe analyses of biotite (continued).

	#19 E3-2013.5 Grain C	#20 G1-1394.5 Grain A	#21 G1-1408.0 Grain A	#22 G1-1408.0 Grain B	#23 G1-2000.0 Grain A	#24 G1-2000.0 Grain B
Na_2O	0.18	0.04	0.16	0.14	0.05	0.22
K_2O	9.25	9.30	8.68	8.89	8.98	9.42
MgO	8.96	14.32	13.06	14.13	12.71	13.16
CaO	0.01	0.00	0.00	0.00	0.00	0.00
MnO	2.66	0.07	0.09	0.06	0.17	0.11
FeO	24.55	16.56	16.73	15.64	16.71	16.98
Al_2O_3	11.93	12.65	13.47	13.25	13.77	13.22
TiO_2	2.35	4.91	5.41	5.10	5.88	4.84
SiO_2	36.45	37.08	36.92	37.08	38.12	36.97
F	na	na	0.70	0.80	0.63	na
Cl	0.01	na	0.04	0.08	0.01	na
$\sum$	96.35	94.91	95.26	95.17	97.03	94.92
O=F	-	-	0.29	0.34	0.27	-
O=Cl	0.00	-	0.01	0.02	0.00	-
$\sum$'	96.35	94.91	94.96	94.82	96.76	94.92
atomic proportions (normalized to 11 oxygens)						
Na	0.027	0.006	0.024	0.021	0.007	0.032
K	0.929	0.899	0.840	0.859	0.850	0.913
Mg	1.051	1.618	1.477	1.595	1.406	1.491
Ca	0.001	0.000	0.000	0.000	0.000	0.000
Mn	0.177	0.004	0.006	0.004	0.011	0.007
Fe^{2+}	1.616	1.050	1.061	0.990	1.037	1.079
Al	1.107	1.130	1.204	1.183	1.204	1.184
Ti	0.139	0.280	0.309	0.291	0.328	0.277
Si	2.869	2.810	2.800	2.808	2.828	2.810
F	-	-	0.168	0.192	0.148	-
Cl	0.001	-	0.005	0.010	0.001	-
$\sum$ cations	7.917	7.798	7.721	7.750	7.670	7.794
$\sum$ oxygens	11.000	11.000	11.000	11.000	11.000	11.000
Mg/(Mg+Fe)	0.394	0.607	0.582	0.617	0.576	0.580
Mg	0.370	0.606	0.581	0.616	0.573	0.579
Fe	0.568	0.393	0.417	0.383	0.423	0.419
Mn	0.062	0.002	0.002	0.001	0.004	0.003

#19 = biotite; nepheline-sodalite syenite, drill hole E3, depth 2013.5 m.
#20 = biotite-phlogopite (rimmed by green chlorite); syenodiorite, drill hole G1, depth 1394.5 m.
#21-22 = biotite-phlogopite; syenodiorite, drill hole G1, depth 1408.0 m.

Table 5. Microprobe analyses of amphiboles.
[Analyses in weight percent; na = not analyzed. All iron computed as FeO.]

	#1 E4-950.2 Grain A	#2 E4-950.2 Grain B	#3 E4-1074 Grain A	#4 E4-1074 Grain B	#5 E4-1256 Grain A	#6 E4-1256 Grain B
Na_2O	9.78	9.88	9.97	10.25	9.15	8.91
K_2O	1.43	1.44	1.42	1.43	1.37	1.37
MgO	9.56	9.48	8.66	8.79	10.22	10.17
CaO	0.75	0.85	0.78	0.70	1.66	1.94
MnO	2.10	1.97	2.67	2.97	1.87	2.08
FeO	18.24	19.39	17.44	17.07	17.38	17.19
Al_2O_3	0.96	1.52	0.66	0.52	1.41	1.76
TiO_2	0.87	1.00	1.13	1.02	1.00	1.10
SiO_2	53.31	51.95	53.57	53.60	52.27	52.26
F	3.00	na	3.03	3.11	2.96	3.12
Cl	na	na	na	na	na	na
$\sum$	100.00	97.26	99.33	99.46	99.29	99.90
O=F	1.26	-	1.28	1.31	1.25	1.31
O=Cl	-	-	-	-	-	-
$\sum'$	98.74	97.26	98.05	98.15	98.04	98.59
atomic proportions (normalized to 23 oxygens)						
Na	2.867	2.911	2.941	3.024	2.695	2.611
K	0.276	0.279	0.276	0.278	0.265	0.264
Mg	2.155	2.148	1.964	1.994	2.314	2.291
Ca	0.122	0.138	0.127	0.114	0.270	0.314
Mn	0.269	0.225	0.344	0.383	0.241	0.266
Fe^{2+}	2.307	2.465	2.219	2.172	2.208	2.173
Al	0.171	0.272	0.118	0.093	0.252	0.314
Ti	0.099	0.114	0.129	0.117	0.114	0.125
Si	8.061	7.896	8.151	8.156	7.940	7.899
F	1.435	-	1.458	1.497	1.422	1.491
Cl	-	-	-	-	-	-
$\sum$ cations	16.326	16.449	16.269	16.331	16.300	16.257
$\sum$ oxygens	23.000	23.000	23.000	23.000	23.000	23.000

#1,2 = magnesioarfvedsonite; aegirine-arfvedsonite syenite, drill hole E4, depth 950.2 m.
#3,4 = eckermannite-magnesioarfvedsonite; aegirine-arfvedsonite syenite, drill hole E4, depth 1074 m.
#5,6 = magnesioarfvedsonite; aegirine-arfvedsonite syenite, drill hole E4, depth 1256 m.

Table 5. Microprobe analyses of amphiboles (continued).

	#7 G1-1394.5 Grain A	#8 G1-1394.5 Grain B	#9 G1-1408.0 Grain A	#10 G1-1408.8 Grain B	#11 G1-2000.0 Grain A	#12 G1-2000.0 Grain B
Na_2O	1.20	1.66	1.28	1.34	2.41	2.29
K_2O	0.43	0.54	0.36	0.38	1.15	1.09
MgO	15.53	15.09	15.81	15.59	12.02	12.25
CaO	11.57	10.95	11.36	11.32	11.06	11.11
MnO	0.38	0.38	0.25	0.28	0.22	0.22
FeO	12.78	13.67	12.36	12.65	13.24	12.79
Al_2O_3	4.29	5.87	3.88	3.86	9.81	9.44
TiO_2	1.09	1.44	0.97	0.86	3.89	3.64
SiO_2	51.89	48.12	51.02	50.44	40.68	41.58
F	na	na	na	na	na	na
Cl	na	na	na	na	na	na
Σ	99.16	97.72	97.29	96.72	94.48	94.41
O=F	-	-	-	-	-	-
O=Cl	-	-	-	-	-	-
Σ'	99.16	97.72	97.29	96.72	94.48	94.41
atomic proportions (normalized to 23 oxygens)						
Na	0.332	0.472	0.361	0.381	0.723	0.684
K	0.078	0.101	0.067	0.071	0.227	0.214
Mg	3.307	3.301	3.428	3.411	2.772	2.814
Ca	1.771	1.722	1.770	1.780	1.833	1.834
Mn	0.046	0.047	0.031	0.035	0.029	0.029
Fe^{2+}	1.527	1.678	1.504	1.553	1.713	1.648
Al	0.722	1.015	0.665	0.668	1.789	1.714
Ti	0.117	0.159	0.106	0.095	0.453	0.422
Si	7.413	7.062	7.421	7.402	6.294	6.406
F	-	-	-	-	-	-
Cl	-	-	-	-	-	-
Σ cations	15.314	15.558	15.354	15.395	15.834	15.764
Σ oxygens	23.000	23.000	23.000	23.000	23.000	23.000

#7,8 = actinolitic hornblende and magnesiohornblende; syenodiorite, drill hole G1, depth 1394.5 m.
#9,10 = actinolitic hornblende; syenodiorite, drill hole G1, depth 1408.0 m.
#11,12 = magnesian hastingsitic hornblende; syenodiorite, drill hole G1, depth 2000.0 m.

Table 6. Microprobe analyses of feldspars.
[Analyses in weight percent; na = not analyzed. All iron computed as FeO in albite and plagioclase, and as Fe_2O_3 in potassium feldspars.]

	#1 E2-1844 Grain A	#2 E2-1844 Grain B	#3 E2-1850 Grain A	#4 E2-1850 Grain B	#5 E2-1856 Grain A	#6 E3-2005.7 Grain A
Na_2O	1.93	6.11	0.43	3.91	0.55	0.63
K_2O	14.34	8.12	16.98	11.06	16.29	15.03
MgO	0.00	0.00	0.01	0.00	0.00	0.00
CaO	0.02	0.05	0.02	0.00	0.01	0.00
SrO	0.00	0.00	0.00	na	0.00	na
BaO	0.00	0.00	0.01	0.01	0.00	na
MnO	0.03	0.03	0.00	0.00	0.01	0.00
FeO	-	-	-	-	-	-
Fe_2O_3	0.31	0.23	0.04	0.18	0.16	0.12
Al_2O_3	18.89	19.15	18.74	18.92	18.76	18.23
TiO_2	0.00	0.04	0.01	0.02	0.00	0.02
SiO_2	65.19	65.83	63.59	66.23	64.68	66.58
$\sum$	100.71	99.56	99.83	100.33	100.46	100.61
atomic proportions (normalized to 8 oxygens)						
Na	0.171	0.535	0.039	0.343	0.049	0.056
K	0.835	0.468	1.010	0.638	0.957	0.873
Mg	0.000	0.000	0.001	0.000	0.000	0.000
Ca	0.001	0.002	0.001	0.000	0.000	0.000
Sr	0.000	0.000	0.000	-	0.000	-
Ba	0.000	0.000	0.000	0.000	0.000	-
Mn	0.001	0.001	0.000	0.000	0.000	0.000
Fe^{2+}	-	-	-	-	-	-
Fe^{3+}	0.011	0.008	0.002	0.008	0.005	0.004
Al	1.017	1.020	1.029	1.007	1.019	0.978
Ti	0.000	0.001	0.000	0.001	0.000	0.001
Si	2.977	2.975	2.963	2.994	2.980	3.031
$\sum$ alkalies	1.007	1.006	1.050	0.981	1.007	0.928
$\sum$ cations	5.013	5.011	5.045	4.989	5.011	4.942
$\sum$ oxygens	8.000	8.000	8.000	8.000	8.000	8.000
Na/$\sum$NaKCa	0.170	0.532	0.037	0.350	0.049	0.060
K/$\sum$NaKCa	0.829	0.465	0.962	0.650	0.951	0.940
Ca/$\sum$NaKCa	0.001	0.002	0.001	0.000	0.000	0.000

#1,2 = Potassium feldspar, cloudy phenocryst (orthoclase + intergrown albite); nepheline-sodalite syenite, drill hole E2, depth 1844 m.
#3,4 = Potassium feldspar, cloudy phenocryst (orthoclase + intergrown albite), weak red-violet cathodoluminescence; drill hole E2, depth 1850 m.
#5 = Orthoclase; nepheline-sodalite syenite, drill hole E2, depth 1856 m.
#6 = Orthoclase, pale red-violet CL; nepheline-sodalite syenite, drill hole E3, depth 2005.7 m.

Table 6. Microprobe analyses of feldspars (continued).

	#7 E4-950.2 Grain A	#8 E4-1074 Grain A	#9 E4-1074 Grain B	#10 E3-1230 Grain A	#11 E3-1230 Grain B	#12 E3-1286.5 Grain A
Na_2O	0.18	0.31	2.64	0.99	8.33	0.40
K_2O	16.00	16.71	12.83	15.55	5.33	15.94
MgO	0.00	0.00	0.00	0.00	0.00	0.00
CaO	0.00	0.01	0.00	0.20	0.61	0.00
SrO	na	0.00	-	0.01	0.00	0.00
BaO	na	0.00	-	0.28	0.22	0.05
MnO	0.00	0.00	0.00	0.02	0.00	0.02
FeO	-	-	-	-	-	-
Fe_2O_3	0.34	0.69	0.49	0.17	0.18	0.13
Al_2O_3	17.69	18.39	18.20	18.96	19.84	18.95
TiO_2	0.00	0.00	0.00	0.00	0.10	0.03
SiO_2	63.49	63.61	65.67	63.14	65.38	65.20
Σ	97.70	99.72	99.83	99.32	99.99	100.72
atomic proportions (normalized to 8 oxygens)						
Na	0.017	0.028	0.234	0.090	0.724	0.036
K	0.966	0.995	0.749	0.927	0.305	0.931
Mg	0.000	0.000	0.000	0.000	0.000	0.000
Ca	0.000	0.000	0.000	0.010	0.029	0.000
Sr	-	0.000	-	0.000	0.000	0.000
Ba	-	0.000	-	0.005	0.004	0.001
Mn	0.000	0.000	0.000	0.001	0.000	0.001
Fe^{2+}	-	-	-	-	-	-
Fe^{3+}	0.012	0.024	0.017	0.006	0.006	0.005
Al	0.987	1.011	0.982	1.044	1.049	1.023
Ti	0.000	0.000	0.000	0.000	0.003	0.001
Si	3.005	2.968	3.005	2.950	2.932	2.986
Σ alkalies	0.983	1.023	0.983	1.032	1.062	0.968
Σ cations	4.987	5.026	4.987	5.033	5.052	4.983
Σ oxygens	8.000	8.000	8.000	8.000	8.000	8.000
$Na/\Sigma NaKCa$	0.017	0.027	0.238	0.087	0.684	0.037
$K/\Sigma NaKCa$	0.983	0.972	0.762	0.903	0.288	0.963
$Ca/\Sigma NaKCa$	0.000	0.000	0.000	0.010	0.028	0.000

#7 = Orthoclase, red CL; aegirine-arfvedsonite syenite, drill hole E4, depth 950 m.
#8-9 = Orthoclase (+ intergrown albite), red CL; aegirine-arfvedsonite syenite, drill hole E4, depth 1074 m.
#10-11 = Alkali feldspar (orthoclase + intergrown albite?); syenite, drill hole E-3, depth 1230 m.
#12 = Orthoclase; syenite, drill hole E-3, depth 1286.5 m.

Table 6. Microprobe analyses of feldspars (continued).

	#13 E3-1810 Grain A	#14 G1-1408.0 Grain A	#15 G1-1408.0 Grain B	#16 E2-1844 Grain A	#17 E1-1850 Grain A	#18 E2-1856 Grain A
Na_2O	0.40	4.09	1.75	10.65	11.87	11.95
K_2O	16.19	10.05	13.19	0.68	0.21	0.05
MgO	0.00	0.00	0.00	0.00	0.00	0.00
CaO	0.01	0.13	0.04	0.02	0.03	0.00
SrO	0.04	na	na	0.00	0.02	na
BaO	0.00	na	na	0.09	0.01	na
MnO	0.01	0.00	0.00	0.00	0.01	0.00
FeO	-	-	-	0.16	0.32	0.16
Fe_2O_3	0.07	0.00	0.04	-	-	-
Al_2O_3	18.44	18.56	17.86	19.67	19.74	19.31
TiO_2	0.00	0.00	0.00	0.00	0.00	0.00
SiO_2	65.26	66.28	66.81	68.37	67.85	69.29
$\sum$	100.42	99.11	99.69	99.64	100.06	100.76
atomic proportions (normalized to 8 oxygens)						
Na	0.036	0.361	0.155	0.905	1.008	1.005
K	0.950	0.583	0.767	0.038	0.012	0.003
Mg	0.000	0.000	0.000	0.000	0.000	0.000
Ca	0.000	0.006	0.002	0.001	0.001	0.000
Sr	0.001	-	-	0.000	0.001	-
Ba	0.000	-	-	0.002	0.000	-
Mn	0.000	0.000	0.000	0.000	0.000	0.000
Fe^{2+}	-	-	-	0.006	0.012	0.006
Fe^{3+}	0.002	0.000	0.002	-	-	-
Al	0.999	0.995	0.960	1.016	1.019	0.987
Ti	0.000	0.000	0.000	0.000	0.000	0.000
Si	3.001	3.015	3.047	2.998	2.973	3.005
$\sum$ alkalies	0.987	0.950	0.924	0.946	1.022	1.008
$\sum$ cations	4.991	4.960	4.933	4.966	5.027	5.005
$\sum$ oxygens	8.000	8.000	8.000	8.000	8.000	8.000
$Na/\sum NaKCa$	0.036	0.380	0.167	0.959	0.987	0.997
$K/\sum NaKCa$	0.963	0.614	0.830	0.040	0.011	0.003
$Ca/\sum NaKCa$	0.000	0.007	0.002	0.003	0.001	0.000

#13 = Orthoclase; syenite, drill hole E3, depth 1810 m.
#14,15 = Potassium feldspar, blue CL; syenodiorite, drill hole G1, depth 1408.0 m; #14 = clear center of phenocryst; #15 = cloudy outer zone.
#16 = Albite; nepheline-sodalite syenite, drill hole E2, depth 1844 m.
#17 = Albite, weak violet-red CL; nepheline-sodalite syenite, drill hole E2, depth 1850 m.
#18 = Albite, clear square euhedral crystal, weak violet-red CL; nepheline-sodalite syenite, drill hole E2, depth 1856 m.

Table 6. Microprobe analyses of feldspars (continued).

	#19 E2-1856 Grain B	#20 E3-2005.7 Grain A	#21 E4-950.2 Grain A	#22 E4-1074 Grain A	#23 E4-1074 Grain B	#24 E3-1230 Grain A
Na_2O	12.36	11.70	11.90	11.77	11.84	10.97
K_2O	0.10	0.13	0.07	0.12	0.10	0.36
MgO	0.01	0.00	0.00	0.00	0.00	0.01
CaO	0.02	0.00	0.00	0.00	0.00	0.76
SrO	0.00	na	na	na	na	0.00
BaO	0.03	na	na	na	na	0.26
MnO	0.01	0.00	0.00	0.00	0.00	0.00
FeO	0.06	0.07	-	0.46	0.59	0.15
Fe_2O_3	-	-	0.89	-	-	-
Al_2O_3	21.02	19.53	18.56	18.77	18.76	20.34
TiO_2	0.00	0.00	0.00	0.00	0.00	0.08
SiO_2	66.98	71.41	68.30	68.71	69.12	69.31
$\sum$	100.59	102.84	99.72	99.83	100.41	102.24
	atomic proportions (normalized to 8 oxygens)					
Na	1.046	0.961	1.014	1.000	1.001	0.912
K	0.006	0.007	0.004	0.007	0.006	0.020
Mg	0.001	0.000	0.000	0.000	0.000	0.001
Ca	0.001	0.000	0.000	0.000	0.000	0.035
Sr	0.000	-	-	-	-	0.000
Ba	0.001	-	-	-	-	0.004
Mn	0.000	0.000	0.000	0.000	0.000	0.000
Fe^{2+}	0.002	0.002	-	0.46	0.59	0.005
Fe^{3+}	-	-	0.029	-	-	-
Al	1.081	0.975	0.962	0.970	0.964	1.028
Ti	0.000	0.000	0.000	0.000	0.000	0.003
Si	2.924	3.025	3.002	3.012	3.014	2.971
$\sum$ alkalies	1.053	0.968	1.018	1.007	1.007	0.971
$\sum$ cations	5.061	4.970	5.011	5.006	5.007	4.978
$\sum$ oxygens	8.000	8.000	8.000	8.000	8.000	8.000
$Na/\sum NaKCa$	0.994	0.993	0.996	0.993	0.994	0.944
$K/\sum NaKCa$	0.005	0.007	0.004	0.007	0.006	0.020
$Ca/\sum NaKCa$	0.001	0.000	0.000	0.000	0.000	0.036

#19 = Albite, replacement of K-feldspar; nepheline-sodalite syenite, drill hole E2, depth 1856 m.

#20 = Albite, 80-μm groundmass crystal, blue CL; nepheline-sodalite syenite, drill hole #3, depth 2005.7 m.

#21 = Albite, red CL; aegirine-arfvedsonite syenite, drill hole E4, depth 950.2 m (Fe computed as Fe_2O_3 because of bright red CL).

#22,23 = Albite; aegirine-arfvedsonite syenite, drill hole E4, depth 1074 m; #22, clear albite crystal, weak or no CL; #23, within partly altered K-feldspar phenocryst, reddish CL.

#24 = Albite; syenite, drill hole E3, depth 1230 m.

Table 6. Microprobe analyses of feldspars (continued).

	#25 E3-1286.5 Grain A	#26 E3-1810 Grain A	#27 G1-1394.5 Grain A core	#28 G1-1394.5 Grain A intermed.	#29 G1-1394.5 Grain A rim	#30 G1-1394.5 Grain B
Na_2O	11.85	11.18	5.48	6.95	9.41	11.44
K_2O	0.11	0.10	0.34	0.46	0.70	0.07
MgO	0.00	0.01	0.00	0.00	0.00	0.00
CaO	0.11	0.13	10.54	7.77	3.14	0.73
SrO	0.00	0.00	na	na	na	na
BaO	0.00	0.00	na	na	na	na
MnO	0.00	0.00	0.00	0.00	0.00	0.00
FeO	0.11	0.26	0.43	0.26	0.10	0.06
Fe_2O_3	-	-	-	-	-	-
Al_2O_3	19.81	20.01	27.92	25.69	21.60	19.79
TiO_2	0.01	0.00	0.06	0.01	0.00	0.01
SiO_2	68.19	68.69	54.36	58.87	63.99	67.61
$\sum$	100.19	100.38	99.13	100.01	98.94	99.71
	atomic proportions (normalized to 8 oxygens)					
Na	1.003	0.942	0.485	0.603	0.815	0.974
K	0.006	0.006	0.020	0.026	0.040	0.004
Mg	0.000	0.001	0.000	0.000	0.000	0.000
Ca	0.005	0.006	0.515	0.373	0.150	0.034
Sr	0.000	0.000	-	-	-	-
Ba	0.000	0.000	-	-	-	-
Mn	0.000	0.000	0.000	0.000	0.000	0.000
Fe^{2+}	0.004	0.009	0.016	0.010	0.004	0.002
Fe^{3+}	-	-	-	-	-	-
Al	1.020	1.025	1.501	1.355	1.137	1.024
Ti	0.000	0.000	0.002	0.000	0.000	0.000
Si	2.978	2.986	2.480	2.635	2.857	2.969
$\sum$ alkalies	1.015	0.954	1.020	1.002	1.005	1.012
$\sum$ cations	5.017	4.975	5.020	5.002	5.002	5.008
$\sum$ oxygens	8.000	8.000	8.000	8.000	8.000	8.000
$Na/\sum NaKCa$	0.989	0.988	0.475	0.602	0.811	0.962
$K/\sum NaKCa$	0.006	0.006	0.019	0.026	0.040	0.004
$Ca/\sum NaKCa$	0.005	0.006	0.505	0.372	0.150	0.034

#25 = Albite; syenite, drill hole E3, depth 1286.5 m.
#26 = Albite; syenite, drill hole E3, depth 1810 m.
#27-29 = Plagioclase, zoned phenocryst, labradorite to oligoclase, blue-green CL; syenodiorite, drill hole G1, depth 1394.5 m.
#30 = Albite, clear patch, weak or no CL; syenodiorite, drill hole G1, depth 1394.5 m.

Table 6. Microprobe analyses of feldspars (continued).

	#31 G1-1408.0 Grain A core	#32 G1-1408.0 Grain A rim	#33 G1-2000.0 Grain A core	#34 G1-2000.0 Grain A rim	#35 G1-2000.0 Grain B core	#36 G1-2000.0 Grain B rim
Na_2O	5.08	6.68	5.59	6.54	4.87	6.66
K_2O	0.24	0.41	0.29	0.43	0.26	0.34
MgO	0.00	0.00	0.00	0.00	0.00	0.00
CaO	11.03	8.35	9.71	7.87	11.47	8.16
SrO	na	na	na	na	na	na
BaO	na	na	na	na	na	na
MnO	0.00	0.00	0.00	0.00	0.00	0.00
FeO	na	na	0.19	0.15	na	na
Fe_2O_3	-	-	-	-	-	-
Al_2O_3	28.77	26.55	27.90	26.32	28.41	26.14
TiO_2	0.00	0.00	0.00	0.00	0.00	0.00
SiO_2	55.29	57.79	57.21	59.42	54.49	57.87
$\sum$	100.41	99.78	100.89	100.73	99.50	99.17
	atomic proportions (normalized to 8 oxygens)					
Na	0.442	0.581	0.482	0.562	0.428	0.582
K	0.014	0.023	0.016	0.024	0.015	0.020
Mg	0.000	0.000	0.000	0.000	0.000	0.000
Ca	0.530	0.402	0.463	0.374	0.557	0.394
Sr	-	-	-	-	-	-
Ba	-	-	-	-	-	-
Mn	0.000	0.000	0.000	0.000	0.000	0.000
Fe^{2+}	-	-	0.007	0.006	-	-
Fe^{3+}	-	-	-	-	-	-
Al	1.521	1.405	1.462	1.375	1.519	1.390
Ti	0.000	0.000	0.000	0.000	0.000	0.000
Si	2.480	2.594	2.544	2.633	2.471	2.610
$\sum$ alkalies	0.986	1.007	0.961	0.960	1.001	0.996
$\sum$ cations	4.987	5.006	4.974	4.973	4.991	4.996
$\sum$ oxygens	8.000	8.000	8.000	8.000	8.000	8.000
$Na/\sum NaKCa$	0.448	0.578	0.502	0.585	0.428	0.585
$K/\sum NaKCa$	0.014	0.023	0.017	0.025	0.015	0.020
$Ca/\sum NaKCa$	0.538	0.399	0.481	0.389	0.557	0.396

#31-32 = Plagioclase, zoned phenocryst labradorite to andesine, blue-green CL; syenodiorite, drill hole G1, depth 1408.0 m.

#33-36 = Plagioclase, zoned phenocrysts, labradorite to andesine, blue-green CL; syenodiorite, drill hole G1, depth 2000.0 m.

Table 7. Range of observed clinopyroxene compositions as determined from microprobe analyses: molecular proportion of acmite (Ac).

Sample	*Rock type*	*Acmite component in clinopyroxene*
E2-1844	feldspathoidal syenite	Ac 90-98
E3-2005.7	feldspathoidal syenite	Ac 95
E4-950.2	arvedsonite syenite	Ac 87-93
E4-1074	arvedsonite syenite	Ac 87-93
E2-1850	feldspathoidal syenite	Ac 68-98
E2-1856	feldspathoidal syenite	Ac 61-90
E3-1810	syenite	Ac 33-75
E3-1286.5	syenite	Ac 13-33
E3-1230	syenite	Ac 13-31
G1-1394.5	syenodiorite	Ac 3
G1-2000.0	syenodiorite	Ac 3

Table 8. Observed composition range of alkali and plagioclase feldspars in Elk rocks

Sample	*Rock type*	*Feldspar compositional range*
E4-950.2	arfvedsonite syenite	orthoclase ($Or_{98}Ab_2$) + albite ($Ab_{99.5}Or_{0.5}$)
E4-1074	arfvedsonite syenite	orthoclase ($Or_{97.5}Ab_{2.5}$) + sanidine ($Or_{76\text{-}91}Ab_{24\text{-}9}$) + albite ($Ab_{99.5}Or_{0.5}$)
E3-2005.7	feldspathoidal syenite	orthoclase ($Or_{90\text{-}94}Ab_{10\text{-}6}$) + albite ($Ab_{99.5}Or_{0.5}$)
E2-1850	feldspathoidal syenite	orthoclase ($Or_{95}Ab_5$) + albite ($Ab_{99}Or_1$), + intermediate compositions (mixtures?) from Or_{95} to Or_{15}
E2-1856	feldspathoidal syenite	orthoclase ($Or_{95}Ab_5$) + albite ($Ab_{99.5}Or_{0.5}$) + mixed intermediate compositions
E2-1844	feldspathoidal syenite	sanidine (microperthite) $Or_{83\text{-}15}$; most common range, $Or_{68\text{-}23}Ab_{32\text{-}77}$; + albite ($Ab_{97}Or_3$)
E3-1286.5	syenite	orthoclase ($Or_{96}Ab_4$) + albite ($Ab_{98}Or_1An_1$) + mixed intermediate compositions
E3-1810	syenite	orthoclase ($Or_{95}Ab_5$) + albite ($Ab_{98}Or_1An_1$) + mixed intermediate compositions
E3-1230	syenite	sanidine (microperthite), typically near $Ab_{61}Or_{37}An_2$; with intermediate compositions extending to near albite ($Ab_{94}Or_3An_3$)
G1-2000.0	syenodiorite	plagioclase, sodic labradorite to calcic oligoclase, $Ab_{43}An_{56}Or_1$-$Ab_{69}An_{29}Or_2$
G1-1394.5	syenodiorite	plagioclase, sodic labradorite to oligoclase, $Ab_{48}An_{51}Or_2$-$Ab_{81}An_{15}Or_4$, + albite, $Ab_{96}An_{3.5}Or_{0.5}$
G1-1408.0	syenodiorite	plagioclase, sodic labradorite to andesine, $Ab_{45}An_{54}Or_1$-$Ab_{58}An_{40}Or_2$, + sanidine, $Or_{88}Ab_{12}$-$Or_{61}Ab_{38}An_1$